1969

The effect of structure on the consolidation of compacted unsaturated clay soils

William Joseph Graham

Department:

THE EFFECT OF STRUCTURE ON THE CONSOLIDATION OF COMPACTED UNSATURATED CLAY SOILS

BY

WILLIAM JOSEPH GRAHAM

A

THESIS

submitted to the faculty of

THE UNIVERSITY OF MISSOURI - ROLLA

in partial fulfillment of the requirements for the

Degree of

MASTER OF SCIENCE IN CIVIL ENGINEERING

Rolla, Missouri

1969

Approved by

John B. Haseley Jr. (advisor) Norbert O. Schmidt

W. B. Vaughan Jr.

ABSTRACT

Contained in this paper are the results of research which was performed to investigate the relation between the volume-change mechanisms of shrinkage and one-dimensional compression for two clay soils, including some samples whose structures had been altered by the addition of flocculating and dispersing agents.

Shrinkage tests were conducted with a special mold designed to facilitate the study of a soil's shrinkage path. Consolidation tests on undisturbed samples and one-dimensional compression tests on unsaturated samples compacted in the vicinity of optimum moisture content were performed. A detailed study was made of a highly plastic red Missouri clay.

Complications arose in the shrinkage tests which prevented a general comparison of the two means of volume reduction. Specific conclusions are drawn as to the mechanism of unsaturated compression of clays and the related effects of structure, and suggestions are made for further study.

ACKNOWLEDGEMENT

The author wishes to express his appreciation to his advisor, Professor John B. Heagler, Jr. whose advice and encouragement guided the preparation of this paper. Special gratitude is extended to the other members of the soil mechanics and foundations staff for their help with particular portions of this thesis and for the instruction given to the author in his graduate studies. Grateful acknowledgement is given to Dr. William Hayes and the Missouri Geological Survey for providing the grant which financed this investigation, and to Mr. Edwin E. Lutzen, of that organization, who furnished the necessary soil samples.

The author is indebted to his wife, Diane, for her patience and understanding during the period of investigation.

TABLE OF CONTENTS

LIST OF FIGURES

LIST OF TABLES

I. INTRODUCTION

One of the basic problems which confronts the foundation engineer is the volume change that takes place in an embankment or in a soil mass beneath a structure. This decrease in volume occurs whenever the soil skeleton is stressed, whether the stress originates from the imposition of an external load or from a decrease in the moisture content upon evaporation of pore water. The compression which results from the application of an external load to a saturated soil has been studied and analyzed since the advent of modern soil mechanics. Recently these investigations have been extended to a three-phase system in which air is present in the liquid medium surrounding the soil particles. Soil shrinkage has received less attention in the same period. Laboratory work has generally been confined to the determination of the shrinkage limit.

This investigation was undertaken to study the shrinkage and compression characteristics of soils whose structures were altered by the use of additives, so that the effects of particle orientation could be detected. In addition, any significant correlations between these two associated mechanisms of volume reduction could be analyzed. To accomplish this, a relatively large shrinkage mold was designed having sides which were removable. It was hoped that these features would aid in the precise determination of the shrinkage paths inherent in the different soil structures. Difficulties were encountered which prevented the completion of a full test series using this mold. One-dimensional compression tests were conducted on saturated undisturbed samples and

on compacted unsaturated samples whose structures were altered. Failure of the shrinkage tests prevented a general comparison of the shrinkage and compressive properties of the soils, but a detailed discussion is given of the results which were obtained, along with recommendations for further research.

II. REVIEW OF LITERATURE

A. Structure of Clays

Investigations into the composition of clay minerals have shown them to be made up of layers of two basic structural units, one having an octahedral configuration and the other a tetrahedral configuration. The octahedral units are comprised of two parallel sheets of oxygen or hydroxyl layers between which are positioned atoms of aluminum, magnesium or iron. Each metallic atom is surrounded by six oxygens or hydroxyls, forming an octahedron. The tetrahedral unit is composed of a silicon atom equidistant from four oxygens or hydroxyls, forming a pyramid or tetrahedron. Specific clay minerals are made up of combinations of these units stacked alternately in the third dimension, or "c" axis. As with the units, most clay minerals are of indefinite length and width, giving rise to a typical platelike shape. Ionic and covalent bonds act to preserve the integrity of these crystal structures.

The balance of charges within a clay mineral can be disrupted in several ways. Termination of the clay's lateral extensions cause a charge imbalance at these edges. These broken bonds are the primary cause of net charges in kaolin minerals. Isomorphous substitution occurs when ions within the lattice, or structural framework, are replaced by other ions having different, usually lower, valances. This substitution is the primary cause of net charge in montmorillonoids. A third and less important cause of imbalance would be the substitution

of another ion for the hydrogen of the exposed hydroxyls along the basal surfaces of a clay mineral. The net charge resulting from these different imbalances is usually negative, resulting in the attraction of cations and polar water molecules to the surface of the clay particle.

The ability of a clay particle to attract and hold water molecules leads to the formation of layers of adsorbed water surrounding the particle. This adsorbed water is taken to be the cause of the plastic properties of clay (1). The closest layer is held tightly to the surface of the clay particle in a strongly oriented position. As the distance from the surface increases, both the attraction and the degree of orientation decrease, allowing this water to be more mobile. At some distance away from the particle, the water is unaffected and behaves as free pore water. Experimental evidence (2) has shown that the adsorbed water closest to the particle has a greater viscosity than that of free water. This viscosity would decrease away from the influence of the surface. The above factor can explain to some degree the viscoelastic properties exhibited by clays.

Theoretical treatment using the principles of colloid chemistry has led to the formation of theories of stabilization of dilute clay-water systems, as presented by H. van Olphen (3) and others. These systems are described as clay particles existing in a medium of water containing free ions. The particles have net surface charges, usually negative, due to lattice imperfections. Consequently, free ions of opposite sign, or counter-ions, are attracted to the charged surface.

The resulting concentration is resisted by the tendency of the ions to diffuse toward more dilute regions of the medium. As the attractive potential between the surface and the ions decreases rapidly away from the surface, the equilibrium distribution will be similar to that shown in Figure 1. In the same fashion, the concentration of anions in the vicinity of the clay particle will decrease as the particle surface is approached. At some distance from the particle, these forces will have dissipated to the extent that the concentration of cations and anions will be unaffected by the particle. The region in which the clay platelet influences the ion concentration is known as the diffuse layer or double diffuse layer of the particle.

The term "structure" refers to the arrangement of the individual particles or aggregations in a soil mass which constitutes the framework through which internal or external stresses are resisted. The existence of the diffuse layer and its relative size can be used to explain the development of this structure. As two particles of colloidal size (< 2 microns) approach each other in a clay-water system, Coulombic forces of repulsion and London-van der Waals attractive forces will be set up between them. The London-van der Waals forces, caused by additive attractions between individual atoms of the two particles, vary in magnitude roughly exponentially with the spacing between the particles. They are affected very little by conditions in the medium. The repulsive forces, on the other hand, are susceptible to changes in several variables, primarily temperature, the concentration of counterions, and their valence (1). The effect of these variables is illustrated in Figure 2. An increase in the concentration of ions in the medium

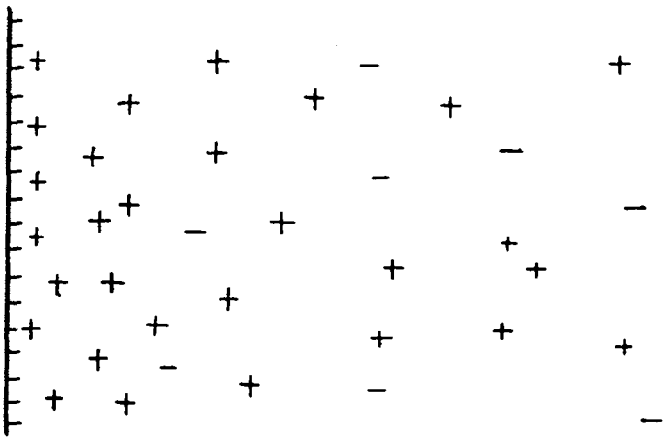

FIGURE 1. DOUBLE DIFFUSE LAYER MODEL (3)

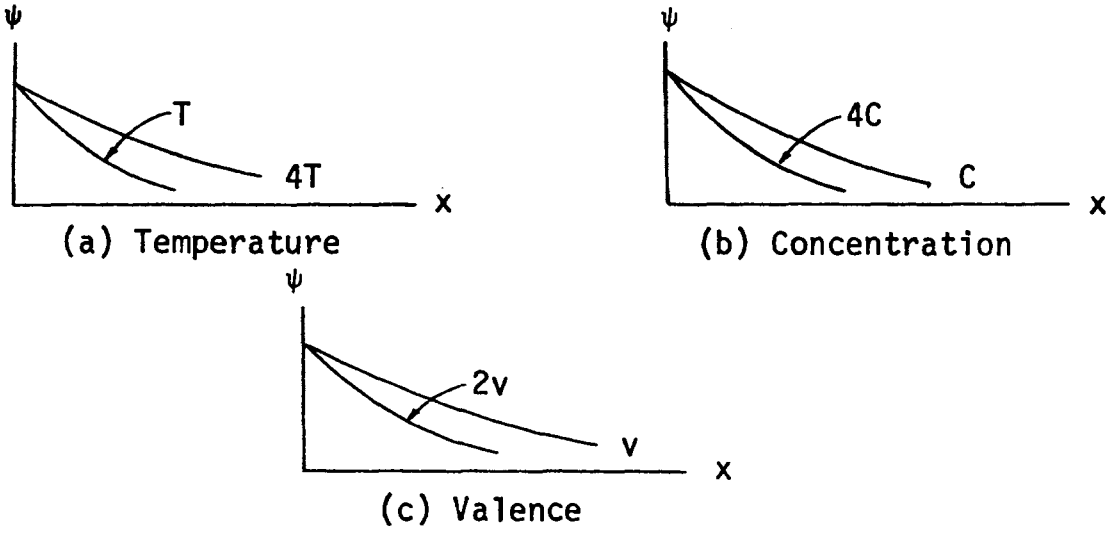

FIGURE 2. EFFECTS OF CHANGES IN VARIABLES ON THE DIFFUSE DOUBLE LAYER (1)

decreases the tendency of ions within the double layer to diffuse outward, resulting in a decrease in the extent of the double layer. Substitution of divalent ions for existing monovalent ions allows the negative surface charge to be satisfied by a lesser number of ions, again reducing the diffuse layer. A plot of the variation of repulsive and attractive energies with particle spacing is shown in Figure 3-a for three diffuse layer systems. The terms "large," "medium," and "small" refer to the size of the layer. It is apparent that compression of the double layer effectively reduces the range of repulsion, while the attractive energy remains unchanged. By adding algebraically the attraction and repulsion curves for each system, the respective net potential curves of particle interaction can be calculated and plotted as in Figure 3-b. The potential curves indicate the amount of work necessary to move the particles closer together. Where the net energy is repulsive, additional energy must be applied to the system before the particles will approach. Until this energy is provided, the particles will remain separated. A clay-water system in this condition is considered dispersed. Should the net energy of the system be attractive at all distances, as in the small diffuse layer of Figure 3-b, the particles will approach each other without hindrance until they merge. This merging action is known as flocculation. The above discussion relates the action of two idealized colloidal particles in a very dilute system. Soil encountered in the field, however, consists of particles varying greatly in size and mineralogy, having intimate interassociation, and with a much lower moisture content. Although these factors may greatly modify the theoretical analysis, it still provides a qualitative basis for studying the structure of a soil. Figure 4 gives examples

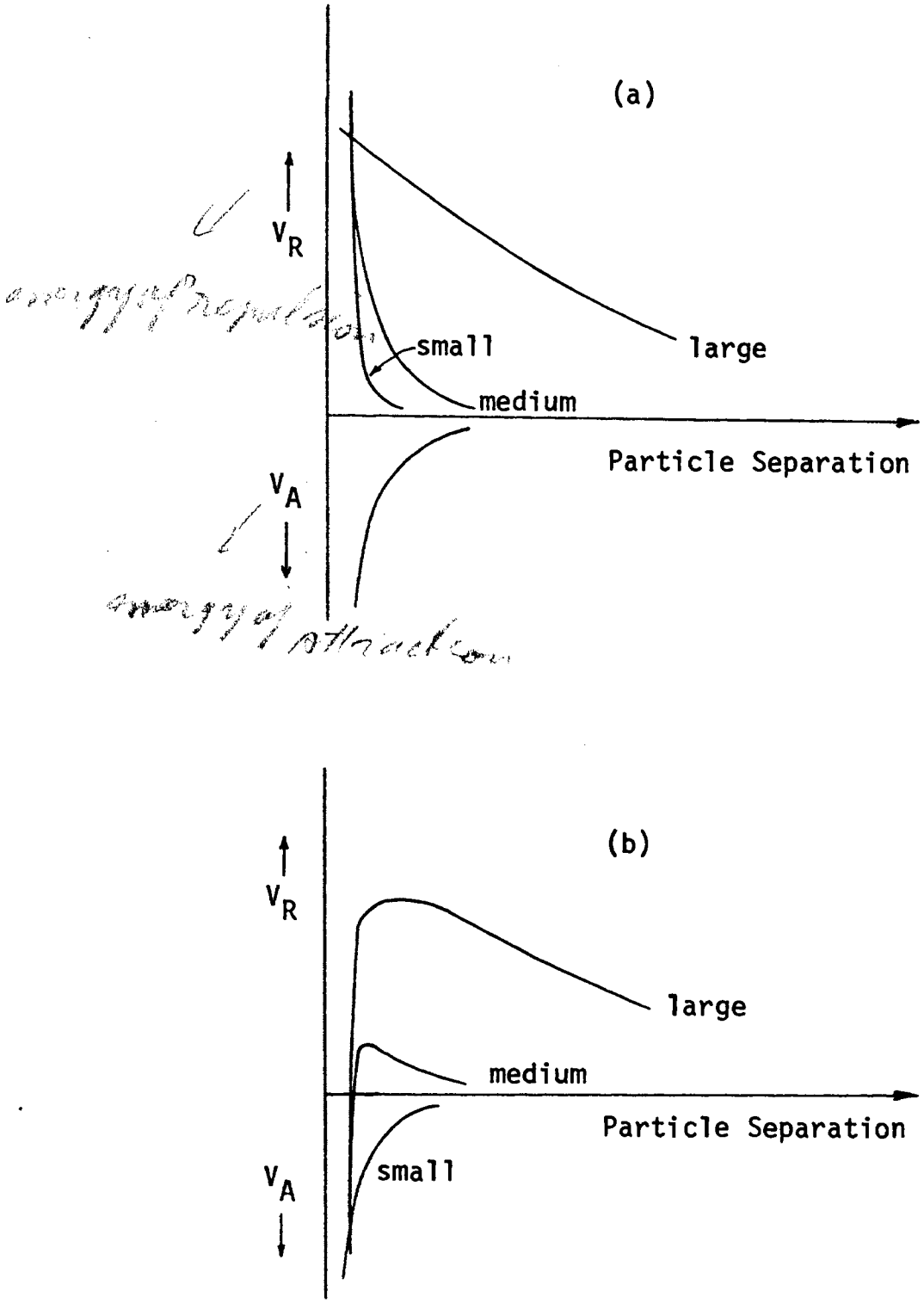

FIGURE 3. ATTRACTIVE AND REPULSIVE ENERGIES, AND NET ENERGIES, VERSUS PARTICLE SEPARATION FOR DIFFERENT LAYER THICKNESSES (3)

of flocculated and dispersed clay structures as described by Lambe (1). The dispersed soil exists in the face-to-face association in which the particles are held apart by repulsive forces.

According to the mechanism given above, flocculation will yield a soil system in which the particles exist primarily in a very intimate face-to-face arrangement called salt flocculation. This aggregation is based on the assumption that a uniform charge is distributed over all surfaces of the particle. However, should the edges of the platelets carry a charge opposite that of the surfaces, an edge-to-face arrangement would occur, as indicated in Figure 4-c for non-salt flocculation. The exact nature of particle contact in clay colloids is not clear, but the consensus of opinion (1) is that this contact is only through partial interpenetration of the adsorbed water layers of the particles.

B. Consolidation

Two of the dominant engineering characteristics of a soil mass are its compressibility and its permeability. These two factors are interrelated in that, for a sautrated system, the rate of change in volume is largely a function of the rate at which water can be removed from the system. A settlement analysis based on this approach was first put forward by K. Terzaghi in 1925. Revisions to this method have been incorporated*, but Terzaghi's basic theory is the only universally

---

*The theory and revisions are discussed in: "Consolidation of Clay with Non-Linear Viscosity," L. Barden (9).

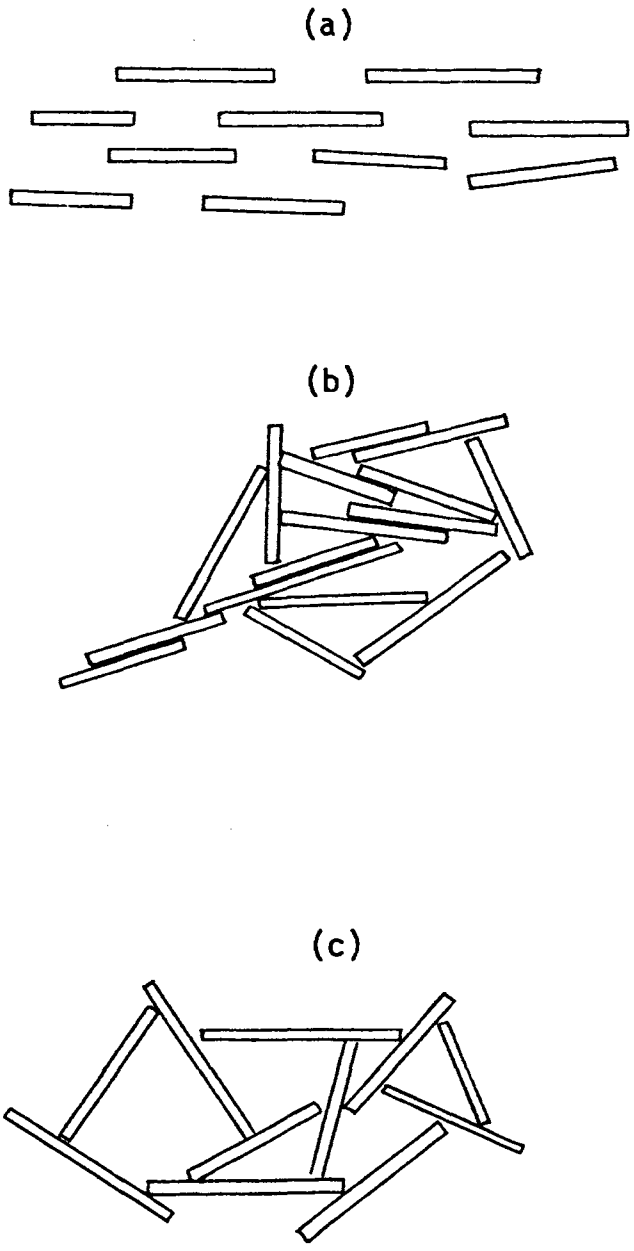

FIGURE 4. VARIOUS CLAY STRUCTURES INCLUDING DISPERSED, SALT FLOCCULATED, AND NON-SALT FLOCCULATED (1)

accepted analysis for the prediction of settlement and the rate at which it occurs.

The compression of a soil mass which occurs with the imposition of externally applied loads can be broken up into three phases (4)(5); initial compression, time-dependent compression or consolidation, and secondary compression. Initial compression consists of an instantaneous volume decrease in the soil upon loading, due to the compression or expulsion of gasses which may exist within the sample. In a "saturated" clay soil, this portion of the total volume decrease is negligible. Crawford (6) has shown that, in a sensitive Leda clay, 80-85% of each load increment was immediately transferred to the pore water. Hamilton and Crawford (7) and Girault (8) have noted a rather large amount of initial compression in saturated samples loaded below the preconsolidation pressure, and have attributed it to the compression of gasses which come out to solution upon removal of overburden pressure during sampling.

Consolidation is that portion of the total volume reduction which takes place as the load is transferred from the incompressible pore fluid to the soil structure. For the transfer to occur, the pressure in the pore liquid must be relieved by expulsion of the liquid through the soil voids. As this movement is time dependent, consolidation is seen to be a rate function, primarily dependent upon the permeability of the soil. The process is considered complete when the pore pressure induced by the applied load has dissipated and this load is carried by the soil structure. Consolidation is often referred to as primary

compression.

After the termination of consolidation, a further compression of the soil normally takes place. This action, known as secondary compression, continues for an indefinite period of time. It is attributed to a plastic flow or creep of the soil structure as adjustment is made for the new load increment. In 1941, Terzaghi (9) described secondary compression as "---a gradual transfer of stress from film to grain bond with an associated period of very slow viscous flow or creep. As the clay particles approach each other, the effective viscosity increases---." Leonards and Girault (10) dispute this, citing experiments in which non-polar pore fluids were used. Results showed that the effect of this substitution for water was negligible, causing them to conclude that the viscosity of oriented water molecules was not the cause of secondary compression. Instead, they endorsed Tan's concept of jumping of bonds as adjustments to the load are made. Barden (11) later amended this conclusion by pointing out that the rate at which this adjustment proceded would be controlled by the viscosity of the adsorbed water layer. Through the use of rheologic models K. Y. Lo (12) has shown that this viscosity is increased with effective stress and decreased with an increase in water content. Barden (9) formulated a model for consolidation in which yielding was dependent on a non-linear viscosity function approaching a Bingham yield behavior.

Secondary compression has been empirically defined as the volume reduction occurring after dissipation of pore pressures (8). However, several investigators (6),(13) have shown that this is a continuous

process starting at the time of application of the load which does not reach a maximum until pore pressure is dissipated. This would tend to indicate that secondary effects are a function of the effective stress.

Studies of the compressibility of a soil are normally performed through the use of the consolidation cell, in which movement in the lateral direction is restrained. Soil properties determined from the results of these tests are dependent on the manner in which the test is conducted. The total compressibility is dependent upon the magnitude and rate of loading, the thickness of the sample, the compressibility of the soil skeleton, and the permeability of the soil (6). Wahls (13) and Leonards and Girault (8) illustrated the effect of the pressure-increment ratio ($\Delta P/P_o$) on the dissipation of pore pressure and the relative amounts of primary and of secondary compression. Wahls concluded that primary compression is a function of the void ratio, independent of pressure increment ratio. In addition, he found that the rate of secondary compression, rather than the amount, is dependent upon the void ratio and the total pressure, again independent of the pressure increment and pressure-increment ratio. The effect of the duration of a load increment on the void ratio-pressure relation is dependent upon the soil itself. Studies by Leonards and Altschaeffl (8) have shown that load duration will have little effect as long as pore pressures are dissipated, the load-increment ratio is sufficiently large, and the soil does not exhibit abnormal secondary effects. The apparent preconsolidation pressure of a Leda clay, however, was appreciably lowered by increasing the duration from the time for pore pressure dissipation to a length of one week (6).

The concept of effective stress is readily applied to the consolidation characteristics of a saturated soil. In a saturated soil mass, the applied load is initially carried by the pore water, setting up a hydraulic pressure which acts equally in all directions. Since water is incompressible and has no shear strength, no volume reduction occurs. This pore water pressure is referred to as a neutral stress, since it does not affect the soil skeleton. If drainage is allowed, the pore pressure is reduced, and the difference between the applied stress and the reduced pore water pressure is the stress which is transferred to the soil grains, with accompanying strain and volume reduction. That portion of the load carried by the soil structure is defined as effective stress. If drainage continues, at some time the load will be carried entirely by the soil structure, and the neutral stress will be reduced to zero. An equation describing this process at any particular point is given below:

$$\bar{\sigma} = \sigma - u \quad \text{- - - - - - - - - - - - - - - - (1)}$$

where

σ = total applied stress

u = induced pore or neutral stress

$\bar{\sigma}$ = effective stress

In recent years several researchers have extended this concept to include unsaturated soil. In 1960, Bishop (14) proposed the following expression for effective stress in a three-phase system:

$$\bar{\sigma} = \sigma - u_a + \chi(u_a - u_w) \quad \text{- - - - - - - - - (2)}$$

where

u_a = pressure in the gas and vapor phase

u_w = pore water pressure

σ = total applied stress

$\bar{\sigma}$ = effective stress

χ = dimensionless parameter which varies with the degree of saturation

When the soil is fully saturated, χ is equal to unity and equation (2) reduces to equation (1).

Several limitations to the application of the extended effective stress principle have been noted. The value of χ is different for volume change-effective stress relationships and for strength-effective stress relations (15). Bishop and Blight (16) found that the paths of $(\sigma - u_a)$ and $(u_a - u_w)$ must be taken into account before utilizing effective stresses in determining the shear strength of unsaturated soils. A critical degree of saturation was proposed by Jennings and Burland (15), below which a unique relation between void ratio and effective stress does not exist. Barden (11) examined the consolidation of compacted unsaturated clays in light of the different permeabilities of air and of water at various stages of saturation. He divided these soils into five groups, depending on their degree of saturation, and analyzed the relationship between the air and the water at each stage.

Experiments with unsaturated soils have generally utilized samples initially formed by compaction in the laboratory. The effect of compaction on the structure of a soil has been covered by Lambe (1) and Seed and Chan (17). The amount of water present in a soil at water contents below that of optimum is not enough to enable full development

of the double layers of the clay particles (1). This water deficiency and double layer depression cause forces of attraction to predominate between particles, so that application of the standard compactive effort at these low water contents results in a flocculated soil structure. As optimum water content is approached, the additional water is less strongly bound to the soil, so that the resistance to movement at the interparticle contacts is more easily overcome. At water contents in the vicinity of optimum, the double layer potential is satisfied and attractive forces no longer predominate. Further additions of water only tend to separate the particles, lowering the dry density and enabling a more dispersed structure to be formed.

The structure of a soil would be expected to affect its compression characteristics to some degree. Lambe (1) indicates that at low pressures flocculated soils offer a greater resistance to compression than do dispersed. At higher pressures, though, the rate of change of void ratio with pressure is greater for the flocculated sample. The deformation taking place in a flocculated soil is caused by localized breakdown of bonds which create the flocculated structure, orienting the particles to some extent. Compression in a dispersed soil results primarily in a decreasing interparticle spacing, with a relatively small amount of orientation. Dispersed structures are found to have larger secondary effects (5).

The interaction of air and water in an unsaturated soil system has been examined in several published studies. The reason for this interest, as pointed out by Bishop and his co-workers (18), lies in the fact that,

due to surface tension, the equilibrium pressures of the two fluids may vary greatly. Investigations concerning fluid movement in soils generally analogize the void space to an interconnected system of capillary tubes having different radii. In these capillaries curved air-water interfaces or menisci will form, accompanied by surface tension stresses in the liquid phase. The magnitude of the pressure deficiency ΔP in the liquid caused by the tensile stresses can be calculated by the equation:

$$\Delta P = \frac{2T}{r}$$

where r is the radius of the capillary and T is the surface tension. If T is held constant, ΔP will increase as r is reduced. The pressure deficiency causes a reduction in the vapor pressure of this water from that of the bulk liquid, decreasing with the size of the radius. As a result of these processes, vapor distillation will cause the larger capillaries to be filled with air, and at the same time, larger pressure deficiencies due to smaller radii will cause water to flow to the smaller capillaries. According to Carman (19), who described the above actions, this movement will occur until equilibrium is established, as evidenced by uniform curvature of the menisci at all points. As a result of the tendency of larger pore spaces to be filled with air, interconnected air channels will exist even at high degrees of saturation (20). This concept is valid for all degrees of saturation; however, the mode of existence of the air at high degrees of saturation is disputed. Hilf (21) believes that bubbles of air cannot exist in equilibrium with water in a soil system undergoing stress, whereas Barden (11) pointed out that this is possible if the bubbles were at pressures greater than atmospheric.

The existence of a pressure deficiency or negative pore pressure in an unsaturated soil was used by Olson as the basis for his effective stress theory of compaction (22). The expulsion of water from an unsaturated sample would be prevented until the suction ($u_a - u_w$) was reduced to zero by the relief of these pore water tensions. A comprehensive investigation of the compressibility of an unsaturated silty clay was conducted by Yoshimi and Osterberg (20). They pointed out that virtually no pore water was extruded from their samples in ranges of saturation from 70% to 97%.

One of the major factors outlined in literature on compression of unsaturated soils is the permeability of air and of water in these three-phase systems. Carman (19) stated that the presence of air in a capillary tube would reduce the permeability of the water by decreasing the cross-sectional area. In their work on compacted clay, Mitchell, Hooper, and Campanella (23) note that as the water content increased dry of optimum, the water permeability slightly increased. Around optimum water content a maximum was reached; wet of optimum it decreased by several orders of magnitude. A principal area of discussion has been on the degree on interconnection of air voids in the vicinity of optimum water content. If the air passages are interconnected, the air permeability will of necessity be higher than if these passages were separated, or occluded. Langfelder, Chen, and Justice (24) found that for the great majority of soils tested, the air permeability changed very little at various moisture contents dry of optimum. As optimum was approached, permeability dropped several orders of magnitude for a single percent moisture increase. At optimum and beyond, the air perme-

ability was essentially zero. Olson (22), in presenting his effective stress theory of compaction, proposed that the maximum dry density occurred when the air permeability went to zero. Matyas (25) offered evidence that the air voids are connected at optimum water content and remain so until the pressure deficiency goes to zero. However, he states that the air permeability may decrease by as much as a factor of 10^5 over the interconnected range. Samples of compacted clay permeable to air under a small pressure gradient at degrees of saturation in excess of 90% have been reported (20).

The interconnection of air voids and the lack of liquid flow in an unsaturated sample are important because these factors point out the lack of a hydrodynamic time lag in the rate of compression of a soil. Yoshimi and Osterberg (20) investigated this point in detail. One-dimensional compression tests were conducted with different sample heights in which conditions of double, single, and no drainage were allowed. Virtually no difference was found provided constant load-increment ratios were used. Variation of $(\Delta P/P_o)$ however, led to results similar to those mentioned previously for saturated soils, regardless of drainage condition or thickness. From these results they reached the following conclusion: "If the pore water movement is negligible the time dependency of the compression is governed by the rheological characteristics of the soil structure. Thus, the time rate of compressive strain is independent of drainage condition or thickness, but is dependent on the stress increment ratio."

C. Shrinkage

The mechanism of shrinkage of a clay soil occurring with a loss in moisture content has been outlined in a number of works on basic soil mechanics (5),(26). This is typically illustrated by a saturated clay-water system in which the individual particles, with their inherent adsorbed water films, are separated in a medium of free water. The boundary of this system is made up of exposed particle surfaces and voids having concave menisci, reflecting the existence of surface tension forces at these air-water interfaces. These forces set up a pressure differential within the system, causing a migration of water from the interior to the surface to establish equilibrium. The pressure imbalance is maintained by evaporation of water from the surface so that a continuous loss of water occurs. As the water is removed, the particles are drawn closer together, effecting a volume decrease in the system. Any resistance of the particles to further approach is met by a tendency of the surface menisci to retreat into the sample, where decreasing radius of the pores would increase the magnitude of surface tension forces. As long as these forces are greater than the resistance to further approach, the sample will continue to decrease in volume. The magnitude of volume change will be equal to the amount of water lost, as illustrated by the line segment AB in Figure 5.

As the shrinkage process continues, a point is reached such that the combination of repulsive forces between particles and any existing random structural interference are great enough to prevent closer approach and the air-water interface will move into the interior of the

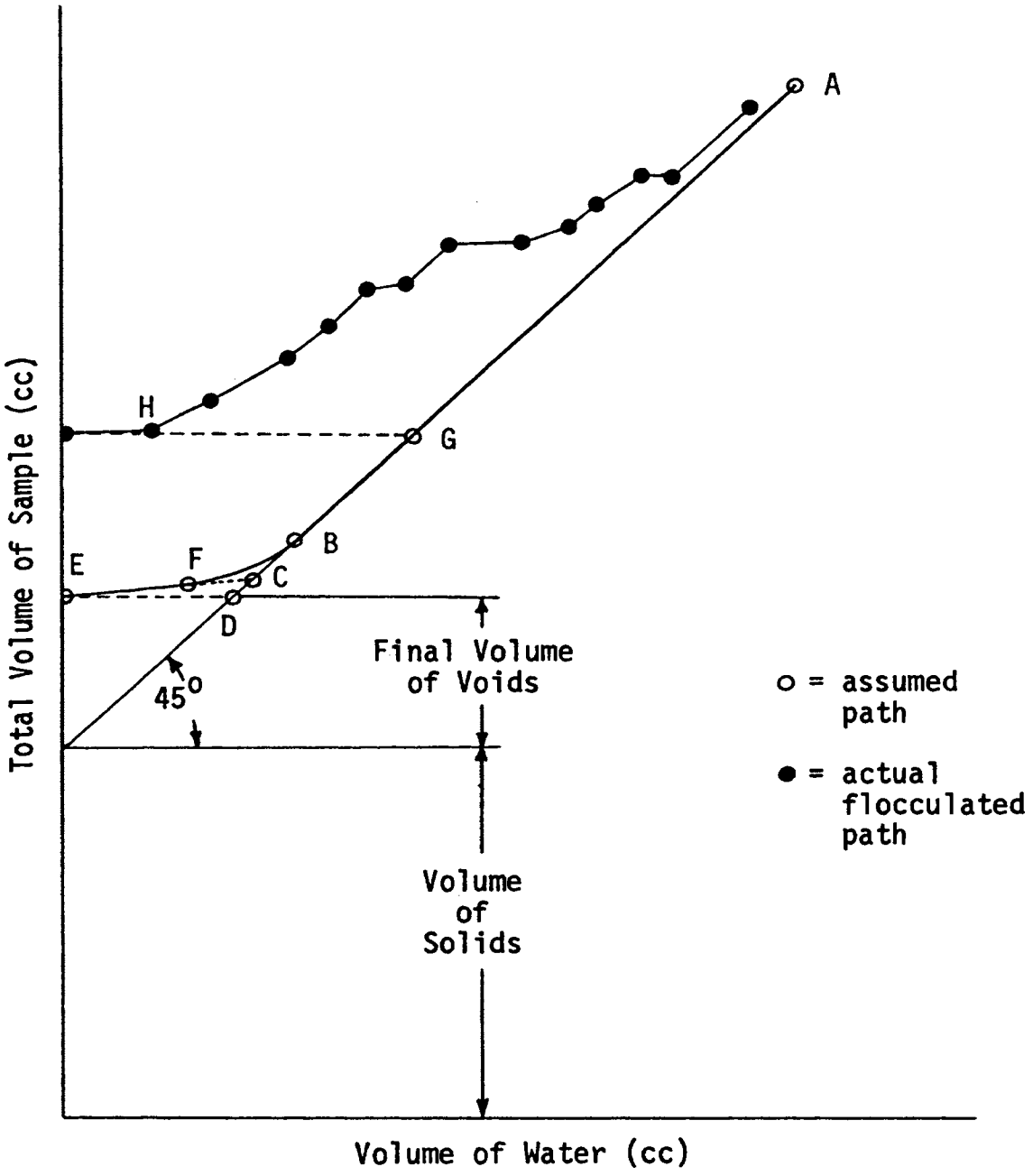

FIGURE 5. ASSUMED AND ACTUAL FLOCCULATED VOLUMETRIC SHRINKAGE CURVE FOR A CLAY SOIL

system. The initiation of this retreat is shown as point B. The sample is now unsaturated and the linear relation no longer exists. The moisture content of the soil at which this proportionality no longer holds true is taken to be the shrinkage limit.

The shrinkage limit is usually defined in some manner similar to the statement of Wu (26): The shrinkage limit is "---the water content at which the soil no longer shrinks in volume on further drying." The equation for calculating the shrinkage limit according to A. S. T. M. Standard Specifications (27) is given as:

$$SL = w - \frac{(V - V_o)}{W_o} \times 100$$

where

SL = shrinkage limit in percent

w = initial water content

V = initial volume of soil mass in cubic centimeters

V_o = volume of oven-dry soil mass in cubic centimeters

W_o = weight of oven-dry soil in grams

The normal procedure for determining this point requires only the initial moisture content, the volume of solids, and the final volume of the sample. This method assumes that the mechanism described above is valid and that no volume change takes place after the sample becomes unsaturated. The shrinkage limit of the soil in Figure 5 would be at point D according to this analysis. Laboratory determinations of the shrinkage path generally show a small amount of residual shrinkage taking place after the normal shrinkage phase is finished. However this discrepancy

involves only a small portion of the total volume loss of a sample which is at a high initial moisture content. The shrinkage limit obtained from the volume-moisture curves will be defined in this paper by point C, the intersection of lines EF and AB, where AB is the plot of the actual shrinkage path of the soil, rather than that figured from the final volume of voids.

Changes in the structure of a soil are accompanied by changes in the shrinkage characteristics. Yong and Warkentin state that "particle interaction leads to unsaturation at a higher water content for random edge-to-face arrangement of particles than for the more parallel arrangement" (5). In addition, DeSantis (28) has shown that clays with a flocculated structure exhibit deviations from the normal shrinkage path at moisture contents well above the shrinkage limit. This is illustrated by the dotted curve in Figure 5. The initial edge-to-face arrangement leads to particle interaction at relatively high moisture contents. Continued evaporation at the surface of the sample causes an increase in the surface tension forces until the strength of the structural arrangement is overcome. The particles then move to closer positions, with an accompanying volume decrease. Repetitions of this interference lead to the irregular appearance of the shrinkage curve. As the particles become more intimately associated with each breakdown in structure, the forces of interattraction become intensified, and a higher surface tension force is necessary to disrupt the structure. When the attractive forces become great enough to resist the maximum tensile forces that can be mobilized through recession of the menisci into the body of the sample, no further volume change occurs and the

sample becomes unsaturated. This cessation of volume change is indicated by point H of the flocculated shrinkage curve.

The shrinkage limit from the standard method of determination would be found using the volume of water indicated by point G, yet the actual shrinkage continues until the moisture content existing at point H is reached. From the above discussion it is seen that while the standard method of determination would indicate that the shrinkage limit of a flocculated soil is greater than that of a soil having an oriented particle arrangement, in actuality the termination of shrinkage could occur at a much lower moisture content.

Other factors influencing the shrinkage characteristics of a soil are the amount and type of clay-size particles (5), and rate of drying (28). The presence of sand and silt-size particles would reduce the total shrinkage of a sample because their bulk and low surface-to-mass ratio would decrease the volume of void space and thus the amount of water in the sample. In addition, the presence of these non-colloidal particles would mask the effects of structure on the shrinkage path. The discussion of the effects of structure on shrinkage given previously was based on the presence of plate-shaped clay particles. Clay minerals characterized by non-planar configurations would not be expected to exhibit structural effects to this degree. The rate of drying controls the rate at which water will evaporate from the surface of a soil. A high drying rate will set up a large moisture gradient between the surface and the interior of the sample. The resulting differences in the moisture content within the sample will cause distortion and cracking,

making accurate measurements of the volume more difficult. In addition, the shrinkage path is plotted using the average water content of the whole sample at the time each volumetric measurement is made. Large variations of the amount of water in different portions of the sample might cause some apparent deviation from the actual moisture-volume relation.

In essence, the shrinkage properties of a clay soil reflect the basic structure of the particle elements making up the soil. This structure in turn, is determined by the nature of the intermolecular and interparticle forces existing between these elements. Particle size and size variation, mineral composition, and drying rate have an appreciable affect on the shrinkage limit and the rate of shrinkage with respect to moisture loss. Structural interference has been seen to cause deviations from the normal shrinkage curve which cannot be detected in the standard shrinkage limit determination. This factor could throw light on the lack of correlation which has been noted (29) between the shrinkage limit of a soil and certain basic properties such as its swelling pressure and capacity for volume change.

III. MATERIAL

Two Missouri soils having different degrees of plasticity were utilized in this investigation. The highly plastic sample was obtained from a bluff near a road cut in Green County, in the N.W. quarter of the N.W. quarter of Section 22, Township 28N, Range 8W. The sample was taken five feet below the A horizon. In this paper, the soil will be referred to as the Springfield soil. The overlying surface material is described as Clarksville Gravelly Loam, which has a high chert content due to the erosion of fine material.

This underlying stiff, fractured clay is typical of the residuum found throughout the Ozark regions of Southern Missouri in association with limestone formations. The soil in this particular area has a higher degree of secondary structure than that found in the other regions (30). Many engineering problems are encountered in this soil because of its unusual characteristics. When used as a fill material it has a low maximum density and a high optimum water content. When standing in natural or compacted slopes it exhibits a high degree of creep. Earth dams located on this material frequently are ineffective because of its high permeability.

The Springfield soil in-situ is predominantly of a deep rusty red color, sometimes erratically interspersed with layers or lenses of an off-white material having similar characteristics. The soil exhibits a high degree of secondary structure. It exists in the form of fractured cubic-to-angular pieces ranging in size from coarse sand to fine

gravel. The surface of these aggregations appear slicken-sided; in some cases they are coated with a thin film of darker material. Undisturbed samples were difficult to obtain because of the stiffness of the clay and its tendency to fragment along the fracture planes. Extreme care had to be exercised when trimming a sample into a consolidation ring. Even then, visible disturbance of the macrostructure was apparent.

The physical properties of the Springfield sample are included in Table I. In all cases Atterberg limits were run on samples of soil which were thoroughly mixed in a soil dispersion cup to moisture contents well above the liquid limit and then allowed to air dry to the necessary consistency. One set of limits was performed on a sample which had never been dried below its natural moisture content. Another set was run on air-dry soil for comparison with the limits of the air-dried treated soils. A pronounced difference was noted in the liquid limits and to a lesser degree in the plastic limits. A line connecting both sets plotted slightly above and parallel to the "A" line of the plasticity chart of Figure 6. The results of the grain-size analysis (Figure 7) shows that the bulk of the sample was smaller than two microns. A standard Proctor compaction test following A. S. T. M. specification D 1557-66, Method A, was performed, yielding a maximum density of 78.9 p.c.f. at an optimum water content of 38.2% (see Figure 8). The soil was allowed to stand overnight after the addition of the mixing water, and then compacted. Immersion of an air dry sample in water was seen to initiate a vigorous slaking action; however, after this action was completed the soil was in the form of

Soil	Springfield				Lebanon		
State	$Ca(OH)_2$	Natural	$Na(PO_3)_6$	Ntl. Moist. Content	$Ca(OH)_2$	Natural	$Na(PO_3)_6$
Liquid Limit, %	89.3	105.6	72.0	144.8	35.5	33.1	30.1
Plastic Limit, %	49.0	34.0	31.9	43.7	22.7	17.5	14.2
Plastic Index, %	40.3	71.6	40.1	101.1	12.8	15.6	15.9
Shrinkage Limit, %	23.0	18.5	15.0		20.0	14.9	12.3
Specific Gravity		2.70				2.675	
Unified Classification	MH	CH	CH	CH	CL	CL	CL
% <2 microns		81-92				21	
Activity		0.78-0.88		1.11-1.26		0.83	
Max. Density, p.c.f.		78.9				113.7	
Opt. Moist., %		38.2				15.9	

TABLE I. PHYSICAL PROPERTIES OF THE TEST SOILS

granules which would not reduce to clay size, even after prolonged submergence.

On the basis of preliminary X-ray diffraction patterns and the resemblance to Missouri cave clays, the soil was initially identified as a poorly crystalline illite-chlorite. After repeated shrinkage tests failed to show the expected structural effect, further X-ray patterns and a differential thermal analysis (D.T.A.) were made in an effort to find the cause of these failures. A comparison of patterns from air dried and glycolated slides showed a very slight shift, with an intensified peak at 7.43 Å (see Figure 9). A slide was made from that portion of the sample smaller than two microns, by allowing the coarser particles to sediment prior to forming the slide (31). The resulting diffraction pattern showed little if any indication of clay minerals. Thus the clay probably exists in the form of aggregations as described below by Terzaghi. Powder slides were run for extended periods to study lower order reflections (Figure 10). A chemically leached powder sample was tested in which the absence of certain peaks indicated the presence of a certain amount of hematite (αFe_2O_3) in the unaltered sample. The results of these studies indicated a kaolin-illite mixture. However, the D.T.A. curve shown in Figure 11 gave an exothermic peak in the vicinity of 480° C, some 80° below the usual kaolin peak. A review of published findings showed this to be indicative of halloysite, a clay mineral of the kaolin group characterized by a tubular shape. This mineral exists in hydrated and unhydrated states, with an irreversible transition from the former to the latter at moisture contents less than 10% (32). The 7.4 Å

reflection of the glycolated diffraction pattern could be attributed to a statistical distribution of hydrated and unhydrated halloysite (33). The powder sample lacked certain reflections normally found in kaolinites. These reflections are either depressed or absent in diffraction patterns for halloysites (34). Illitic peaks are noted in the 10 Å range and are substantiated by second-order reflections at 5 Å. Lack of the large endothermic peak between 900°-1000° C usually found for kaolins could be explained by the presence of the illite. Depression of this peak in kaolinite-illite mixtures is illustrated by Grim (33).

Further evidence of the presence of halloysite in the Springfield soil is noted in its engineering properties. Lambe and Martin (32) stated that "halloysite, hydrated or unhydrated, has: low maximum compacted density, high optimum water content, high permeability, and high frost susceptibility." They further pointed out that a flat compaction curve is apparently characteristic of halloysite. In an investigation of two halloysitic Kenya clays, Newhill (35) noted a large variation in the liquid limits of air dry and natural-moisture-content samples. Terzaghi (36) described the Sasumua soil, a partially hydrated halloysite, as having a clay fraction which "occurs in the form of clusters of hard porous grains with rough surfaces, each of which consists of a great number of firmly interconnected mineral particles."

The Springfield sample could not be identified beyond a doubt as containing some form of halloysite, primarily because of the lack of

resolution in the X-ray diffraction patterns. However, the physical and mineralogical properties do give strong indications that this is the case. If this soil does indeed contain halloysite, it would substantiate the hypothesis that this soil is of lateritic origin (37).

For comparative purposes, a second soil of low plasticity was tested. This soil was obtained locally from the "C" horizon of the Lebanon association, and is classified as Lebanon Silt Loam. Its physical properties are given in Table I. Classification and compaction tests were performed in the same manner as the Springfield soil. X-ray diffraction showed the presence of a large amount of non-clay minerals, primarily quartz. Illitic and kaolinitic tendencies were noted. The Lebanon soil had a liquid limit of 33.1 and a plastic index of 15.6, yielding a CL classification. The standard Proctor maximum density was 113.7 p.c.f. at an optimum moisture content of 15.9.

The structures of the test soils were modified to what was considered flocculated or dispersed conditions by the respective addition of calcium hydroxide ($Ca(OH)_2$) or sodium hexametaphosphate ($Na(PO_3)_6$). While complete dispersion may not have been attained a greater degree of particle orientation was gained in the sodium-treated samples in comparison with the unaltered and lime-treated soils. The optimum ($Ca(OH)_2$), or lime, content was determined by visually comparing the amount of sedimentation which took place in dilute clay-water mixtures containing various amounts of lime. It was considered desirable to add only that amount which would effectively flocculate the soil, to ensure that little excess would be available for cementation (38).

Three percent lime by dry weight of soil was found to be entirely satisfactory for both soils. Previous works (28)(39) have indicated that three percent ($Na(PO_3)_6$) would provide maximum dispersion, and that further concentrations would have negligible effect.

IV. EQUIPMENT AND PROCEDURE

A. Shrinkage

For this investigation a shrinkage mold was designed incorporating collapsible sides, in order to attain a more uniform moisture distribution in the sample after it had taken an initial "set". The mold was basically a 2" x 3" x 5" box made up of five 1/4" stainless steel plates, held in place by C-clamps. Tongue-and-groove joints served to align the sections and prevent leakage. The inside surfaces of the mold were buffed smooth to lessen the adhesion of the soil to the sides. The relatively large size of the mold was dictated by the desire to increase the accuracy of the measurements made on the soil sample. Preliminary shrinkage tests indicated that it would be necessary to lubricate the inside surfaces of the mold to prevent adherence of the soil. As testing proceded, high-vacuum silicone grease, an aerosol "Teflon" spray, and petroleum jelly were utilized with limited success.

The soil for shrinkage tests was obtained from bag samples which were allowed to air-dry. It was then ground in a Lancaster mixer for a minimum of 15 minutes, after which it was sieved. Only that portion passing the #40 sieve was utilized in the test. The soil was then mixed with water in a soil dispersion cup, with a minimum mixing time of 15 minutes. Enough water was added to form a fairly viscous slurry which could be easily deaired. During this time, pre-measured amounts of the desired additive, if needed, were mixed in with the soil. Upon completion of mixing, the slurry was set aside for at least 24 hours to

assure uniform hydration. The sample was then reagitated in the dispersion cup. The hydrated soil was de-aired using a bell jar connected to an aspirator-type vacuum system. This operation was continued until no air bubbles were observed at the surface of the sample for a period of five minutes. The slurry was then placed in the shrinkage mold in three layers, tapping the mold against a hard surface when pouring each layer. The top of the sample was struck off with a straight edge. The slurry in the mold was de-aired as before, after which the top of the sample was again made plane. The sample was weighed, then exposed to air at room temperature until it reached a gelation point or semi-rigidity sufficient to withstand higher temperatures (24-48 hours). Then it was placed in a drying oven heated to 105^{o} C. At intervals of 1-2 hours it was removed, weighed to the nearest gram, measured with a vernier caliper to the nearest millimeter, reweighed, and returned to the oven. After the soil had attained sufficient consistency, the sides of the mold were removed to facilitate reduction of the moisture gradient. Upon reaching constant dimensions, the sample was left in the oven for 24 hours; then the final weight and volume were obtained. The sample was broken up, and the volume of portions of it were measured as a check using standard shrinkage limit equipment. Three standard shrinkage limit determinations were run in conjunction with each test for purposes of comparison. These were made using excess material from the shrinkage path determinations.

Successful tests were accomplished only on the natural and the flocculated Springfield samples. Cracking of the rest of the samples, caused by excessive moisture gradients and high moisture contents, made

volume determinations impossible. A second series of shrinkage tests was performed using circular glass dishes approximately 9.2 centimeters in diameter by 1.8 centimeters deep, yielding an initial sample volume of roughly 120 cubic centimeters. These were shallow enough that no appreciable moisture gradient was set up and de-airing could be accomplished at a lower moisture content, resulting in an absence of cracking. The test procedure was the same as that used for the larger samples.

B. Compression

Two series of one-dimensional compression tests were conducted for this study. The first group consisted of consolidation tests on undisturbed samples of the Springfield soil, SU-1 and SU-2, and on the Lebanon undisturbed sample, LU-1. The second set of tests was made on unsaturated samples which were compacted at standard Proctor effort in the vicinity of optimum moisture content. Structural variations were imparted to these soils through the addition of flocculating and dispersing agents. The natural, calcium-treated and sodium-treated Springfield samples are designated SCN, SCC, and SCS, respectively. The Lebanon samples are similarly identified as LCN, LCC, and LCS.

All tests were performed using fixed-ring Bishop cells 2.50 inches in diameter by 0.77 inches high. Loading was accomplished with a two-bank lever frame of 16 TSF capacity. The dispersed soils were loaded in a similar frame having a greater capacity. Time-dependent machine deflection determinations were made so that the continuing compression

of filter paper, porous stones, and loading head could be taken into account at each reading. Prior to each test, the inside surface of the ring was coated with a thin film of vacuum grease.

In order to maintain the compacted samples at a constant moisture content during the unsaturated portion of compression, it was necessary to prevent evaporation. To accomplish this, a thin sheet of clear polyethylene film was placed over the cell after it was assembled and secured with rubber bands. Holes cut in the sheet for the loading head and mounting brackets were made slightly smaller to ensure a snug fit.

Undisturbed samples were extruded from three-inch shelby tubes and immediately transferred to the moist room for trimming into the consolidation ring. A trimmed sample was weighed and placed in the consolidation cell. After assembly the cell was positioned on the loading frame, a 100 gram seating load was applied, and the deformation guage positioned. The sample was then flooded and allowed to stand for a number of hours to check for swelling tendencies. An initial load equivalent to 0.26 TSF was applied and time-deformation readings taken until secondary compression was established. Additional loads were applied until the approximate preconsolidation pressure was reached. The sample was unloaded to its initial pressure, and then recompressed to the maximum load, approximately 17 TSF. A load-increment ratio of one was used except when rebounding the sample. After dissipation of pore pressure from the final load, the sample was rebounded in stages, removed from the cell, and a final moisture content determination was made.

The same procedure was followed for the unsaturated soils after they were extruded from the compaction mold, except for the following steps. The samples were not flooded, but kept at a constant moisture content. Porous stones and filter paper discs were premoistened, and several drops of water were placed inside the cell away from the stone to ensure a humid atmosphere. A seating load of 200 grams was used and no intermediate rebound was performed. The sodium-treated samples were loaded to 20.8 TSF.

V. DISCUSSION

A. Shrinkage

The shrinkage tests conducted using the large collapsible molds were successfully completed for only the natural and the lime-treated Springfield samples. All attempts with the Lebanon soils met with failure. Cracks would develop in the top surface of a sample early in the test and grow progressively worse as shrinkage continued. Failure caused by these cracks was thought to stem from the high moisture gradients set up in the sample, with accompanying differential rates of shrinkage between the interior of the sample and its outer surfaces. To combat this, the sample was placed in a large dessicator and periodically exposed to the atmosphere for short periods. While this was successful in lowering the moisture gradient, cracks still developed in the sample. The cause of this cracking arose from the necessity of mixing the sample at a high moisture content, as explained below. The samples were agitated in the soil dispersion mixer as this was the most effective way to attain uniform hydration in a reasonable amount of time, especially for the Springfield soil. This procedure incorporated a large amount of air into the slurry, making deairing necessary. This could be effectively attained only when the samples had a consistency such that air bubbles could migrate easily to the surface. Complications arose after the sample had been deaired in the mold. As shrinkage away from the mold was initiated, a capillary meniscus was formed which tended to prevent further lateral movement at this interface. The slurry at its high water content was not strong

enough to resist this tendency, causing tension cracks to form away from the interface. These cracks widened and became more numerous as shrinkage continued. In the sodium-treated samples this effect was particularly noticeable. The top surface would "gel," forming a thin skin over the rest of the slurry, which remained liquid. At the same time tension cracks would form and widen. A second layer would then occur within this disruption and it too would crack. A terracing effect resulted as the sample dried. Attempts were made to prevent the formation of this meniscus by repeatedly separating the soil from the inside of the mold with a thin knife-edge, but this proved impractical. Several layers of moist gauze were placed on the top surface of the sample in an effort to prevent any cracks from widening, but with no success. Shrinkage curves plotted from the results of the two completed tests are shown in Figures 12 and 13.

The second series of tests was completed with relatively little trouble. As mentioned previously, the reduction in moisture gradient and the ability of these samples to be deaired at lower moisture contents held cracking to a minimum. The smaller size of the samples made volume determinations less accurate, but it is felt that they are still indicative of the true shrinkage paths of the samples. The pronounced step effect expected of the lime-treated samples could not be observed in this series of tests. Some tendency to depart from the normal shrinkage curve can be seen in the flocculated samples of Series II (Figures 15 and 18), but not to the extent observed by DeSantis (28). In addition, the final void ratio of the flocculated Springfield soil, while higher than the natural or dispersed (Table II), was not of the

magnitude that DeSantis encountered. His tests were performed on a highly plastic cave clay which was originally thought to be similar to the Springfield sample. However, little indication of halloysite could be detected in X-ray diffraction patterns of this material. This difference, coupled with the lack of structural response and the low void ratio, might indicate that the tubular halloysite particles of the Springfield clay are unable to form a flocculated structure having the resistance to breakdown shown by the plate-shaped cave clay. Lambe and Martin (32) pointed out the possibility that the structure of halloysite would differ from other particles.

The shrinkage limits obtained from the shrinkage curves of the different samples are shown in Table II, along with the results of standard A. S. T. M. determinations. Also included are the final void ratios for all tests. Examination of these values shows that, for a given soil and type of test, the shrinkage limit and final void ratio is indicative of the type of structure existing in the particular sample, as would be anticipated. These values for the natural and lime-treated Springfield samples do not show a great variation, particularly for the shrinkage path determinations. However, the plastic limit, a sensitive indicator of the effect of lime treatment on the structure of a clay (38), showed a 44% increase for the limed over the air-dry natural sample. The liquid limit and plastic index of both the lime-treated samples were considerably lower than that of the air-dry natural soil. While substantiating the attainment of flocculation, it does lend uncertainty to the degree of dispersion in the sodium-treated soil. The shrinkage limits and consequent final void ratios for this

Soil	Springfield Series I		Springfield Series II				Lebanon Series II			
Property	Shrinkage Limit	Final Void Ratio	Shrinkage Limit %		Final Void Ratio		Shrinkage Limit %		Final Void Ratio	
Calculated from:	Curve	Curve	Curve	Std.	Curve	Std.	Curve	Std.	Curve	Std.
Natural	30.4	0.61	32.1	18.5	0.79	0.63	14.5	14.9	0.40	0.42
$Ca(OH)_2$	33.7	0.76	32.5	23.0	0.81	0.65	16.0	20.0	0.45	0.59
$Na(PO_3)_6$		0.57	24.4	15.0	0.67	0.43	12.4	12.3	0.34	0.35

TABLE II. SHRINKAGE LIMIT AND FINAL VOID RATIO VALUES FROM SHRINKAGE CURVES AND FROM STANDARD SHRINKAGE TESTS

treatment did yield a significant decrease over the other samples which is best accounted for as a result of appreciable particle orientation. The Springfield shrinkage limits obtained from the shrinkage curves are 41-73% higher than those of the corresponding standard test. The Lebanon soil, however, shows a significant difference only for the lime-treated sample. A possible explanation for this behavior would be that the shrinkage limit of a halloysitic soil may depend upon test conditions such as the initial mass of the sample and the relative shape of the mold. It is felt that the absence of any appreciable departure from the normal shrinkage curve in the flocculated Springfield soil is attributable to the presence of the tubular halloysite clay. The low clay content of the Lebanon soil would account for the failure of these samples when tested in the large mold and for the lack of particle interference in the flocculated sample.

B. Compression

Dial reading-time curves for the compression tests were plotted on five cycle semi-logarithmic paper as shown in Figures 20 through 28. It was generally impossible to find the initial height of the unsaturated samples at each load increment by using normal graphic construction. Becuase of this the initial dial reading was used as D_0 in all cases to calculate void ratio-pressure relations. This value is given in the figures for each load. The final height of sample under any particular load was taken to be the point of intersection of the slope of secondary compression with that of primary compression. For those loads in which the straight-line portion of

secondary compression was reached before 0.1 minutes, the dial reading at that time was assumed to be D_{100}. Several of the dial reading-log time plots showed a normal consolidation portion but had no reduction in slope after sufficient time had elapsed for pore pressure dissipation. When this condition occurred, D_{100} was selected at a time comparable with those of adjacent curves.

The SU-1 sample was at a moisture content well below its plastic limit at the time of testing. The granular secondary structure was particularly distinct at this point. The time-compression characteristics, seen in Figure 20, show a large amount of initial compression occurring before the first reading could be taken. Only at the last load increment did an appreciable portion of primary compression continue to occur after 0.1 minutes. This behavior, similar to that of a granular material, indicates that the macrostructure of the soil governed the rate at which the soil was compressed. To check this result, a second undisturbed sample which had a higher water content and void ratio was tested. This sample, SU-2, was from a different location, but its X-ray diffraction pattern was essentially identical to the first sample except that a higher illite content was indicated (see Figure 10). Its liquid and plastic limits were slightly lower, but in the same range as the SU-1 sample, and it had a similar physical appearance. The same coarse macrostructure could be seen in this soil, but the granules were relatively soft at its higher moisture content. Dial reading-log time curves for SU-2 are shown in Figure 21. The first loads resulted in rather flat curves similar to SU-1 until the preconsolidation pressure was reached. After this, the curves

assumed the typical Terzaghi shape expected of a saturated clay. Thus it could be concluded that secondary structure has an affect on the rate of compression which varies with the natural moisture content of the soil.

The void ratio-log pressure curves for SU-1 and SU-2 are given in Figure 29. Values for the compression index (C_c) and the preconsolidation pressure (P_c) are listed on this Figure and in Table III. The slope of the final rebound curve for sample SU-2 is much higher than those for the SU-1 or compacted Springfield samples. No swelling pressure was indicated, however, when this sample was first placed on the loading frame.

Figure 22 shows the dial reading-log time curves for sample LU-1. These plots, typical of a soil having low plasticity, signify that pore pressures were largely dissipated within 5-15 minutes. The first four loads show a lack of reverse curvature in the primary stage. Until the applied pressure was four times as great as the preconsolidation pressure, the hydrodynamic effect did not appear to be the dominant influence on the rate of compression. The void ratio-pressure relation seen in Figure 30 shows that LU-1 gave a well-defined virgin compression curve.

The dial reading-log time curves for the compacted unsaturated samples are shown in Figures 23 through 28. Compacted in the vicinity of optimum moisture content, all of these samples except the SCC became saturated at some intermediate load. The initial moisture content was

used to establish the point at which saturation occurred. This point is denoted on the respective curves. The dependence of post-saturated compression upon the rate of expulsion of pore water is evident. Upon saturation, or at the preceding load, the rate of primary compression began to plot as a reverse curve. One exception was the flocculated Lebanon sample, where the water permeability after expulsion of air was high enough that this curvature could not be seen. Examination of the sets of curves for the natural, flocculated, and dispersed samples of the two soils points out the variations in rate of compression which took place as a result of structural changes. In the flocculated soils previous to saturation primary compression occurred before the initial dial reading was made, and the compression-log time data plotted a straight line. Primary compression did not take place quite so rapidly in the natural soils. Dial reading-log time graphs of the load increments, prior to saturation, show that some time was required for the establishment of straight-line secondary compression. The dispersed samples showed the greatest retardation of unsaturated primary compression. It was necessary to extend the duration of each load for several days in order to define the secondary compression rate. The shape of the time-compression curves before saturation approached that of the Type II curves discussed by Leonards and Girault (10). For these curves, the majority of dial readings in the secondary phase were taken at long time intervals. As a result, daily temperature fluctuations noticeably affected these portions of the plots. The SCS sample shoed a surprising lack of volume reduction over the first three load increments. This tendency was also noted in another test on the same sample which was halted before completion. The best

explanation would be that dispersion of the soil was accomplished such that the natural aggregations were broken up and the repulsive forces of the individual particles resisted appreciable compression at low pressures. There was no sharp break in any of the compression-time at the point where saturation was reached. Several factors acted to prevent such an occurance. The occlusion of air pores takes place gradually, the smaller pores becoming cut off first. In addition, the distribution of air is probably not uniform throughout the compacted samples. At a high degree of saturation, some areas of the sample are saturated while others are not. Thus, the compression-time curves would not show a distinct transition from immediate to permeability-dependent primary compression as the last of the air is dissolved or expelled from the sample.

Void ratio-log pressure curves for the compacted Springfield and Lebanon samples are given in Figures 31 and 32. Comparison of the initial and final moisture contents from Table III generally show that small moisture losses occurred during some stage of the compression test. Sample SCC, which remained unsaturated until the final portion of the last load, had no appreciable change in moisture content. This would indicate that negative pore water pressures prevent extrusion of water until the degree of saturation is nearly 100%. The increase in the final water content of the SCS sample may have been caused by the use of too much water when premoistening the porous stones. The void ratios of the compacted samples at an applied pressure of 16.0 TSF were obtained from these curves and listed in Table III. For this load, the void ratios of the flocculated soils were the highest, particularly the

Soil	Springfield					Lebanon			
Sample	SU-1	SU-2	SCN	SCC	SCS	LU-1	LCN	LCC	LCF
Initial Water Content, %	26.8	47.2	38.5	37.2	33.3	16.7	16.9	17.7	17.0
Final Water Content, %	24.9	46.1	37.4	37.2	34.3	17.2	14.4	15.8	15.0
Initial Void Ratio, e_i	0.819	1.344	1.088	1.095	1.018	0.679	0.532	0.498	0.515
Void Ratio @ 16.0 TSF	0.679	1.073	0.899	1.055	0.865	0.429	0.375	0.434	0.357
Applied Load at Saturation, TSF			4.2	17.2	10.4		4.2	4.2	1.3
Compression Index, C_c	0.156	0.260	0.221	0.070	0.173	0.152	0.111	0.066	0.117
Preconsolidation Pressure, TSF	4.2	2.2	3.8	8.1	2.4	1.0	1.2	3.4	~3.0
Slope Ratio, β	0.108	0.586	0.210	0.071	0.292	0.101	0.094	0.063	0.107

TABLE III. COMPRESSION CHARACTERISTICS OF THE TEST SOILS

Springfield sample. Although they were compacted at slightly lower moisture contents than the natural or flocculated samples, the dispersed soils attained the lowest void ratios at this pressure. Values of the compression index, the preconsolidation pressure, and the slope ratio (β) for all tests are found in Table III and a detailed discussion of these characteristics is given below.

Compression indices for the Springfield samples were rather low, considering the large amount of clay-size material making up this soil. Terzaghi (36) pointed out this characteristic in his discussion of halloysitic Sasumua soils. For both soils, the compression indices of the flocculated samples were smaller than those of the dispersed. This is not in accord with the compressive reactions proposed for these soils (1)(5). It is probable though, that the straight-line portions of the compression curves had not yet been attained at the maximum test load and the structure was not destroyed, in which case the true values would have been much higher. There was no significant difference between the natural and dispersed indices for either soil.

The preconsolidation pressures, found through use of the Casagrande construction method, seem to be indicative of the structural makeup of the compacted samples. The edge-to-face structure of the flocculated soils would cause these samples to resist compression on account of the bond strength of the interparticle contacts. At some point in the loading cycle, however, the effective applied pressure would be great enough to cause wholesale rupture of these bonds, accompanied by large compressions. This would show up as a distinct preconsolidation pressure.

In dispersed soils, increases in pressure serve to push the parallel particles closer together, until they reach an equilibrium point with the increasing repulsive forces. At higher void ratios and particle separations, the lower value of repulsive forces would allow these movements to be of greater magnitude than in the flocculated soils. Determination of a precise value of the preconsolidation pressure for LCS is difficult as a large amount of compression took place even at the lightest loads. Such a reaction to loading is not surprising, as little particle interference was present to inhibit the closer approach of particles.

Comparison of the slopes of compression and rebound for each test gives an indication of the extent to which the swelling potential of the different soil structures is realized. The slope ratio β is equal to the slope of the rebound portion of the void ratio-log pressure curve divided by the compression index. According to Yong and Warkentin (5), a value of β greater than 0.2 would suggest a moderately swelling soil. Sample SU-2 shows a value much in excess of this, yet it exhibited no swelling tendency prior to the initial load. The compacted Springfield samples had β values which were in accord with their different structures. Sample SCC had the lowest value, indicating that no swelling tendencies would be expected. The same held true for the flocculated Lebanon sample. The SCS soil had a higher slope ratio than the natural. Its oriented particle arrangement was more susceptible to the readsorption of excess water from within the sample as the load was removed. The low clay content of the Lebanon soil is reflected in the small β values obtained for these samples. None of these possess

any appreciable swell potential. The treated soils bounded the compacted natural sample, but the undisturbed had a value even greater than the dispersed sample.

Figure 33 is a plot of the time rate of secondary compression, R_s, versus log pressure. Calculated after Wahls (13), R_s is equal to the amount of secondary compression per log cycle. The dispersed soils, while having very erratic patterns, did give the highest values. The flocculated soils show little change in slope at lower pressures, but then increase more rapidly in the higher ranges. The natural soils, both compacted and undisturbed, generally have larger changes at low pressures, tending to level off as larger pressures are applied. Sample SU-1 has a curve which is concave upward, similar to the flocculated soils. These differences are a result of the varying resistance to compression offered by the different soil structures. The dispersed soils, with little compressional interference from particle contact, show the largest rates of secondary compression. The natural soils would have intermediate degrees of particle orientation, giving greater compressional resistance. Little increase in the rate of secondary compression occurs in the flocculated samples until the applied loads are great enough to cause significant movements at the interparticle contacts.

The change of rate of secondary compression in the compacted soils seems to be affected whenever these samples become saturated. A decrease in this change takes place either immediately before or after, or in conjunction with the load at which saturation occurs. It

is interesting to note that this also takes place in two of the three undisturbed, supposedly saturated samples, at that load wherein their initial moisture contents would indicate that they became saturated. These two are the SU-2 and LU-1 samples, at 1.04 and 4.16 TSF respectively. No indication is seen in the SU-1 sample, which reached this point at the 8.32 TSF load. This might make questionable the assumed saturation of undisturbed samples which have been flooded prior to a consolidation test.

Initial compression is that decrease in volume which occurs immediately after application of the applied load. Figure 34 gives that amount of compression which occurred before the 0.1 minute reading for the compacted samples. For both the Springfield and the Lebanon soils, the unaltered samples generally had larger initial deflections than did the treated. This would mean that greater degrees of structural resistance are produced in both dispersed and flocculated soils than in intermediate structures. The resistance to structural breakdown is evident in the lime-treated samples for both soils. Large immediate deflections are resisted until a pressure is reached high enough to overcome the stability of the particle arrangement.

For comparative purposes, a percent initial compression was calculated as defined below:

$$C_i = \frac{\Delta H_{0.1}}{\Delta H_{1000}} (100) \quad - - - - - - - - - - - - (3)$$

where

$\Delta H_{0.1}$ = change in height for 0.1 minutes

ΔH_{1000} = change in height for 1000 minutes

C_i = initial compression as a percentage of the compression at 1000 minutes

Figures 35 and 36 give the percent initial compression occurring with each load for the Springfield and Lebanon samples. The initial compression is seen to be somewhat dependent on the structure of the soil; however, it is not as indicative as had been expected. The flocculated samples had larger initial percent deflections than the dispersed, but did not seem to delineate limits between which the untreated samples would fall. The percentage initial deflection of the untreated samples reflect the point at which saturation occurred, as seen by the decreasing amount of immediate compression that took place after this point was reached. The treated samples did not behave so consistently. They increased, decreased, or remained at the same level, showing no particular pattern. Sample SU-2, at a higher void ratio and water content than SU-1, had much smaller initial compressions. Both of these samples, along with SCN, exhibited a large initial compression upon imposition of the first load. While it is possible that this could have been due to imperfections on the top and bottom surfaces, the seating loads should have negated this effect. A more plausible explanation would be that this first immediate compression was caused by an adjustment in the granular aggregations of clay particles comprising the macrostructure of these soils. The undisturbed Lebanon sample exhibited a large amount of percent initial compression throughout its cycle of loading. This action is consistent with that of a soil having such a low clay content.

The immediate compression of an unsaturated soil is dependent upon

the compression and expulsion of air, the dissolving of air in the pore liquid, and the elastic deformation of soil particles. Assuming a constant temperature, the use of Boyle's Law provides a check on the amount of air compression which could possibly take place with each load. This computation was made for each compacted sample using the following equation:

$$\Delta H_a = H_{a1} - H_{a2} = H_{a1} - \frac{P_{a1}(H_{a1})}{P_{a2}} \quad - - - - - (4)$$

where

H_{a1} = equilibrium height of air under load L_1

H_{a2} = height of air in the sample immediately after load increment $(L_2 - L_1)$ is applied

P_{a1} = equilibrium absolute air pressure under load L_1

P_{a2} = absolute air pressure immediately after load increment $(L_2 - L_1)$ is applied

ΔH_a = initial change in height of air with the application of load increment $(L_2 - L_1)$

The equilibrium height of air is found by subtracting the initial sample height at each load from the combined heights of the solids and the water found from the initial moisture content. The amount of air dissolved in the pore liquid was not taken into account as its small value at normal temperature had little effect on the overall accuracy of the calculations. This simple pressure-volume relationship was utilized with two different assumptions concerning the state of equilibrium of the air pressure prior to the addition of a load increment. In the first case, the air voids were assumed to be interconnected and open to the atmosphere, so that the air pressure prior to each load was

dissipated to that of atmospheric. For the second case, the air passages were taken to be interconnected but completely occluded, or closed to the atmosphere. This would cause the equilibrium air pressure to be equal to the applied pressure on the sample. These two cases are taken to define limiting conditions for the mode of existence of the pore air. In both instances the initial air pressure at the start of the tests was assumed to be atmospheric.

The calculated change in the height of air, ΔH_a, was substituted for $\Delta H_{0.1}$ in Equation (3) so that these results could be included in Figures 35 and 36. The samples SCN, LCN, and LCC reached their calculated points of saturation after they had compressed only a few dial divisions under their indicated load of saturation. The computed percent air compression at these loads was not included on the figures as it was very small and highly subject to any inaccuracies in the assumed initial height and moisture content of the samples. Generally the actual percent compression was much less than that computed for either the dissipated or occluded states until saturation was imminent. At this point the actual deflection approached or coincided with that value calculated for the occluded condition. These results infer that a structural retardation acted in all samples, regardless of their degree of orientation. This retardation was not particularly dependent upon the equilibrium air pressures within the sample until the degree of saturation was very high, at least above 95%. Here the amount of compression indicated that the air voids were becoming occluded.

From a structural standpoint the rate of compression in an unsatu-

rated soil depends upon the time required for the free and loosely bound water to be extruded from between approaching clay particles into adjacent air voids, and the rate at which the resulting air pressure can be dissipated. In an oriented three-phase soil system, the free water between the approaching clay platelets must travel some finite distance to an air void or the surface. This movement of water would require a certain amount of time. In an edge-to-face arrangement, it could be assumed that air voids exist between the particles. The rearrangement of these particles upon loading would involve movements at the contact points, with little or no mass movement of water. As compression of this flocculated structure continues with loading, the volume of air is reduced while the water content remains essentially constant. At the same time particle reorientation results in a more parallel arrangement. Consequently, the number and size of the air voids are reduced, and the free and loosely bound water between the particles must now move some distance, bringing hydrodynamic effects into play. The above process can be seen in a comparison of the shape of the natural and flocculated compression-time curves. As the degree of saturation increases, these plots generally show a retardation of initial compression caused by the increased distance which the pore fluid must move to reach an equilibrium point.

The plots of actual and calculated initial compression given in Figures 35 and 36 indicate that the initial amount of deformation is less than that which would occur because of the compression of air upon loading, regardless of structural configuration. Flocculated samples would have an initial delay caused by interference at the particle

contacts. The geometry of this arrangement would allow the elastic, frictional, and viscous characteristics of the particle-adsorbed water system to control the rate of compression. Because water movement is not a factor, a straight-line secondary compression-time relation is essentially established within a very short period. In the dispersed state, any compression or escape of air transfers the load to the oriented particle system so that further deformation is controlled by the movement of water from between these particles.

As saturation is approached the air voids are no longer open to the atmosphere, and the amount of initial compression is somewhat dependent upon the buildup and dissipation of pressures in the air-water interphase. This point might also be indicated by a disruption in the change in rate of secondary compression with increasing load.

Structural implications are apparent throughout the data obtained from the unsaturated compression tests. The resistance of the calcium-treated soil to compression can be seen in the relatively high void ratio at maximum loading, the low compression index, the high preconsolidation pressure, and the initially small rate of secondary compression. The slope ratio β of the flocculated Springfield sample is roughly one-third of the value for the untreated soil. The Lebanon samples give a two-thirds relation for this comparison. The attainment of significant degrees of dispersion is emphasized in the steeper slopes of secondary compression and the relatively small initial compressions of the sodium-treated sample.

The mechanism of compression of unsaturated clay soils is a complex function of many variables, as discussed in the review of literature given previously. In a saturated soil all of the applied pressure increment is assumed to be taken up by the pore water pressure increase. In the two-phase system at time zero, the pore water pressure is equal to the applied load increment and the effective pressure is zero. The time lapse before the effective pressure is equal to the applied pressure increment is controlled by the permeability and structural characteristics of the soil. In a three-phase system of soil, water, and gas no such simplifying assumption can be made about the individual pore fluid pressures. At the present there is no way to quantitavely evaluate the separate pressures in the liquid and gaseous phases or the rate of effective stress increase during the performance of a one-dimensional consolidation test. However, it is logical that the compressibility of the gaseous phase allows an immediate transfer of some portion of the applied load to the soil skeleton. Furthermore, if this transfer is not essentially complete within 0.1 minutes, a retardation of the development of straight-line secondary compression would occur, regardless of the structure of the soil. This type of delay would be evident in the dial-reading-log time curves as an initially steep slope which decreases to the straight-line secondary plot. Examiniation of the unsaturated compression-log time curves of Figures 25 and 26 does not show this decreasing curvature until the point of saturation is approached. No appreciable lag is noted in the development of secondary compression over a wide range of three-phase compression. It is seen then, that the process of compression in an unsaturated soil is essentially rheological, in that there is little if any depen-

dence on the rate of movement of the pore fluid to the boundary of the sample. Applied pressures are transferred immediately to the soil grains, and the rate and amount of compression is controlled by the microstructure of the soil. As the system moves toward saturation, the size and number of the air voids decrease, and these pores become cut off from the surface of the sample. Positive pore water pressures develop, reducing the soil suction ($u_a - u_w$) to zero, and Terzaghi's concept comes into play. That is, the rate of compression becomes a function of the movement of pore water to the extremities of the sample.

VI. CONCLUSIONS

This investigation involved a study of the shrinkage and compression characteristics of soils whose structures were modified to flocculated and dispersed configurations by the addition of electrolytes. Because of the inability to obtain significant shrinkage data, no general statements could be made concerning the interrelation of these two aspects of volume reduction. The following conclusions are drawn:

1. The open, edge-to-face arrangement of the flocculated soil particles produces higher shrinkage limits and final void ratios than do the more oriented structures.

2. The variation in the Springfield shrinkage limits and final void ratios for the different molds brings about the observation that the determination of shrinkage limits for non-plate-shaped particles is dependent upon initial volumetric or spatial conditions of the sample.

3. The effect of structural changes is evident in the compressive behavior of the compacted soils. During the unsaturated portion of the compression tests the dial reading-log time curves of flocculated soils attain straight-line secondary compression immediately, whereas the natural and dispersed samples take an increasingly larger amount of time to reach this condition. Dispersed soils are marked by high rates of secondary compression (R_s). Flocculated soils show consistently small rates until a load is applied of sufficient magnitude to

break down the structural stability. R_s-log pressure curves show an upward concavity caused by this breakdown of resistance to compression. For soils with intermediate degrees of orientation the structural resistance is overcome at lighter loads, giving R_s-log pressure plots which are concave downward. This compressive resistance is apparent in the e-log p curves for flocculated and dispersed samples. Flocculated soils yield higher preconsolidation pressures and final void ratios than do the more oriented particle arrangements.

4. The presence of air in the soil-pore fluid system may affect the slope of secondary compression. Most of the R_s-log pressure curves for compacted samples showed a decrease in the rate of change of the secondary compression when the point of saturation was approached.

5. A resistance to initial compression exists in unsaturated compacted soils, independent of the particle orientation. However, the cause of this resistance is different for flocculated and for dispersed structures. The retardation of compression in flocculated soils is a function of the geometry of interparticle structural arrangement as movements take place at edge-to-face contacts. In more oriented structures, this resistance is a result of the time required for free and loosely bound water to move some finite distance from between approaching clay particles.

6. A comparison of the plots of actual and calculated percent initial compression indicates that the air voids in a three-phase soil system remain open to the atmosphere until a high degree of saturation

(>95%) is reached.

7. Compression of compacted unsaturated soil having air voids which are not occluded results in an immediate transfer of the applied pressure to the existing soil structure. Further compression is governed entirely by the structural characteristics of the soil.

8. The Springfield soil is assumed to contain aggregations of the clay mineral halloysite, thus accounting for a number of its unusual properties.

VII. RECOMMENDATIONS

Further research is necessary to confirm and elaborate upon several factors brought to light in this investigation.

1. More refined testing equipment is necessary to pursue the study of the shrinkage characteristics of different soil structures.

2. In order to eliminate any existing structural effects unique to the particular sodium and calcium additives used in this investigation, further research should be undertaken using various compounds containing these elements.

3. Additional testing should be performed to investigate the occlusion of air voids as saturation is approached.

4. A comprehensive testing program involving the properties and mineralogy of the Springfield soils would aid in the understanding of its compacted and in-situ behavior.

BIBLIOGRAPHY

1. LAMBE, T.W. (1960) Compacted clay (a symposium). Transactions, ASCE, vol. 126, p. 681-756.

2. ROSENQUIST, I.T. (1959) Physico-chemical properties of soils: soil-water systems. Journal of the Soil Mechanics and Foundations Division, ASCE, vol. 85, no. SM2, p. 45.

3. VAN OLPHEN, H. (1963) An introduction to clay colloid chemistry. New York, Interscience Publishers (John Wiley & Sons) p. 30-50.

4. LAMBE, T.W. (1951) Soil testing for engineers. New York, John Wiley & Sons, p. 76.

5. YONG, R.N. and B.P. WARKENTIN (1966) Introduction to soil behavior. New York, Macmillan, p. 152-158, p. 155, p. 191-226.

6. CRAWFORD, C.B. (1964) Interpretation of the consolidation test. Journal of the Soil Mechanics and Foundations Division, ASCE, vol. 90, no. SM5, p. 87-102.

7. HAMILTON, J.J. and C.B. CRAWFORD (1959) Improved determination of preconsolidation pressure of a sensitive clay. ASTM, Spec. Tech. Pub. 274, p. 266.

8. LEONARDS, G.A. and A.G. ALTSHAEFFL (1964) Compressibility of clay. Journal of the Soil Mechanics and Foundations Division, ASCE, vol. 90, no. SM5, p. 133-155.

9. BARDEN, L. (1965) Consolidation of clay with non-linear viscosity. Geotechnique, vol. 15, no. 4, p. 345-362.

10. LEONARDS, G.A. and P. GIRAULT (1961) A study of the one-dimensional consolidation test. Proc. 5th Internatl. Conf. on Soil Mechanics and Foundation Engrg., vol. 1, Paris, p. 215.

11. BARDEN, L. (1965) Consolidation of compacted and unsaturated clays. Geotechnique, vol. 15, no. 3, p. 267-286.

12. LO, K.Y. (1961) Secondary compression of clays. Journal of the Soil Mechanics and Foundations Division, ASCE, vol. 87, no. SM4, p. 61-87.

13. WAHLS, H.E. (1962) Analysis of primary and secondary consolidation. Journal of the Soil Mechanics and Foundations Division, ASCE, vol. 88, no. SM6, p. 229. 207

14. BISHOP, A.W. (1960) Discussion, Conf. on pore pressure and suction in soils. London, Butterworths, p. 63.

15. JENNINGS, J.E.B. and J.B. BURLAND (1962) Limitations to the use of effective stresses in partly saturated soils. Geotechnique, vol. 12, no. 2, p. 125-144.

16. BISHOP, A.W. and G.E. BLIGHT (1963) Some aspects of stress in saturated and partly saturated soils. Geotechnique, vol. 13, no. 3, p. 177-197.

17. SEED, H.B., J.K. MITCHELL, and C.K. CHAN (1960) The strength of compacted cohesive soils. Proc. Res. Conf. on Shear Str. of Coh. Soil, ASCE, Boulder, Colo., p. 877-964.

18. BISHOP, A.W., I. ASPAN, G.E. BLIGHT, and I.B. DONALD (1960) Factors controlling the strength of partly saturated cohesive soils. Proc. Res. Conf. on Shear Str. of Coh. Soil, ASCE, Boulder, Colo., p. 504.

19. CARMAN, P.C. (1953) Properties of capillary-held liquids. Journal of Phys. Chem., vol. 57, p. 57-64.

20. YOSHIMI, Y. and J.O. OSTERBERG (1963) Compression of partially saturated cohesive soils. Journal of the Soil Mechanics and Foundations Division, ASCE, vol. 89, no. SM4, p. 1-24, p. 20.

21. HILF, J.W. (1956) An investigation of pore-water pressure in compacted cohesive soils. Bureau of Reclamation Tech. Memo. 654, p. 29-43.

22. OLSON, R.E. (1963) Effective stress theory of soil compaction. Journal of the Soil Mechanics and Foundations Division, ASCE, vol. 89, no. SM2, p. 40.

23. MITCHELL, J.K., D.R. HOOPER, and R.G. CAMPANELLA (1965) Permeability of compacted clay. Journal of the Soil Mechanics and Foundations Division, ASCE, vol. 91, no. SM4, p. 41-65.

24. LANGFELDER, L.J., C.F. CHEN, and J.F. JUSTICE (1968) Air permeability of compacted cohesive soils. Journal of the Soil Mechanics and Foundations Division, ASCE, vol. 94, no. SM4, p. 981-1001.

25. MATYAS, E.L. (1967) Air and water permeability of compacted soils. ASTM Spec. Tech. Pub. 417, p. 160.

26. WU, T.H. (1966) Soil mechanics. Boston, Allyn and Bacon, p. 16.

27. ASTM STANDARDS (1968) Shrinkage factors of soils. D 427-61, Part II, p. 231.

28. DeSANTIS, E. (1966) The shrinkage characteristics of plastic clay. M.S. thesis presented to the University of Missouri-Rolla, p. 28, p. 53.

29. SEED, H.B., R.J. WOODWARD, and R. LUNDGREN (1962) Prediction of swelling potential for compacted clays. Journal of the Soil Mechanics and Foundations Division, ASCE, vol. 88, no. SM3, p. 53-87.

30. LUTZEN, E.E. (1969) Personal communication.

31. SCHMIDT, N.O. (1968) Personal communication.

32. LAMBE, T.W. and R.T. MARTIN (1955) Composition and engineering properties of soil (III). H.R.B. Proceedings, vol. 34, p. 570, p. 566-582.

33. GRIM, R.E. (1953) Clay mineralogy. New York, McGraw-Hill, p. 53, p. 246.

34. BRINDLEY, G.W. (1961) Kaolinite and related minerals. The X-ray identification and crystal structure of clay minerals, edited by G. Brown, London, Mineralogical Society, p. 114.

35. NEWHILL, D. (1961) A laboratory investigation of two red clays from Kenya. Geotechnique, vol. 11, no. 4, p. 308.

36. TERZAGHI, K. (1958) Design and performance of Sesumua Dam. Proc. Institution of Civil Engineers, London, vol. 9, p. 376. (Reprinted in Harvard Soil Mechanics Series, no. 55, under the same title).

37. HEAGLER, J.B., Jr. (1969) Personal communication.

38. HILT, G.H. and D.T. DAVIDSON (1960) Lime fixation in clayey soils. H.R.B. Bull. 262, p. 20-32.

39. SUKOW, D.E. (1966) The effect of structure on the consolidation characteristics of a clay soil. M.S. thesis presented to the University of Missouri-Rolla, 64 p.

APPENDIX

FIGURES ILLUSTRATING CHARACTERISTICS AND PROPERTIES OF THE TEST SOILS

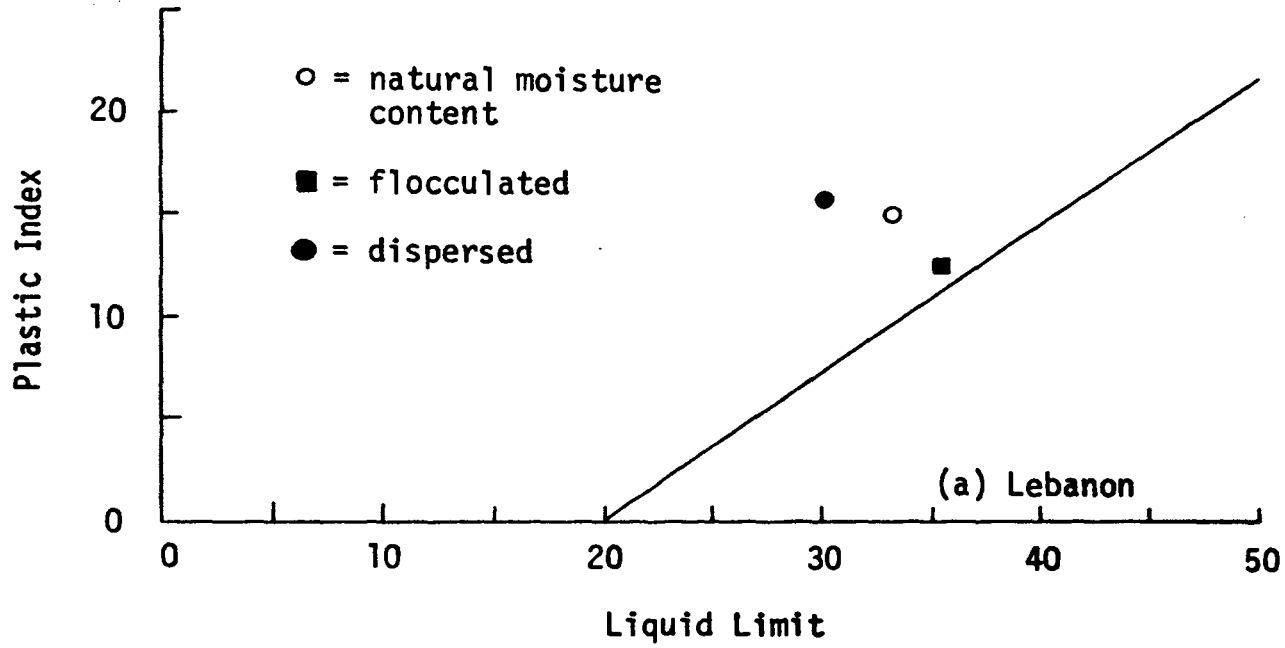

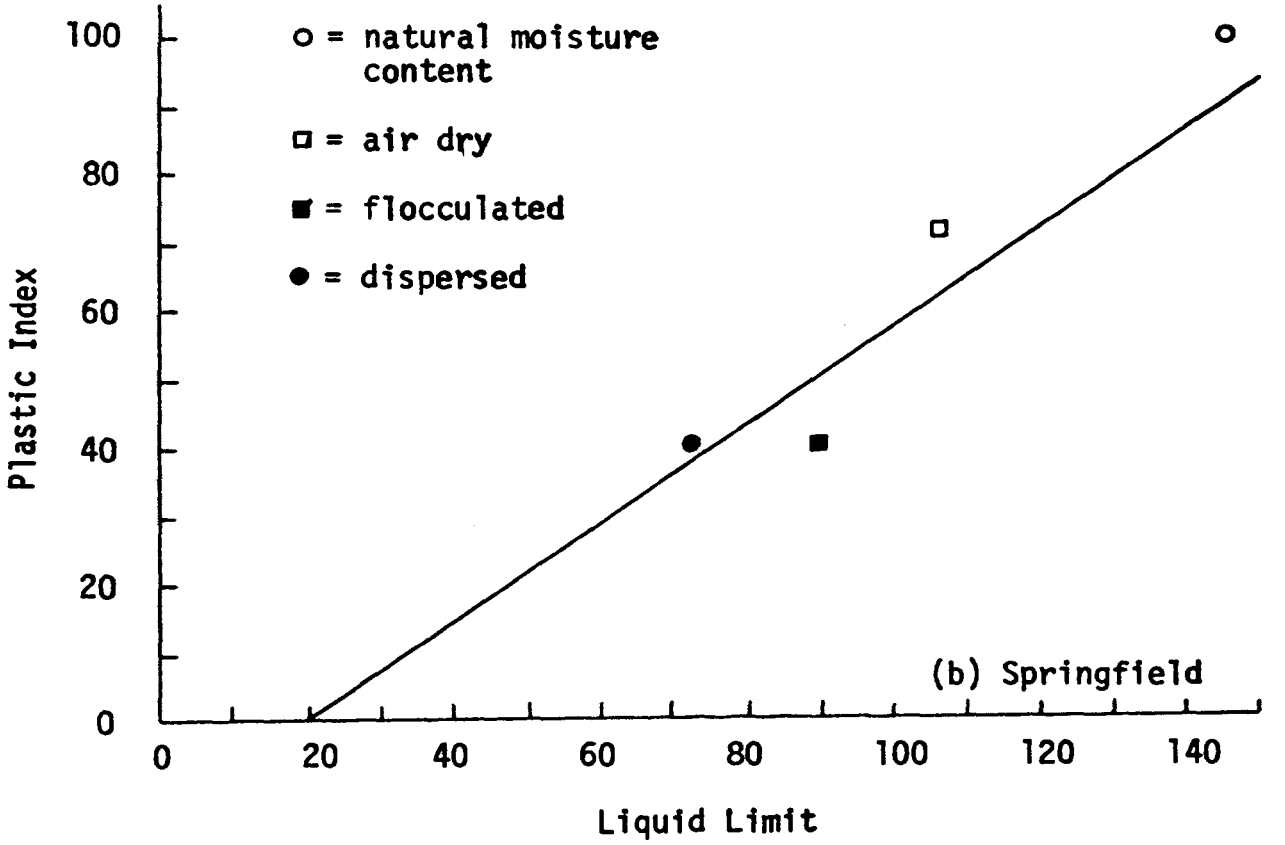

FIGURE 6. PLASTICITY CHART

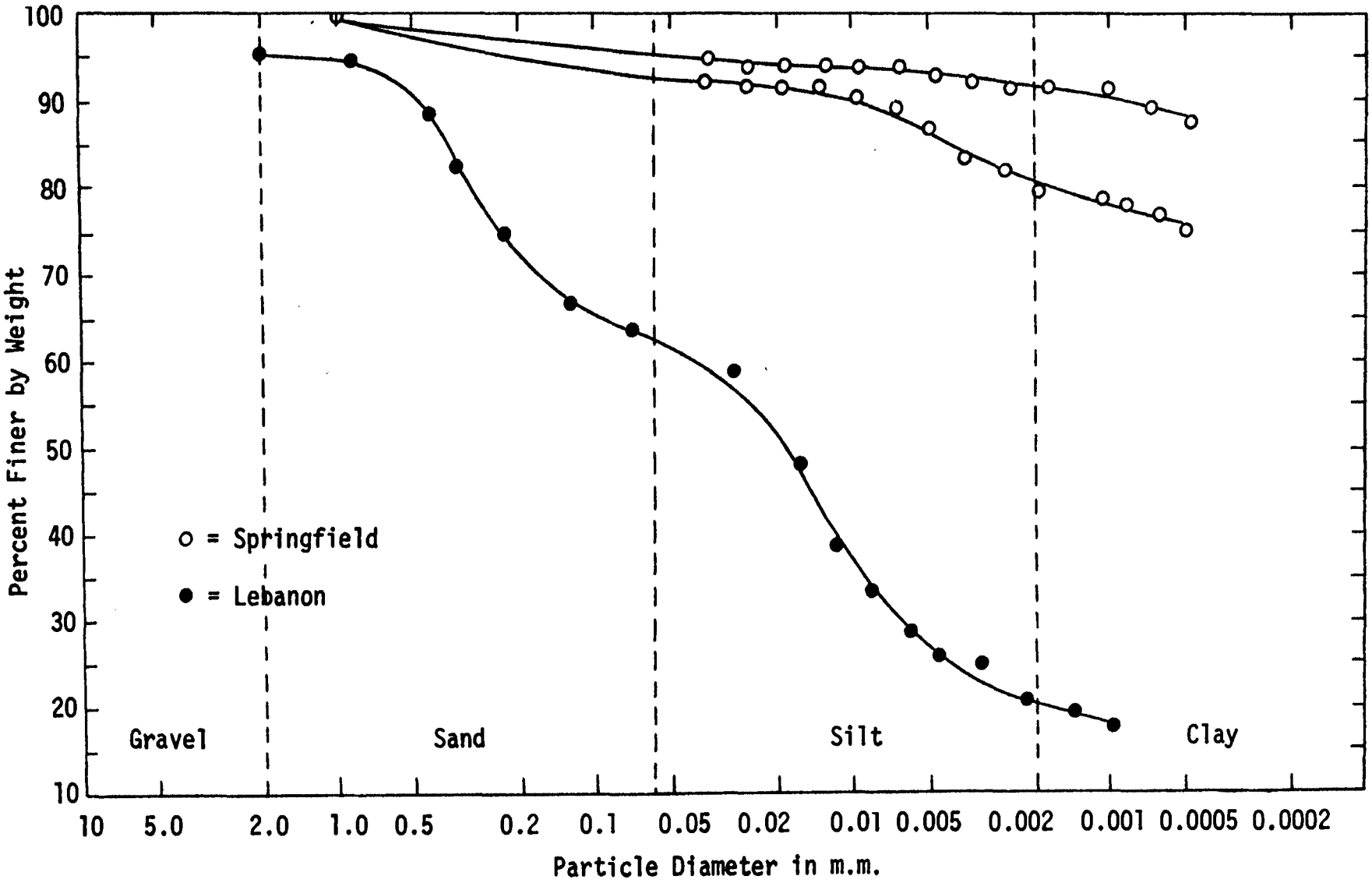

FIGURE 7. GRAIN SIZE ANALYSIS FOR SPRINGFIELD AND LEBANON SOILS

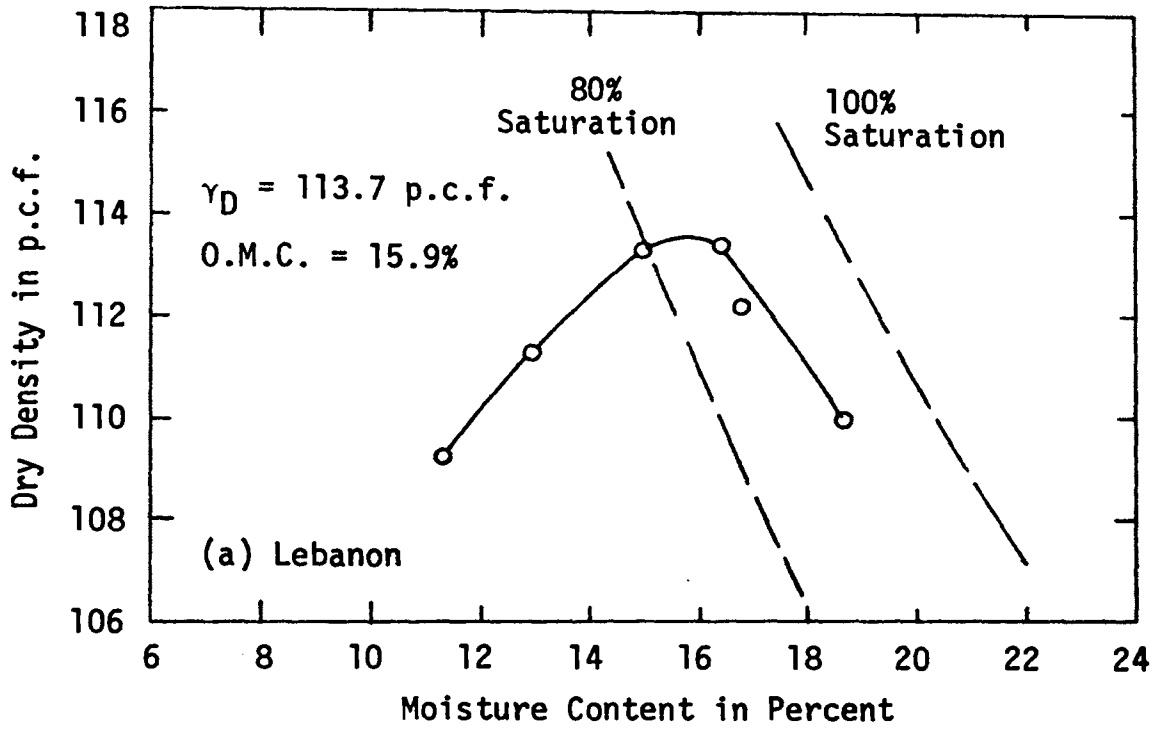

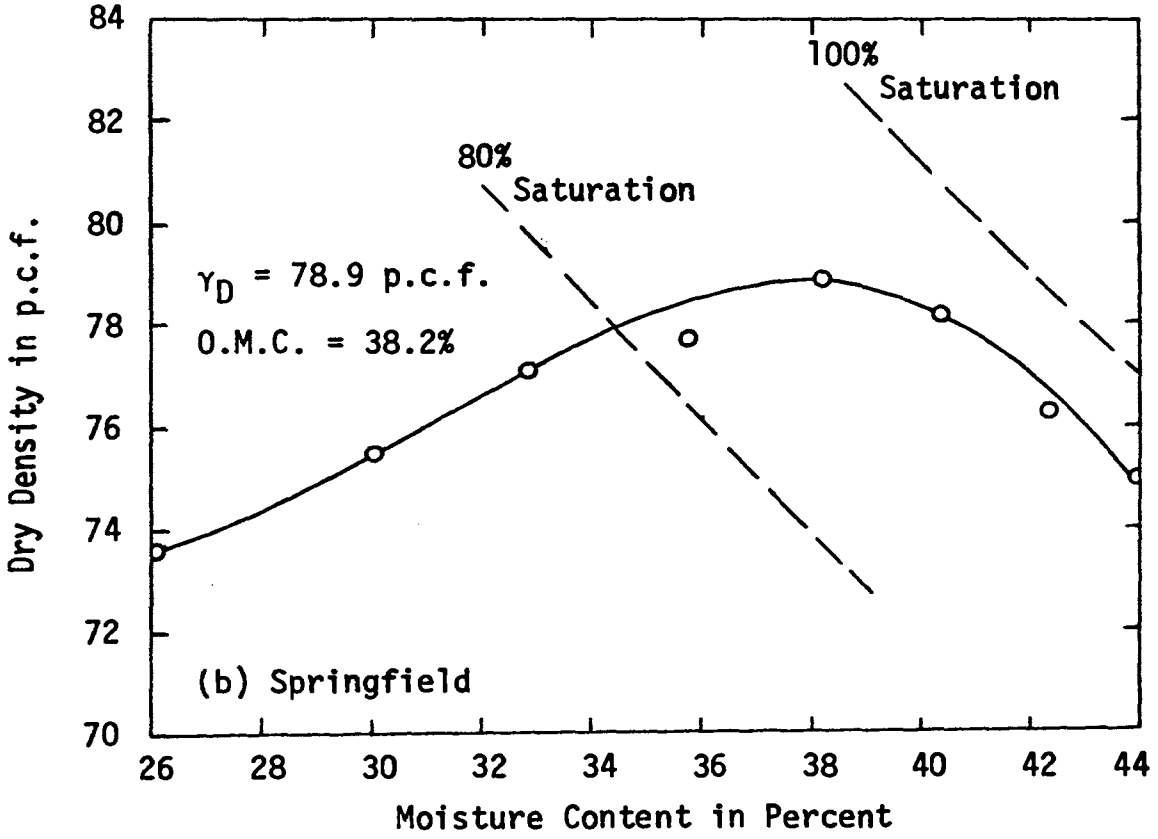

FIGURE 8. MOISTURE-DENSITY RELATIONS

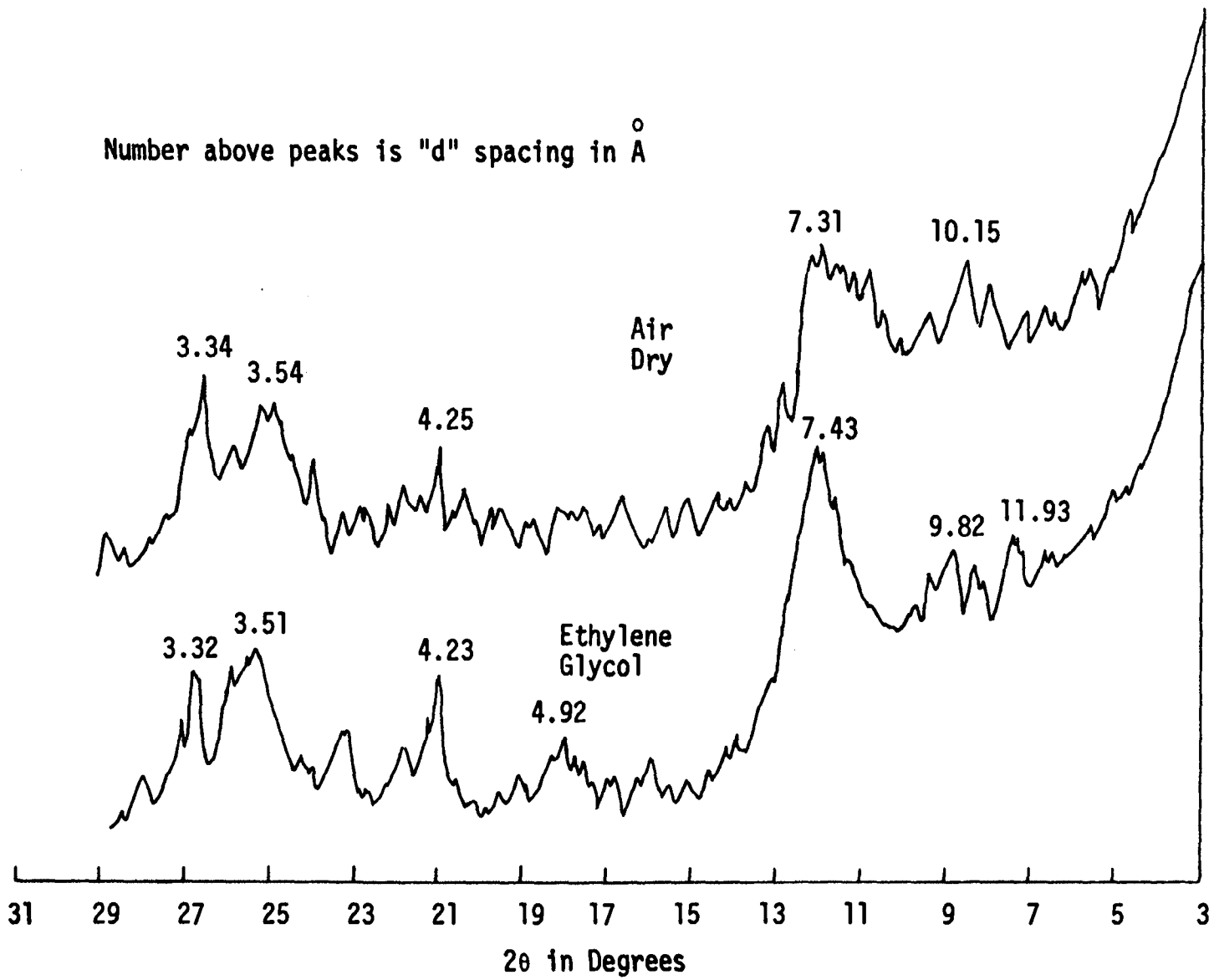

FIGURE 9. X-RAY DIFFRACTION PATTERNS FOR SPRINGFIELD SEDIMENTED SLIDES

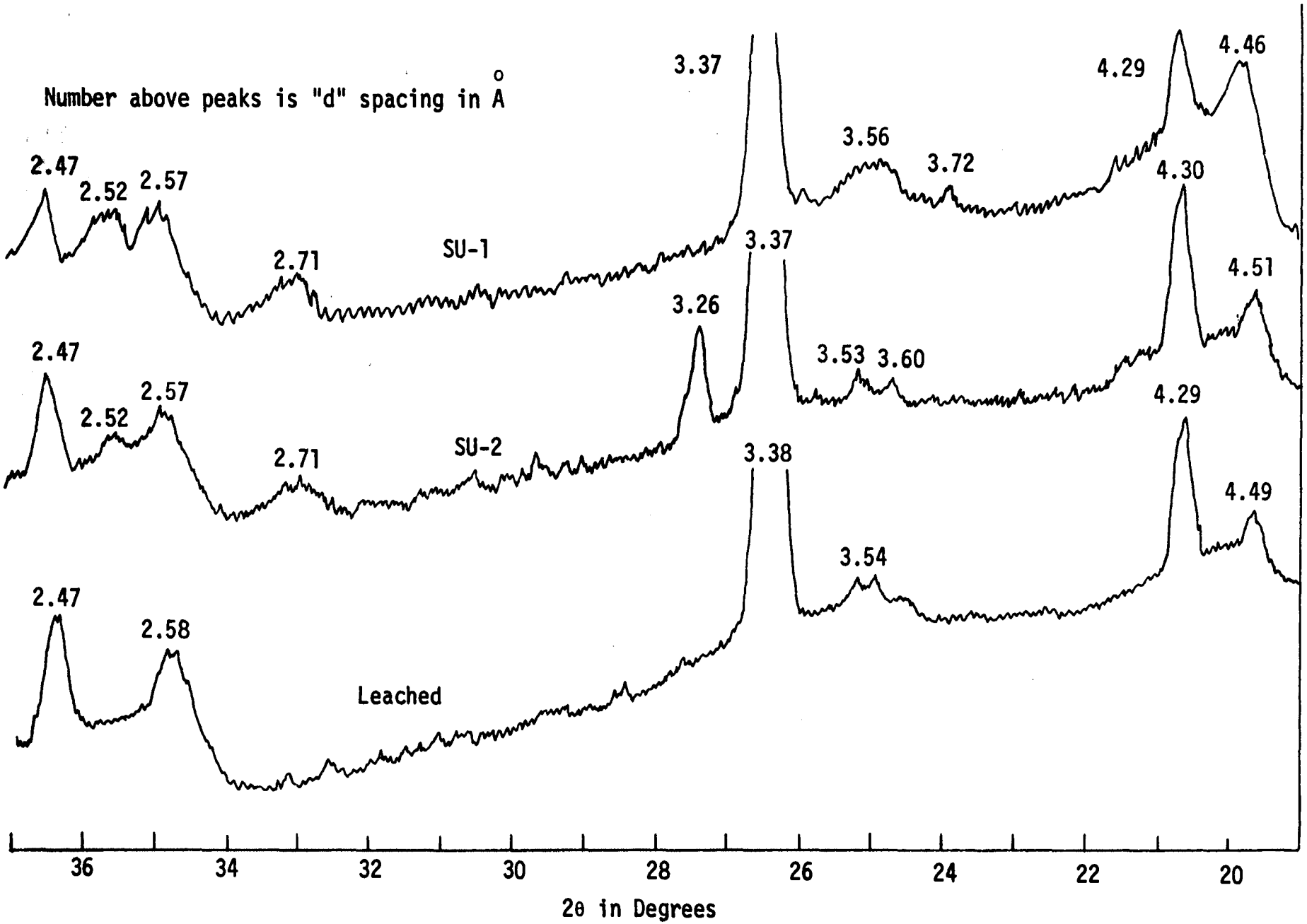

FIGURE 10-a. X-RAY DIFFRACTION PATTERNS FOR SPRINGFIELD POWDER SLIDES

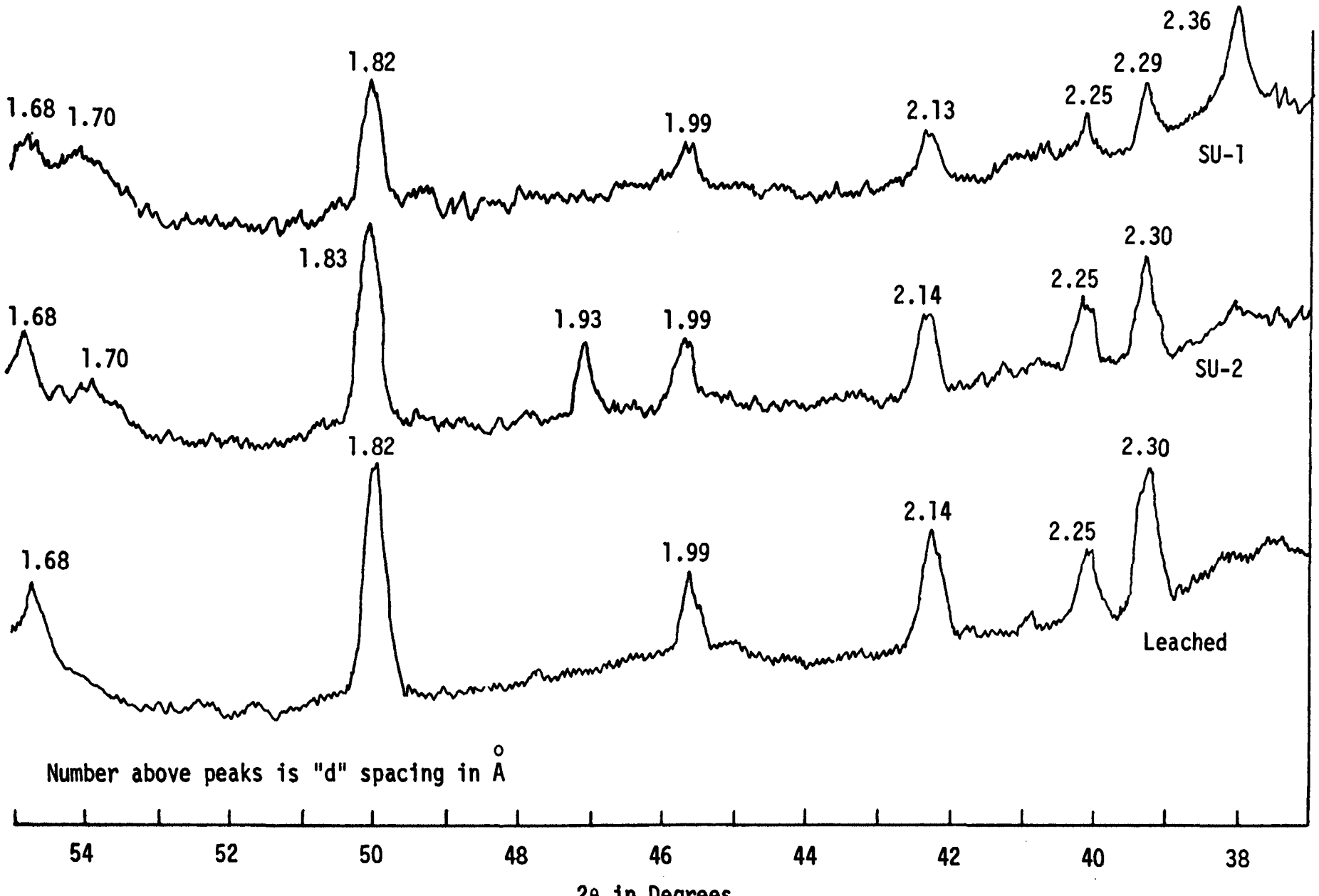

FIGURE 10-b. X-RAY DIFFRACTION PATTERNS FOR SPRINGFIELD POWDER SLIDES

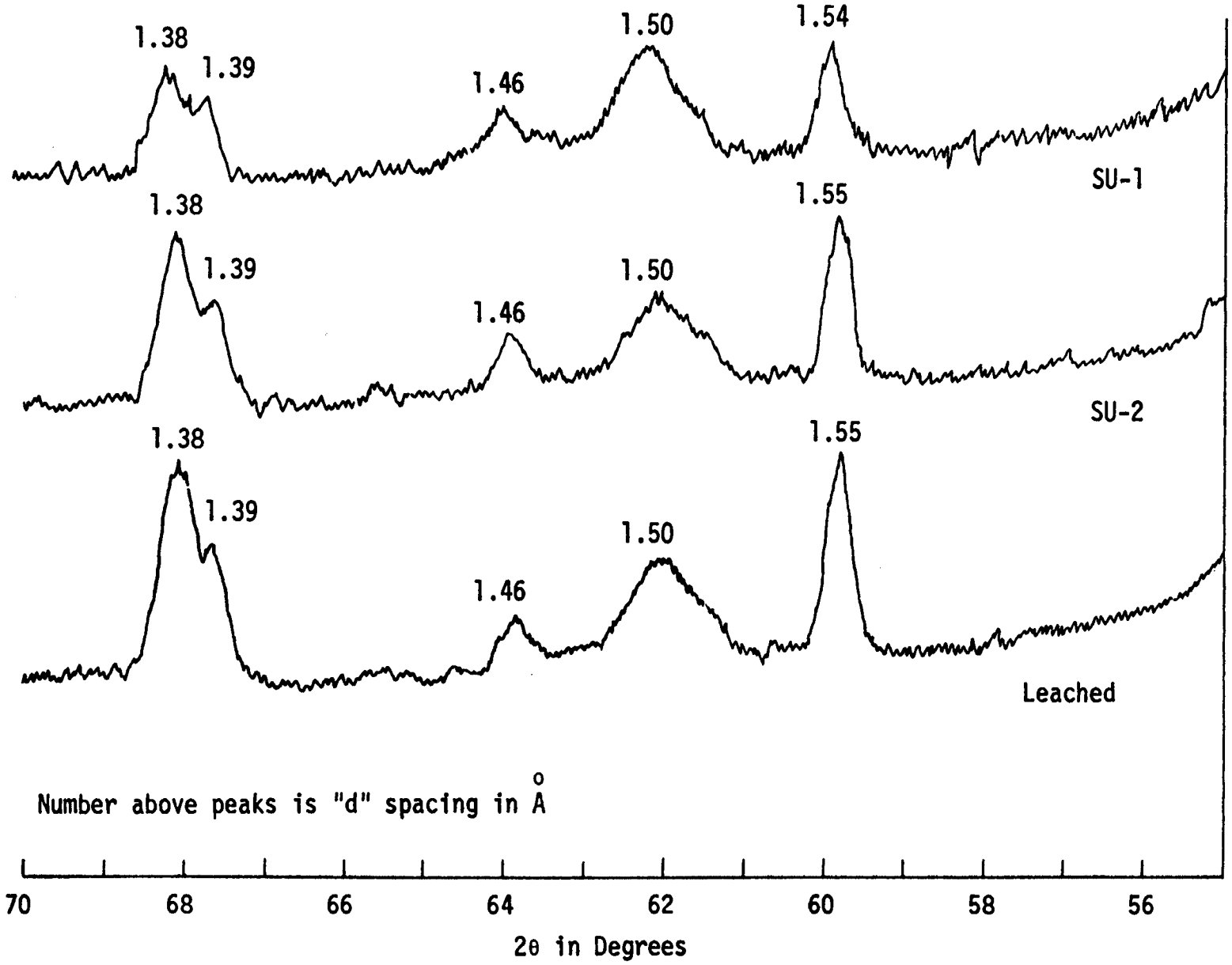

FIGURE 10-c. X-RAY DIFFRACTION PATTERNS FOR SPRINGFIELD POWDER SLIDES

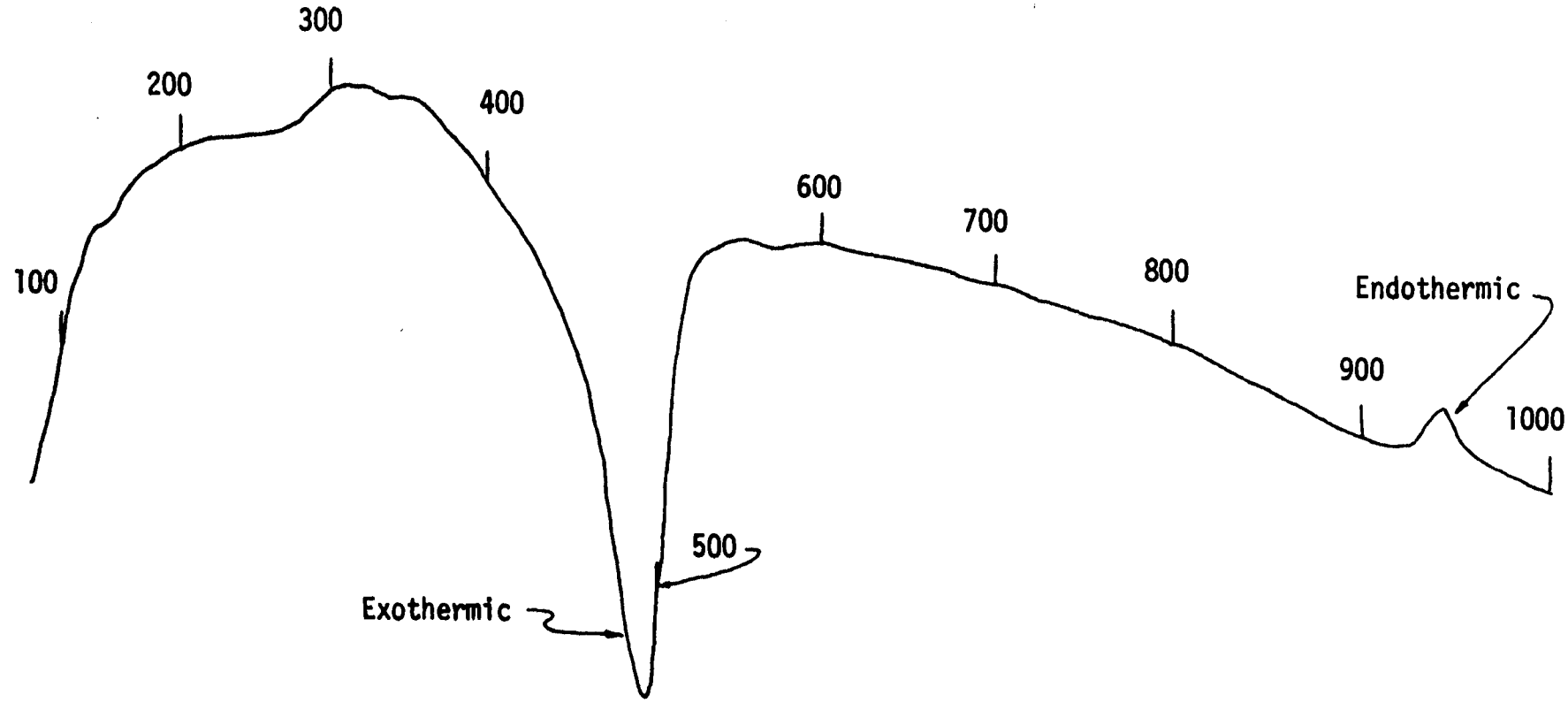

FIGURE 11. DIFFERENTIAL THERMAL ANALYSIS PATTERN FOR THE SPRINGFIELD SOIL

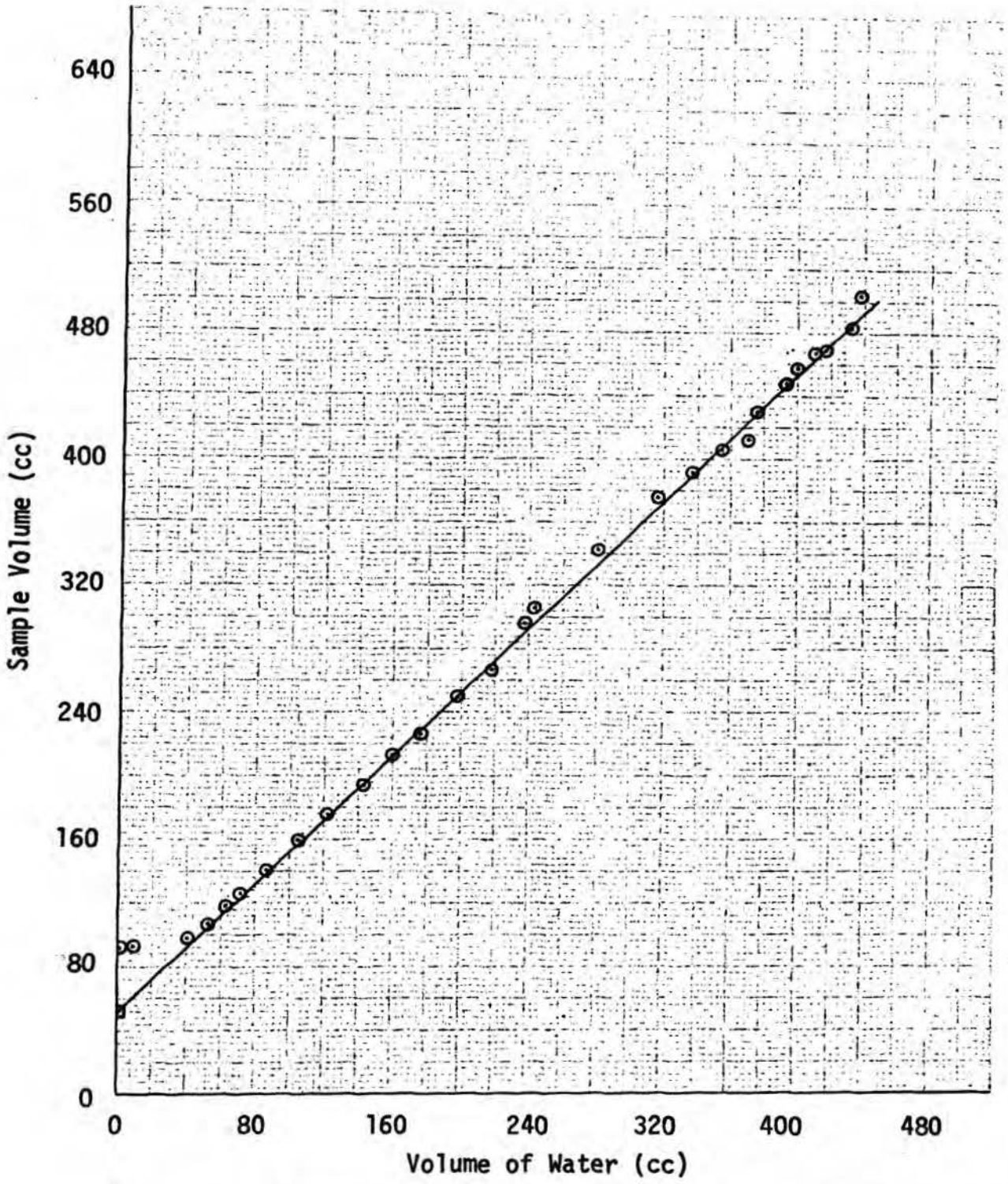

FIGURE 12. SHRINKAGE CURVE FOR SPRINGFIELD NATURAL, SERIES I

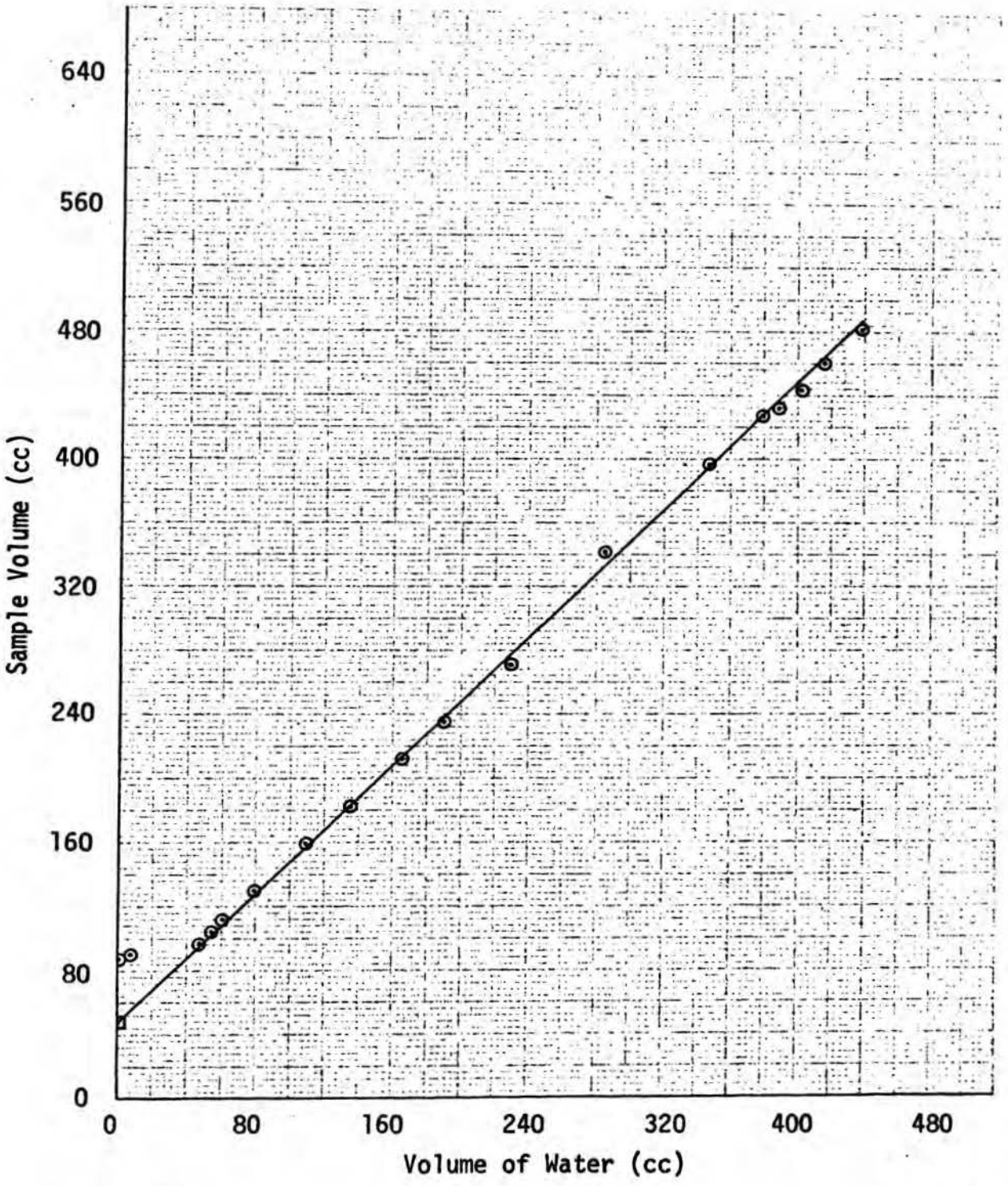

FIGURE 13. SHRINKAGE CURVE FOR SPRINGFIELD FLOCCULATED, SERIES I

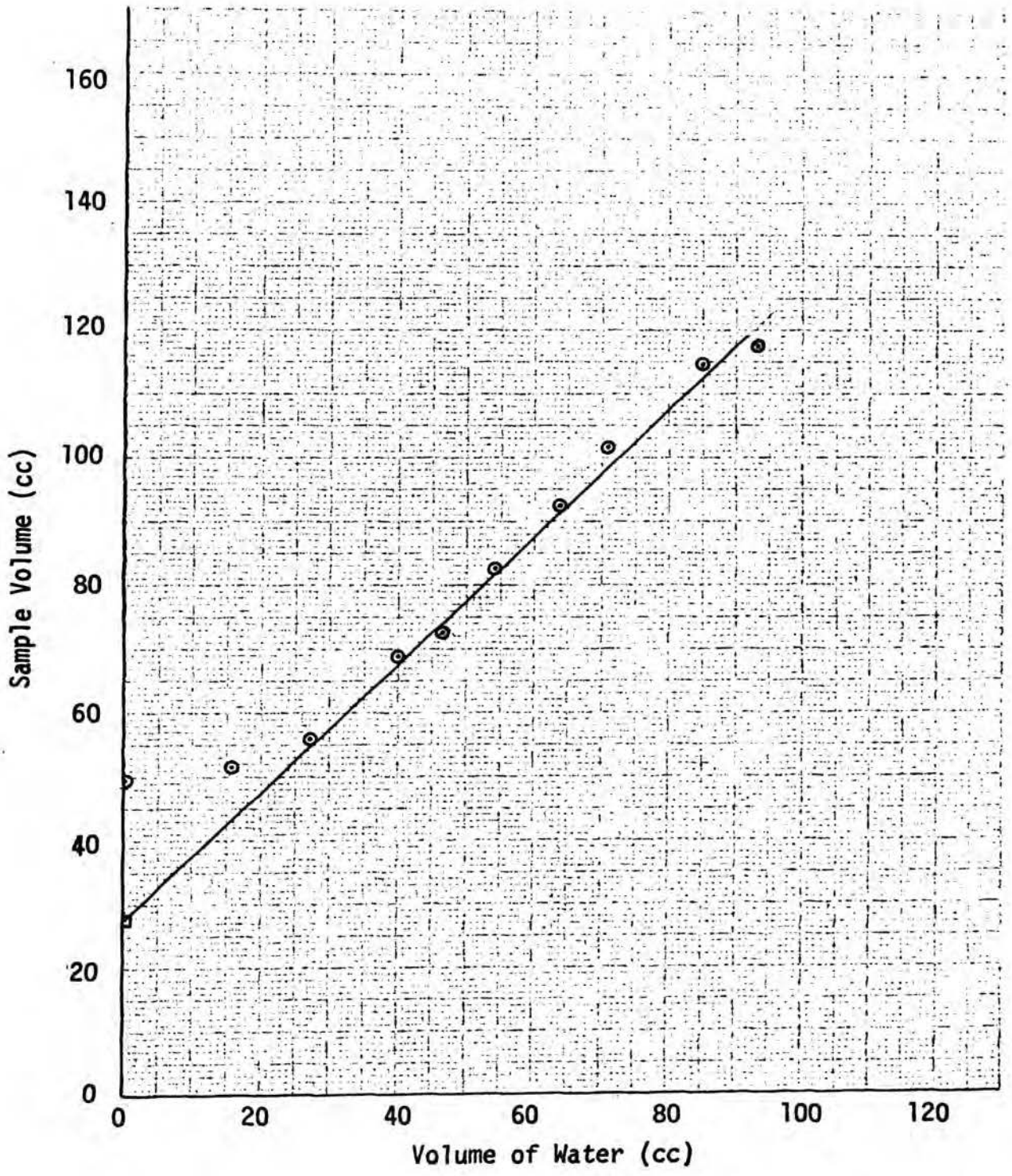

FIGURE 14. SHRINKAGE CURVE FOR SPRINGFIELD NATURAL, SERIES II

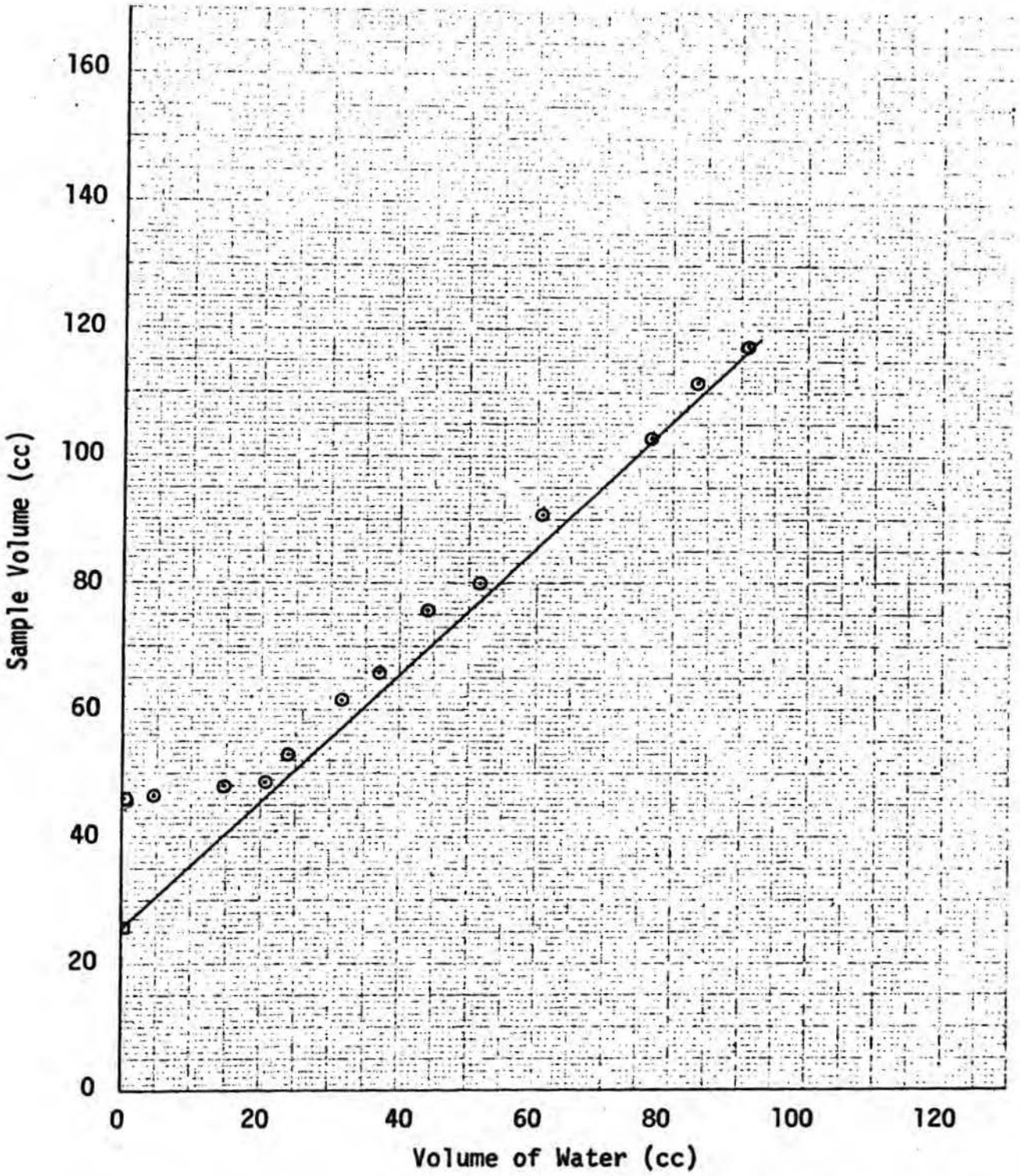

FIGURE 15. SHRINKAGE CURVE FOR SPRINGFIELD FLOCCULATED, SERIES II

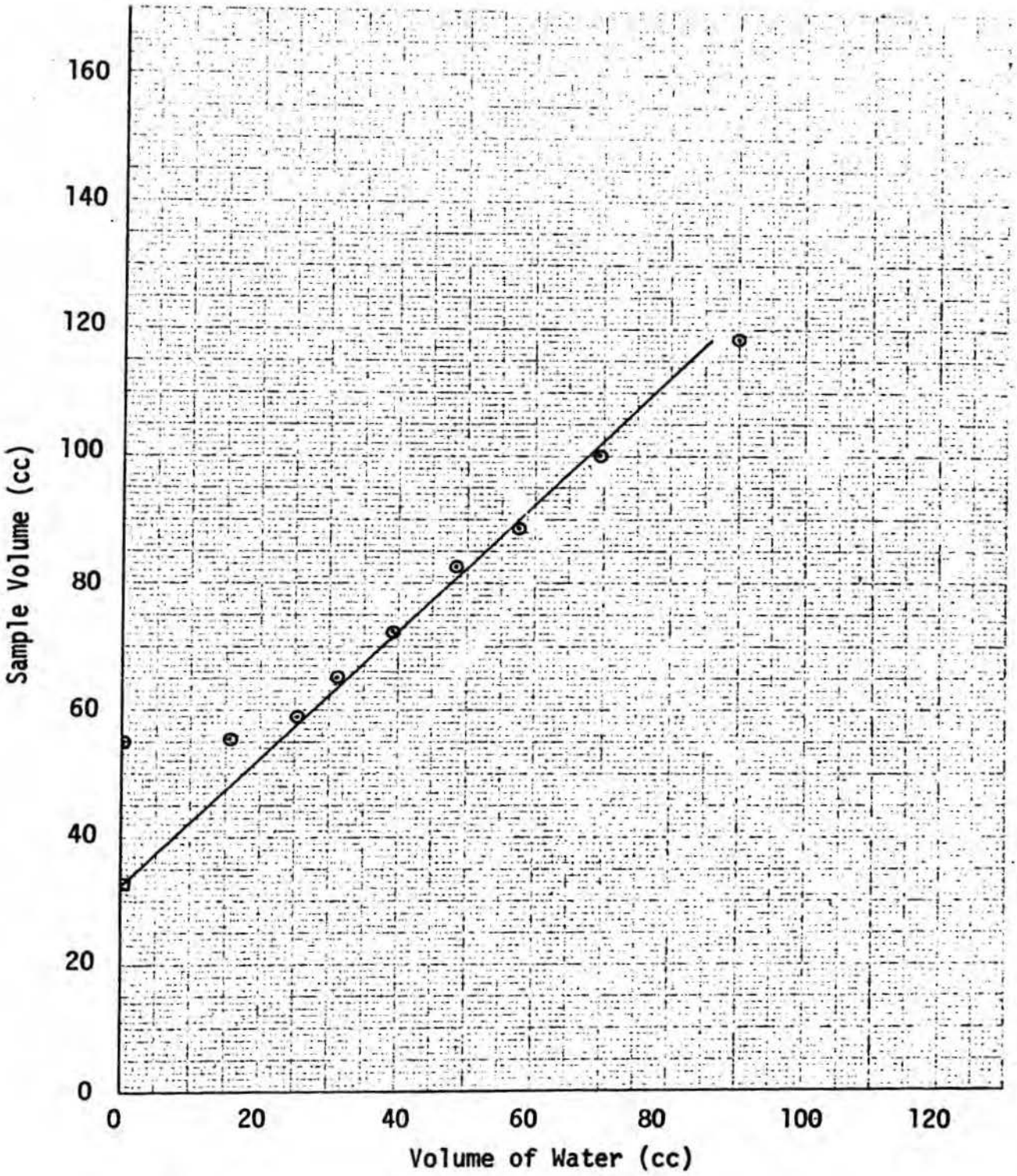

FIGURE 16. SHRINKAGE CURVE FOR SPRINGFIELD DISPERSED, SERIES II

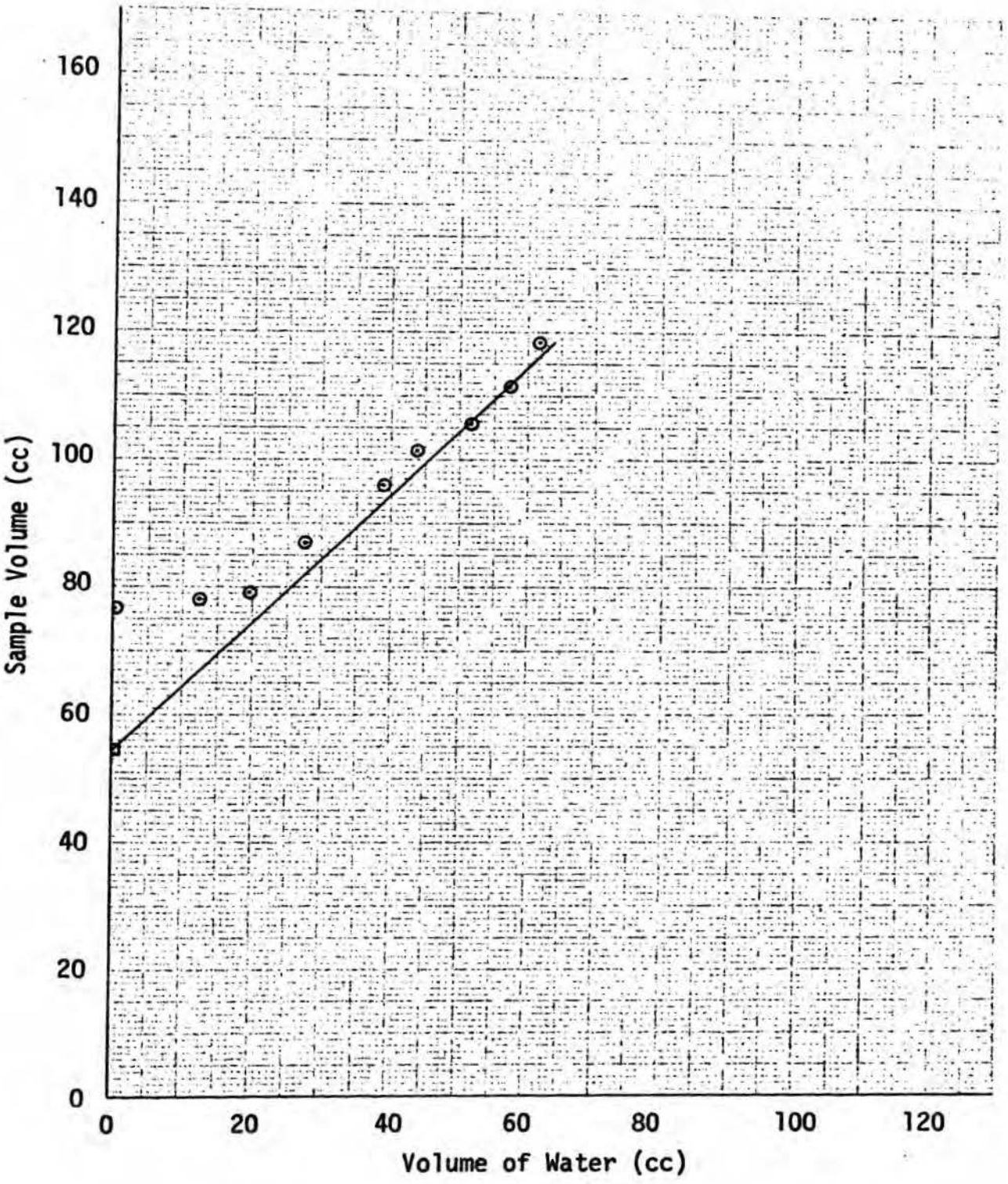

FIGURE 17. SHRINKAGE CURVE FOR LEBANON NATURAL, SERIES II

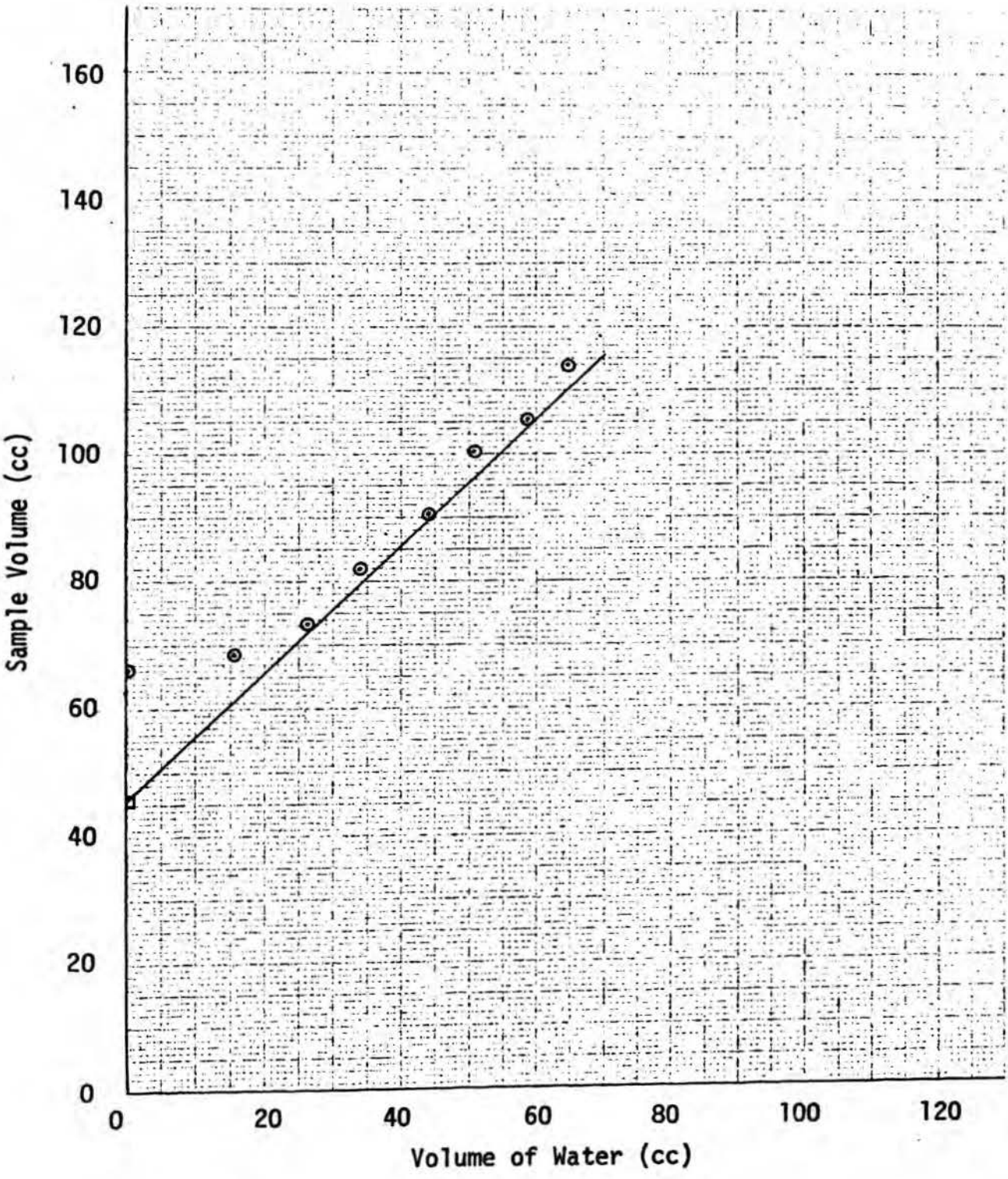

FIGURE 18. SHRINKAGE CURVE FOR LEBANON FLOCCULATED, SERIES II

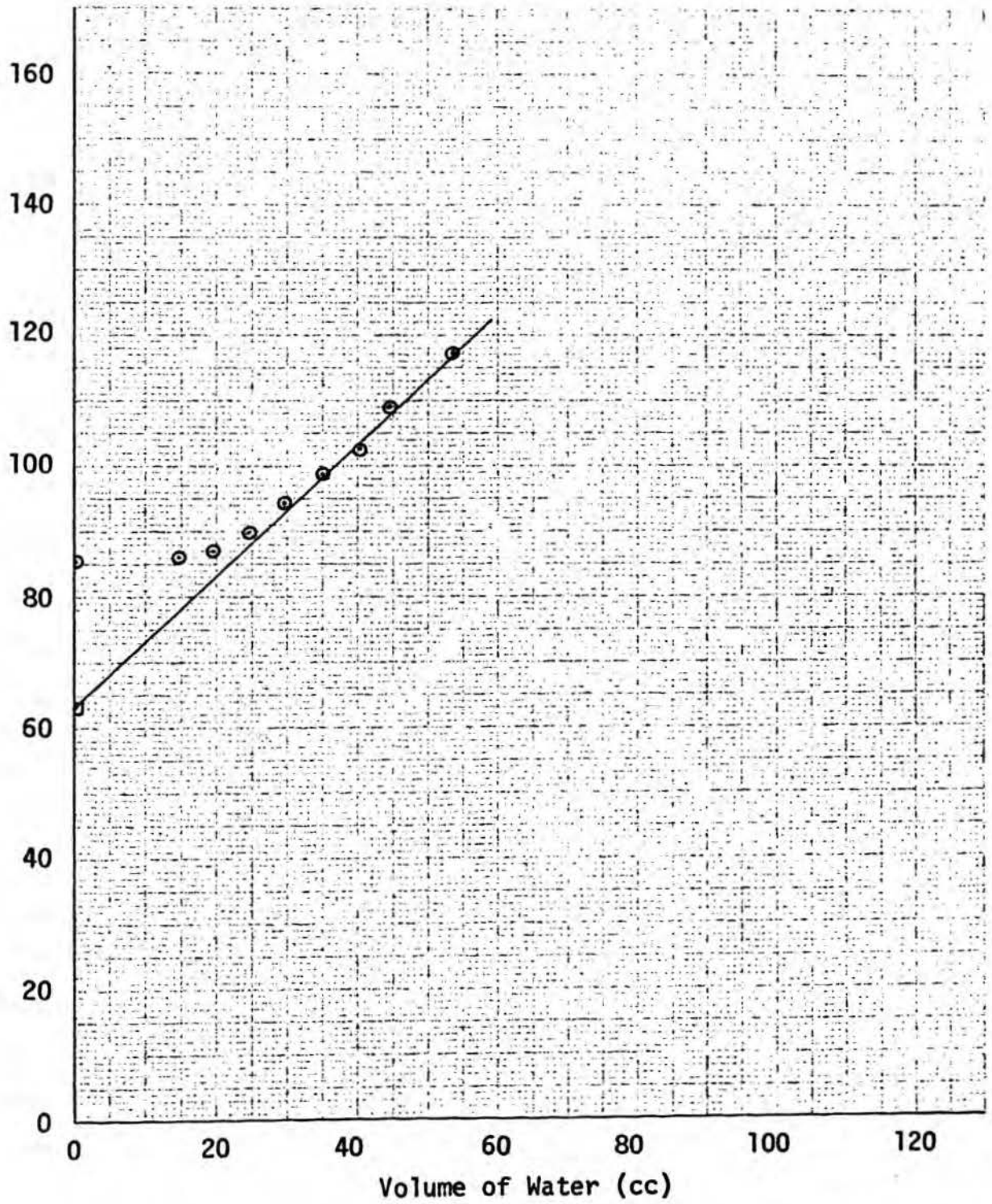

FIGURE 19. SHRINKAGE CURVE FOR LEBANON DISPERSED, SERIES II

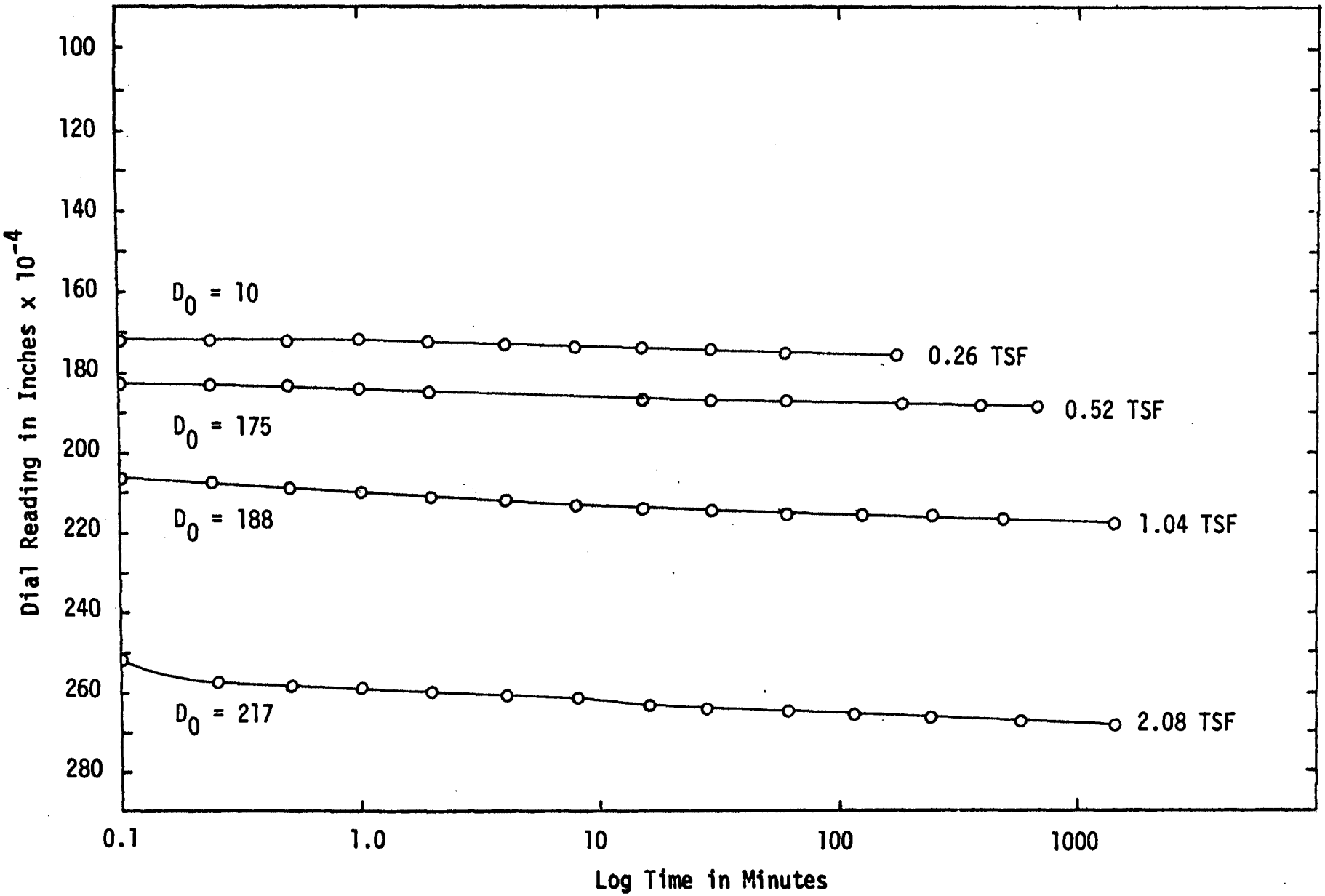

FIGURE 20-a. DIAL READING VERSUS LOG TIME FOR SAMPLE SU-1

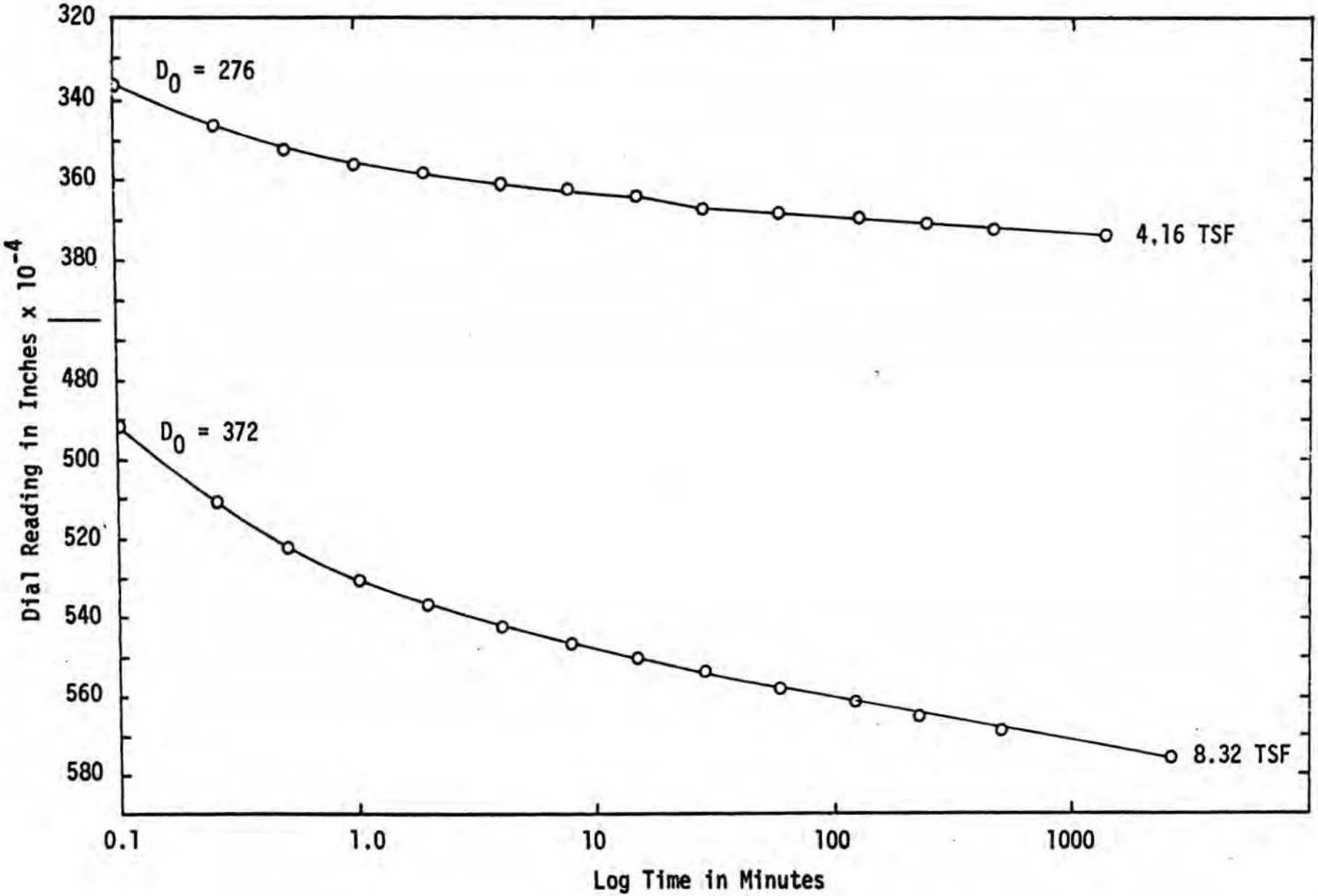

FIGURE 20-b. DIAL READING VERSUS LOG TIME FOR SAMPLE SU-1

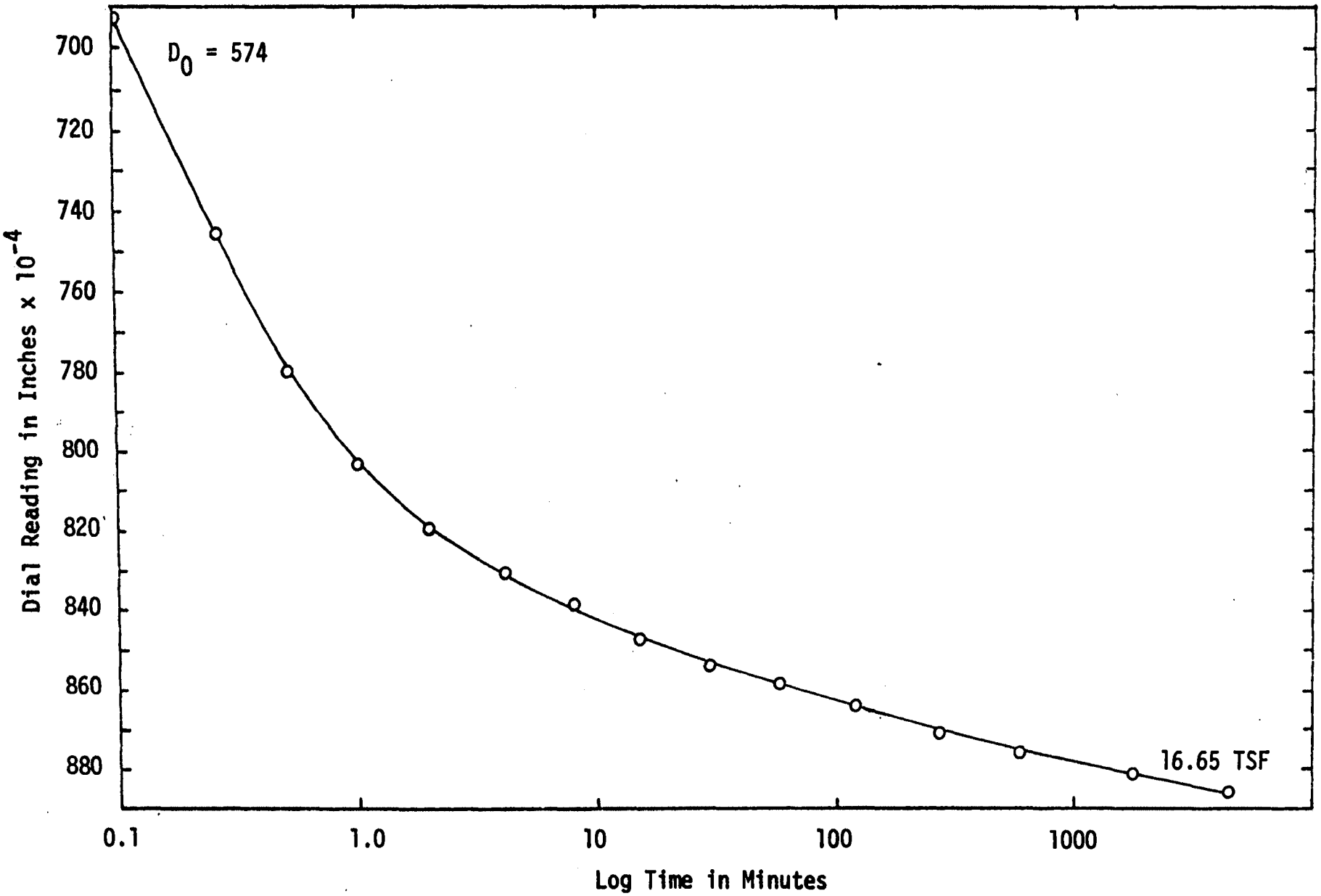

FIGURE 20-c. DIAL READING VERSUS LOG TIME FOR SAMPLE SU-1

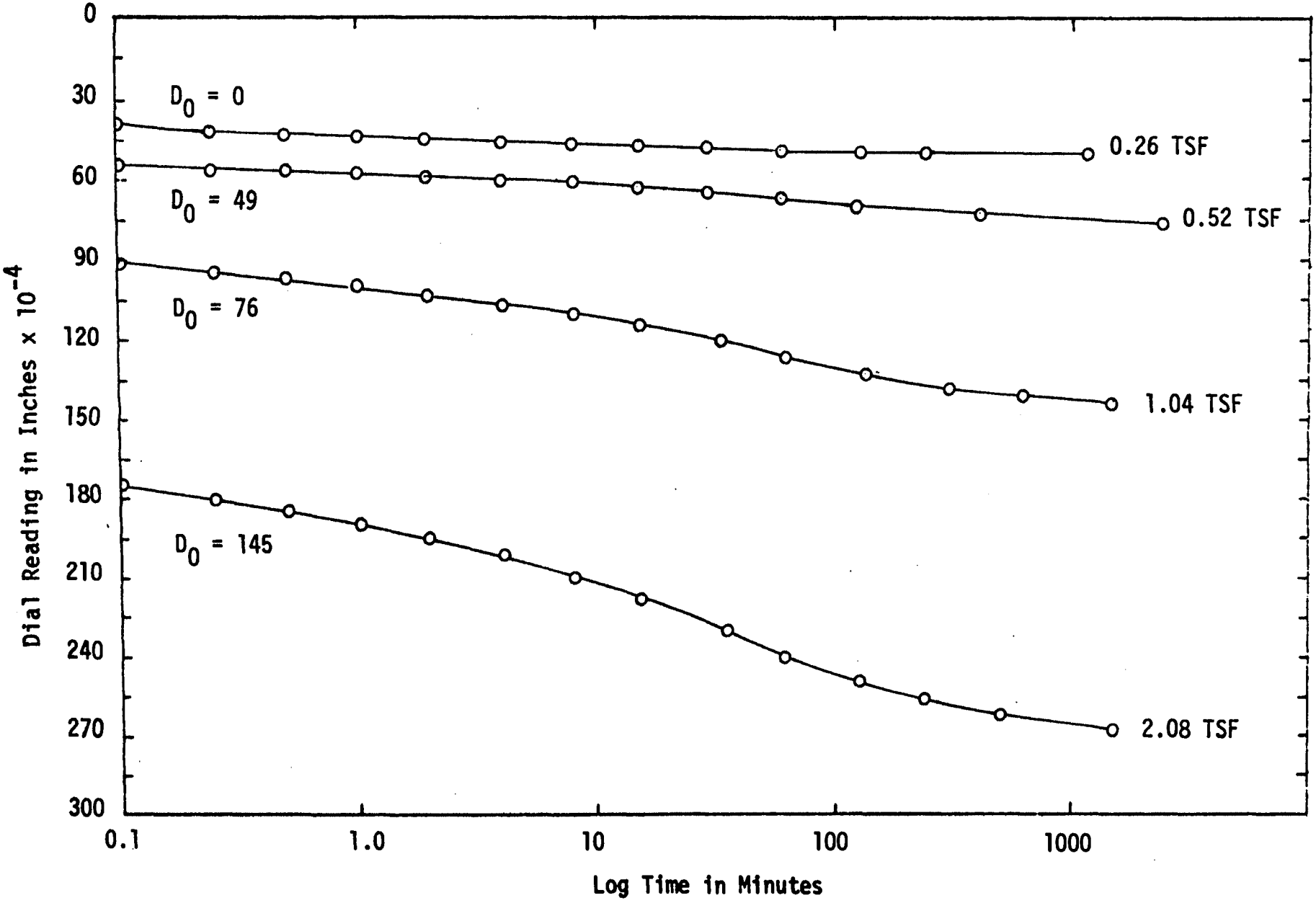

FIGURE 21-a. DIAL READING VERSUS LOG TIME FOR SAMPLE SU-2

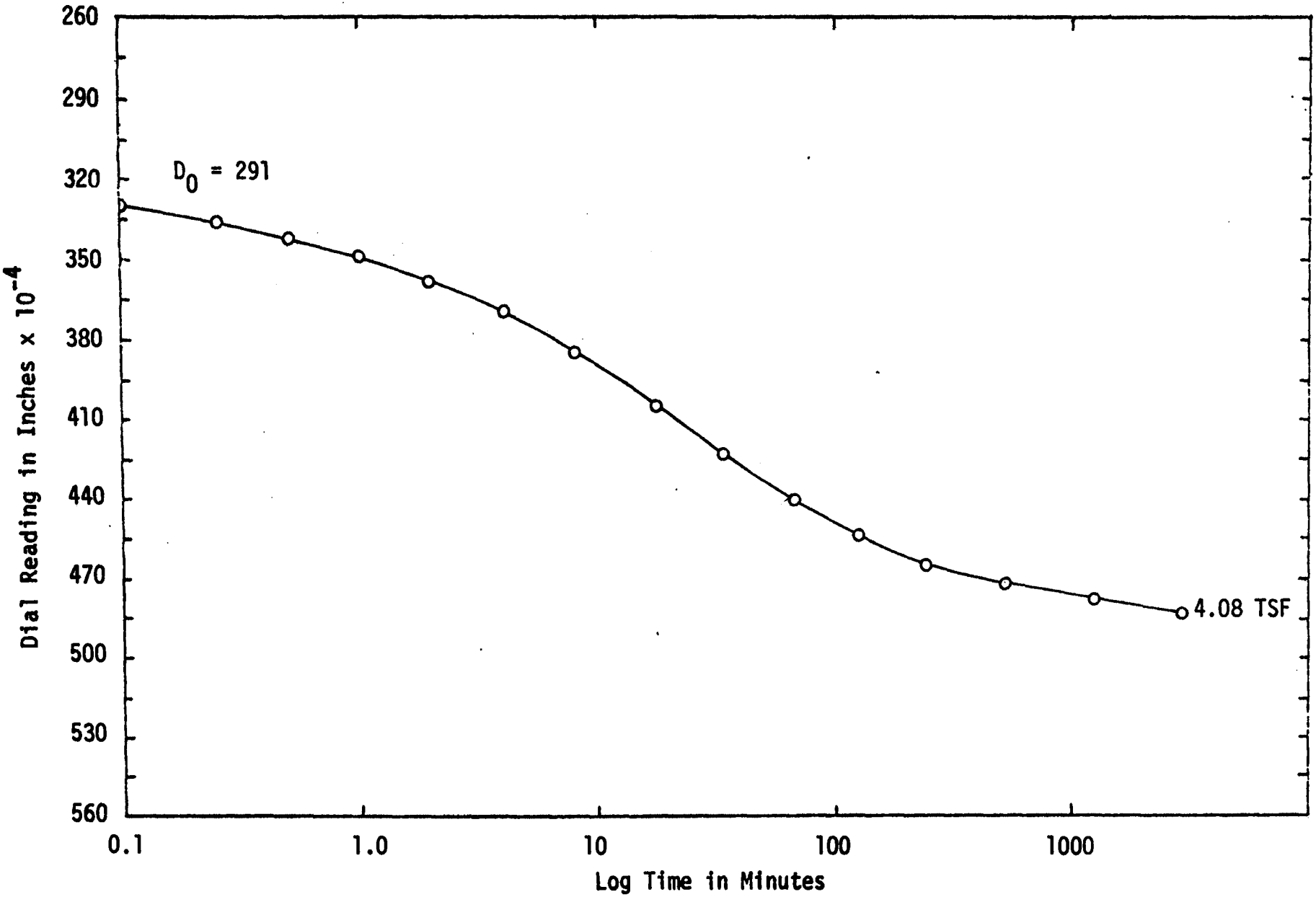

FIGURE 21-b. DIAL READING VERSUS LOG TIME FOR SAMPLE SU-2

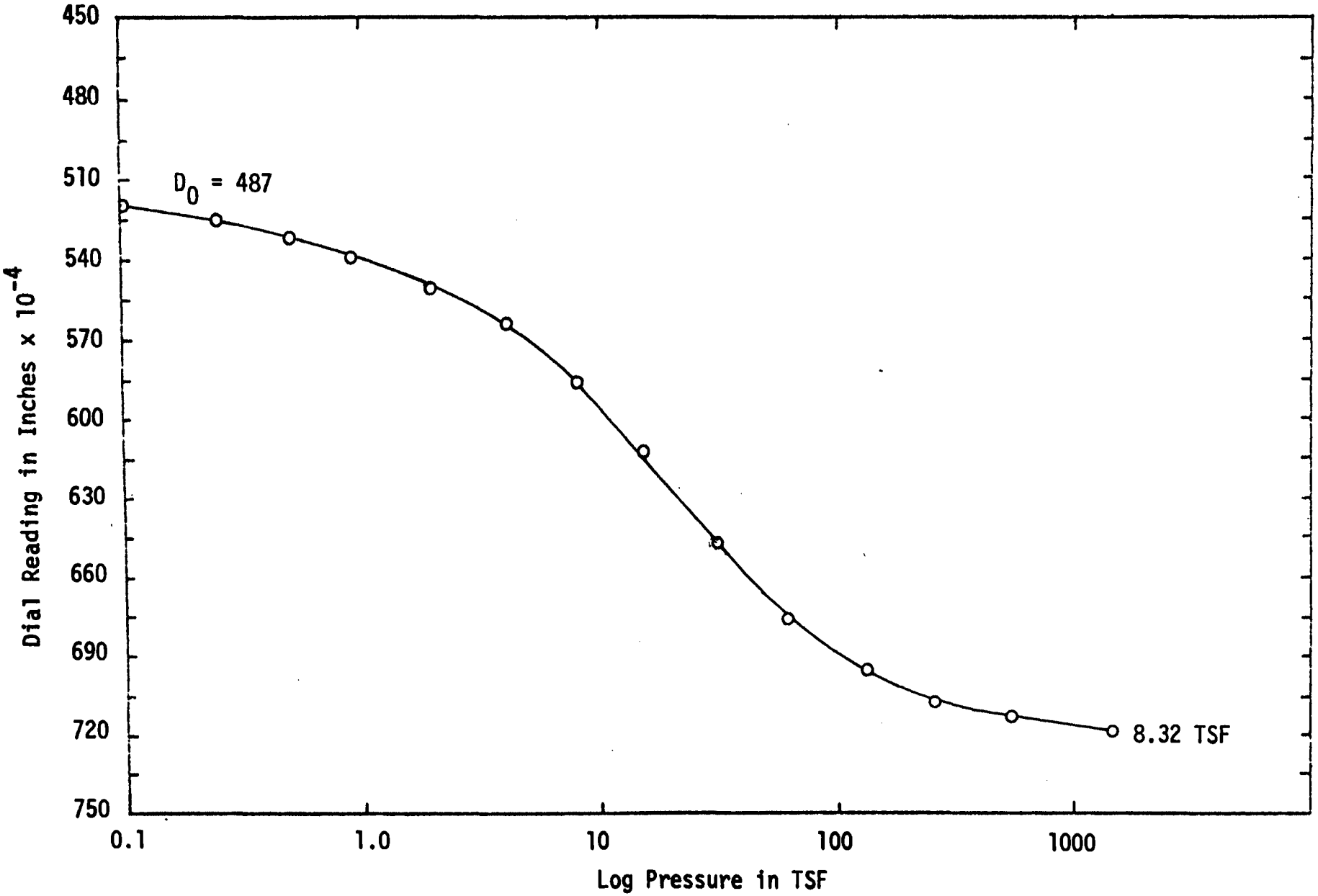

FIGURE 21-c. DIAL READING VERSUS LOG TIME FOR SAMPLE SU-2

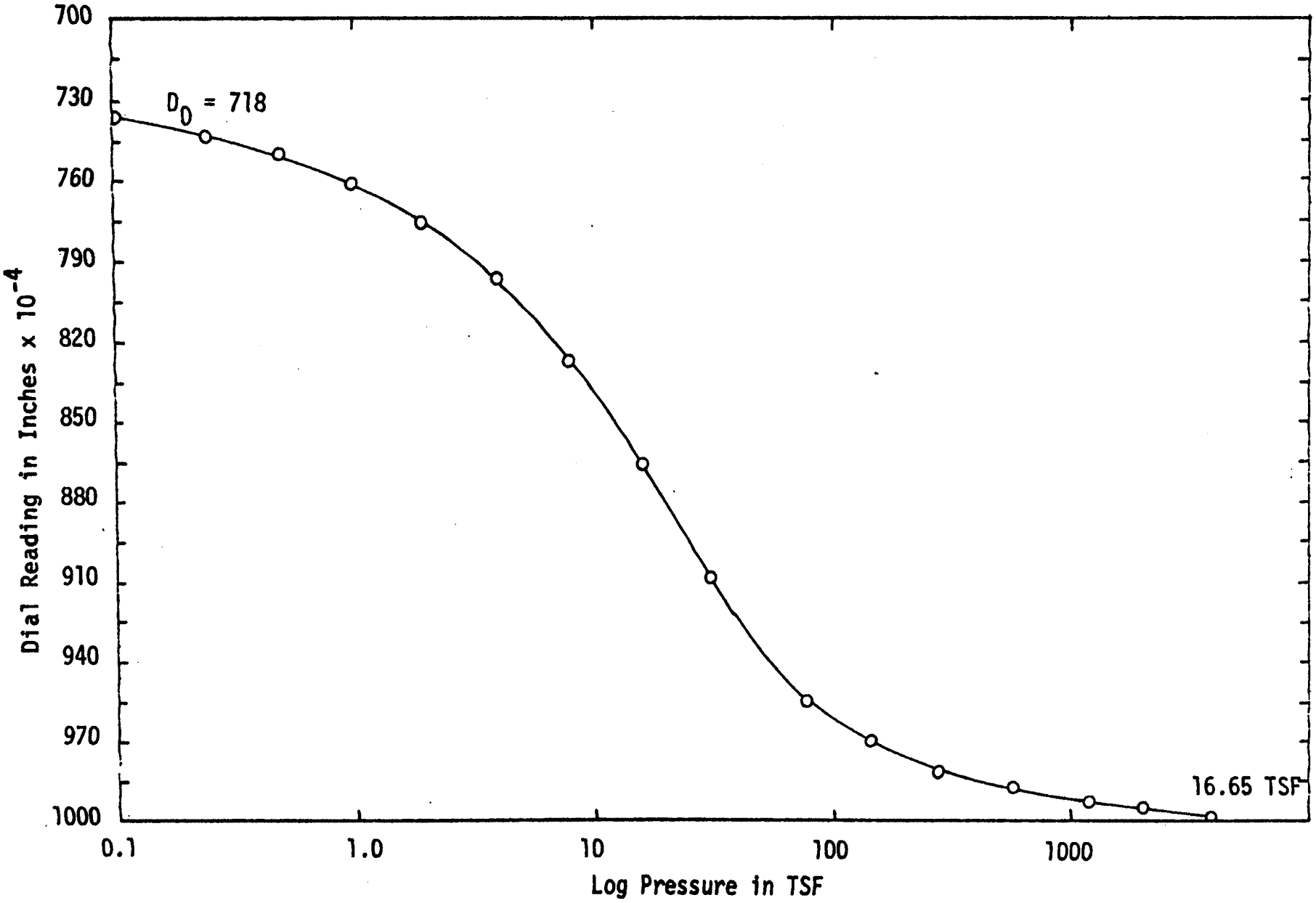

FIGURE 21-d. DIAL READING VERSUS LOG TIME FOR SAMPLE SU-2

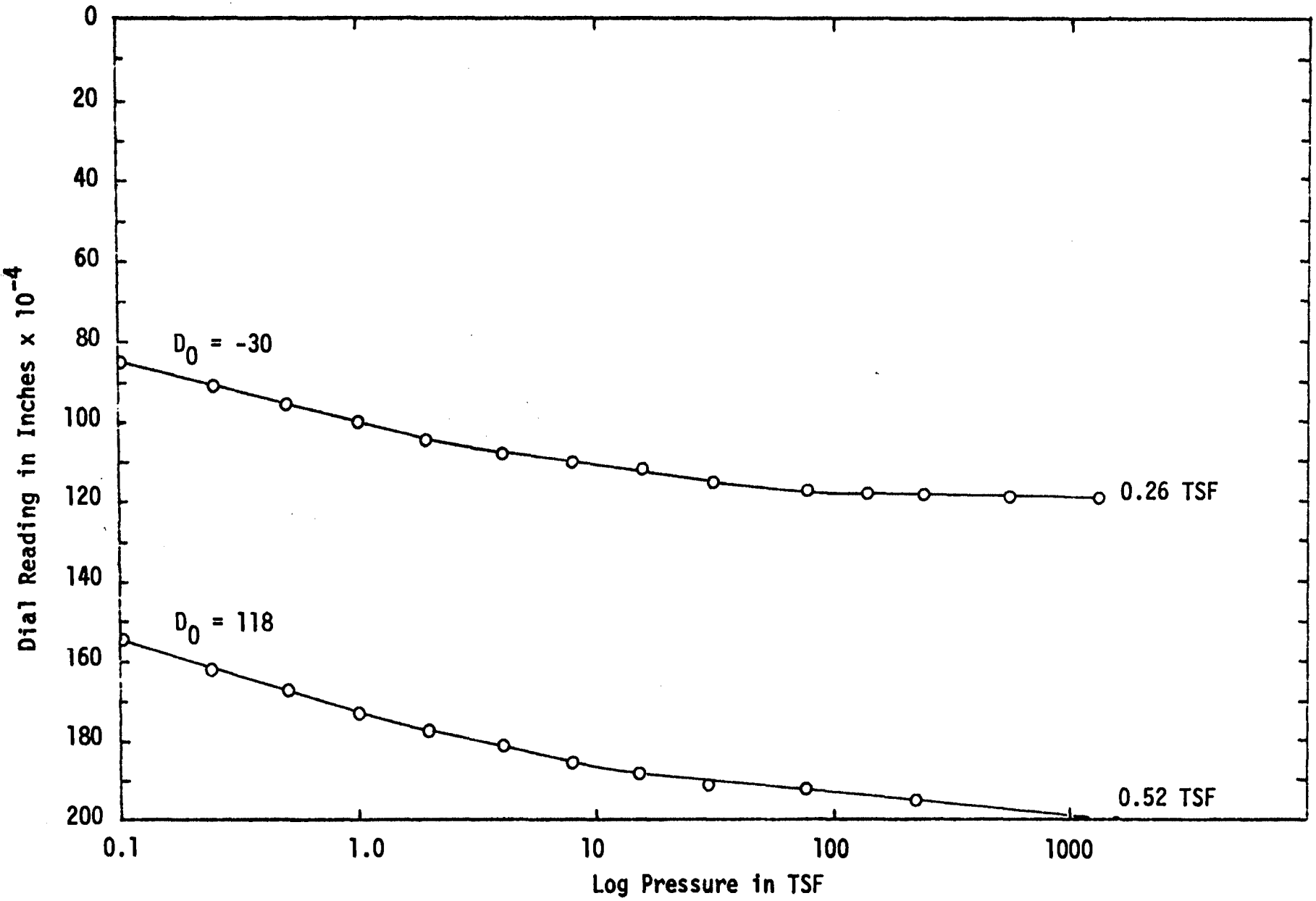

FIGURE 22-a. DIAL READING VERSUS LOG TIME FOR SAMPLE LU-1

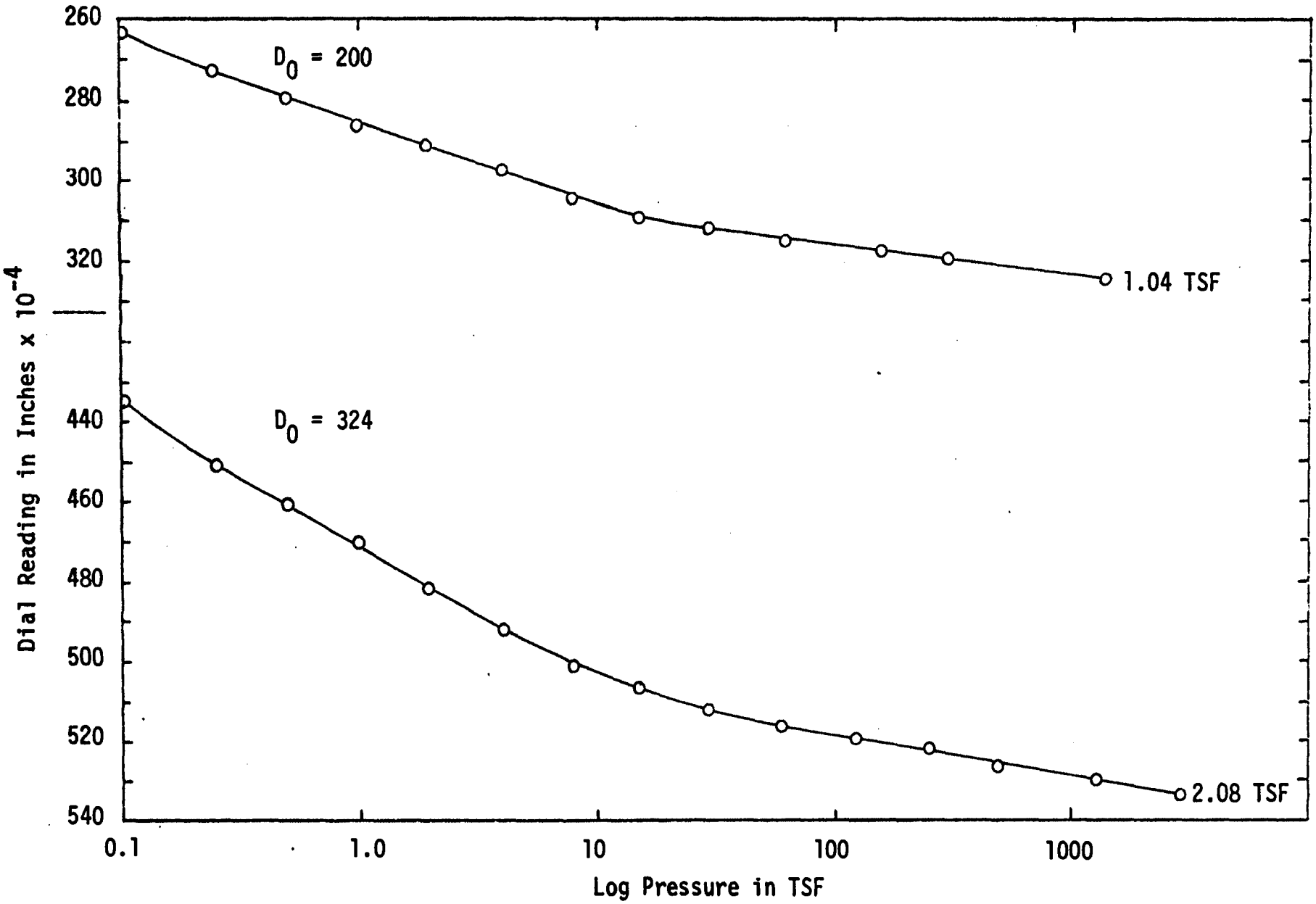

FIGURE 22-b. DIAL READING VERSUS LOG TIME FOR SAMPLE LU-1

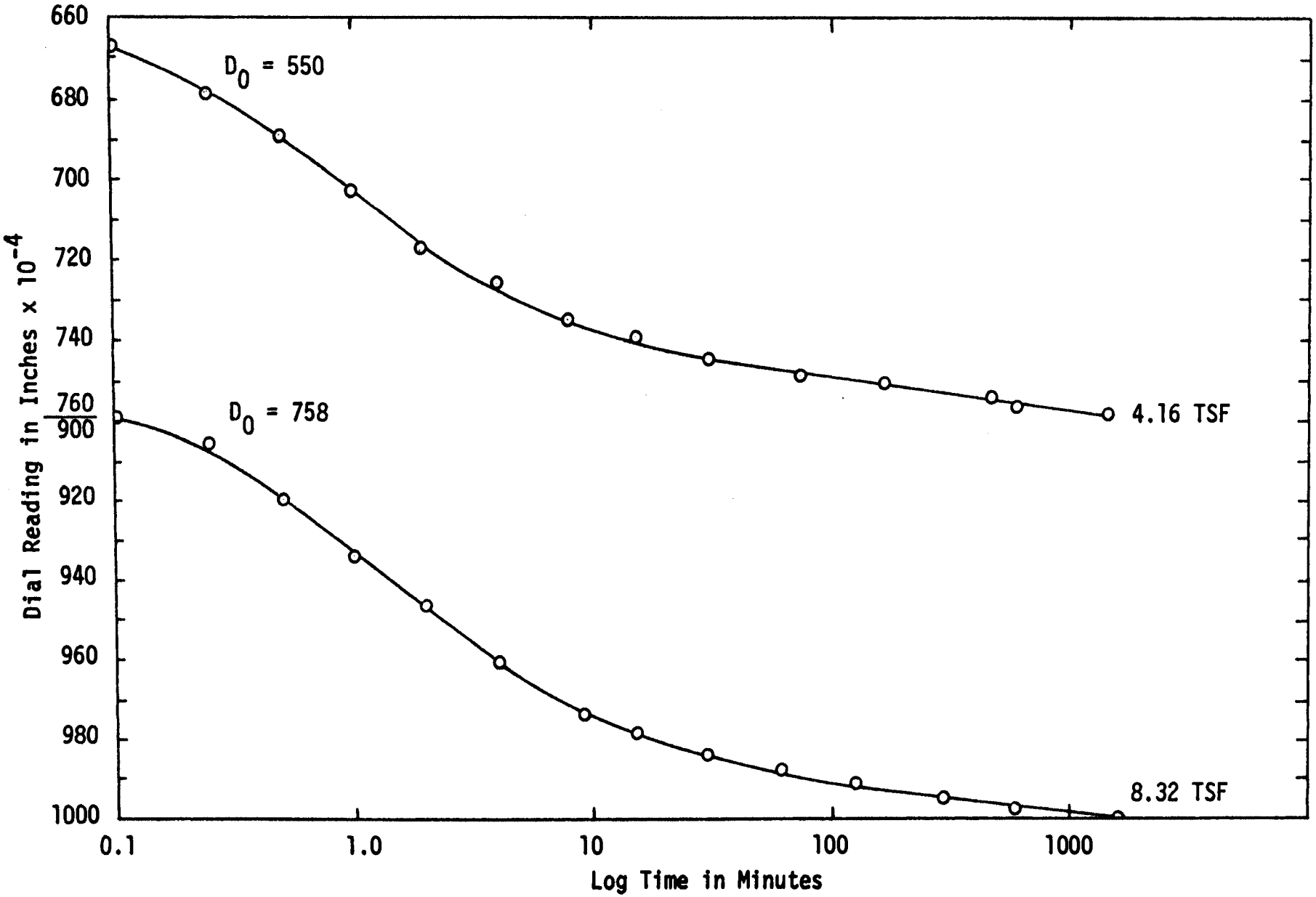

FIGURE 22-c. DIAL READING VERSUS LOG TIME FOR SAMPLE LU-1

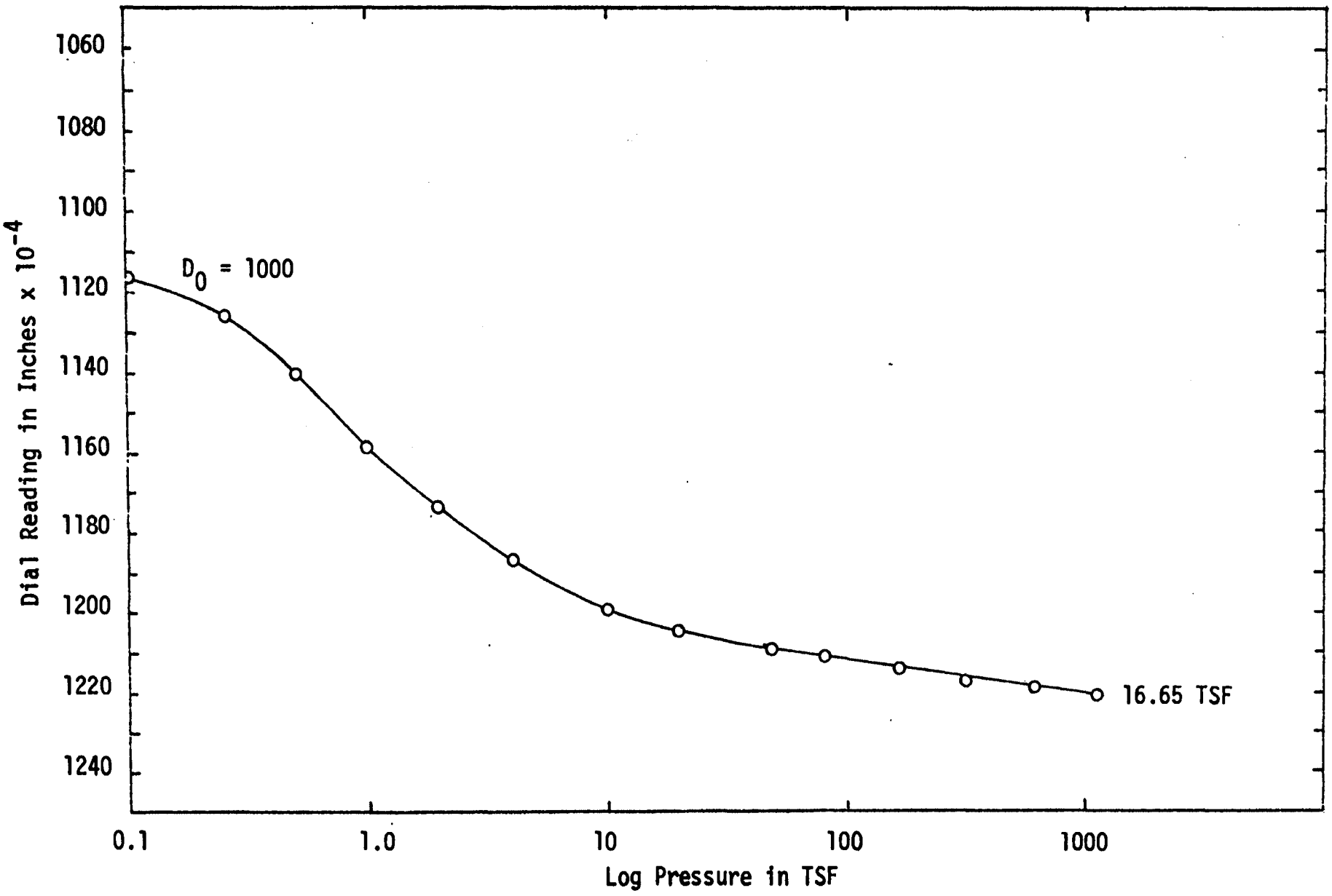

FIGURE 22-d. DIAL READING VERSUS LOG TIME FOR SAMPLE LU-1

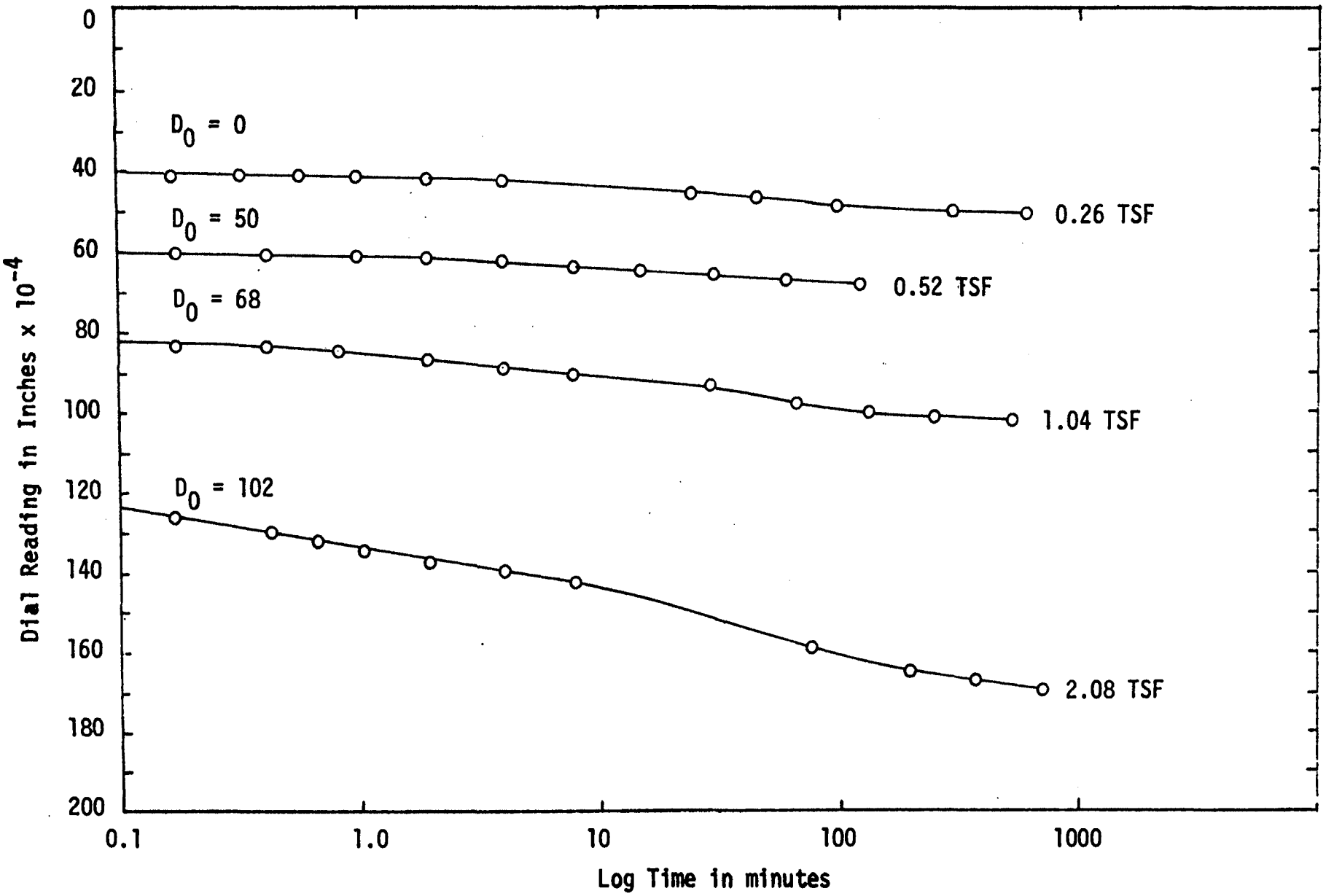

FIGURE 23-a. DIAL READING VERSUS LOG TIME FOR SAMPLE SCN

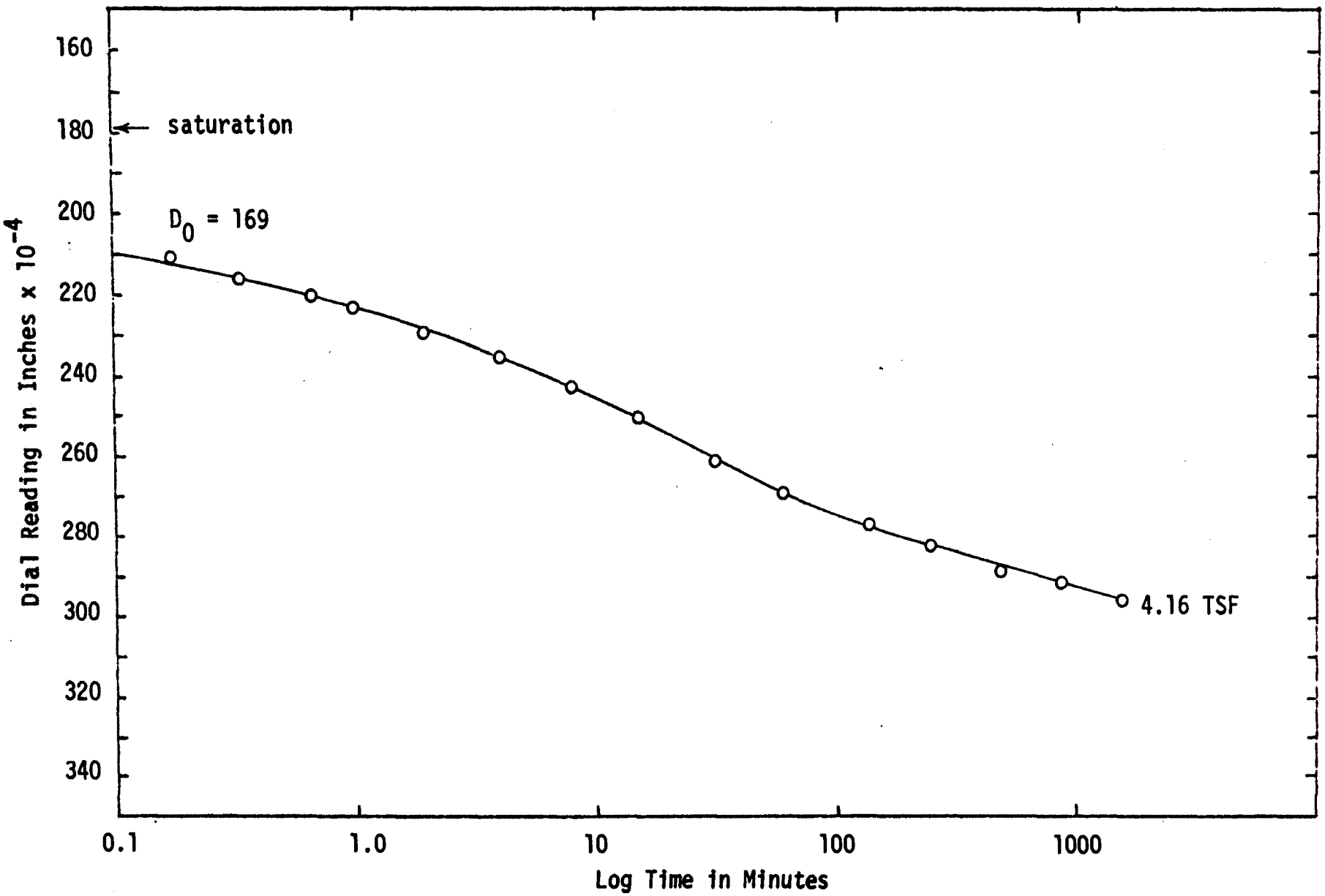

FIGURE 23-b. DIAL READING VERSUS LOG TIME FOR SAMPLE SCN

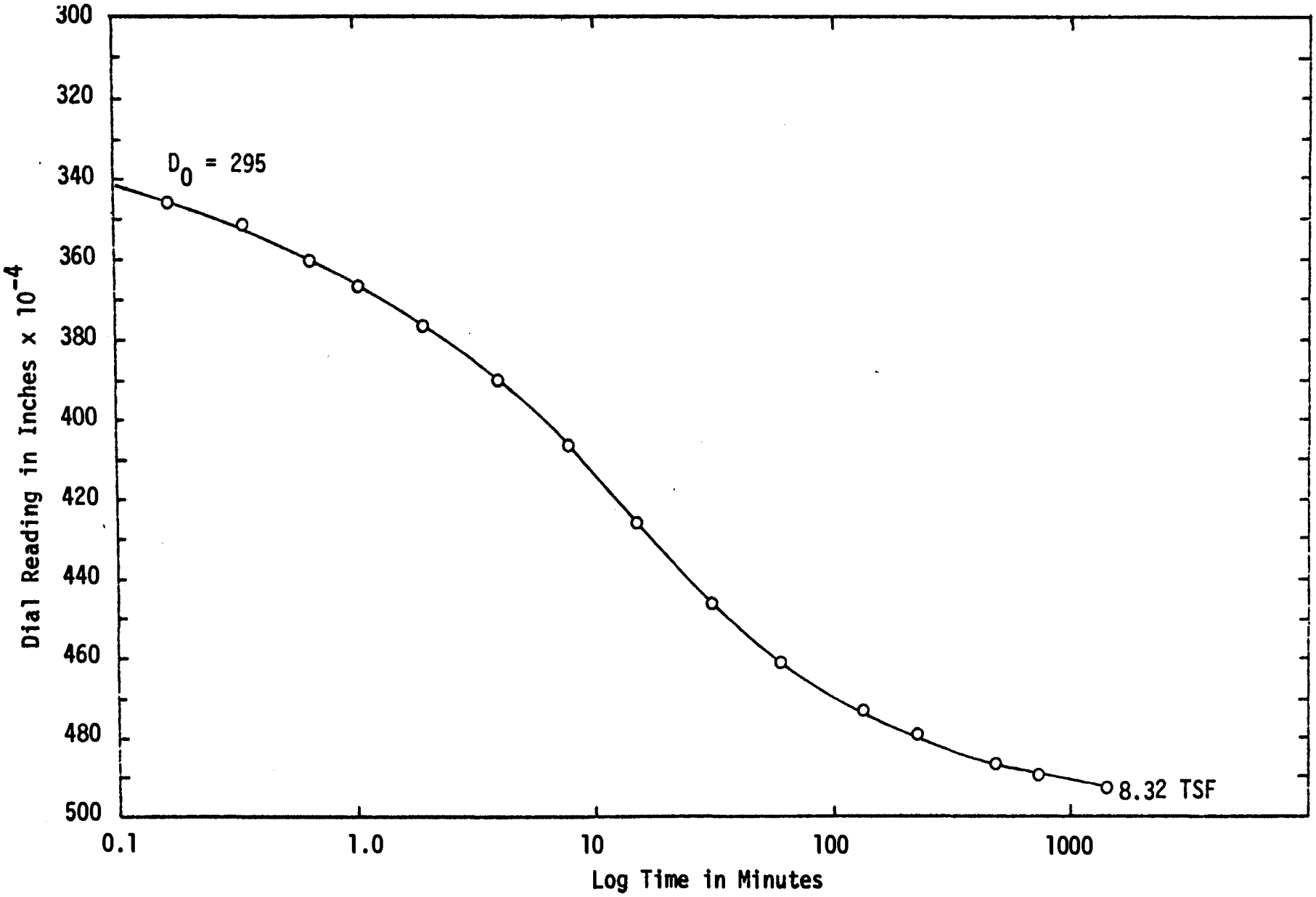

FIGURE 23-c. DIAL READING VERSUS LOG TIME FOR SAMPLE SCN

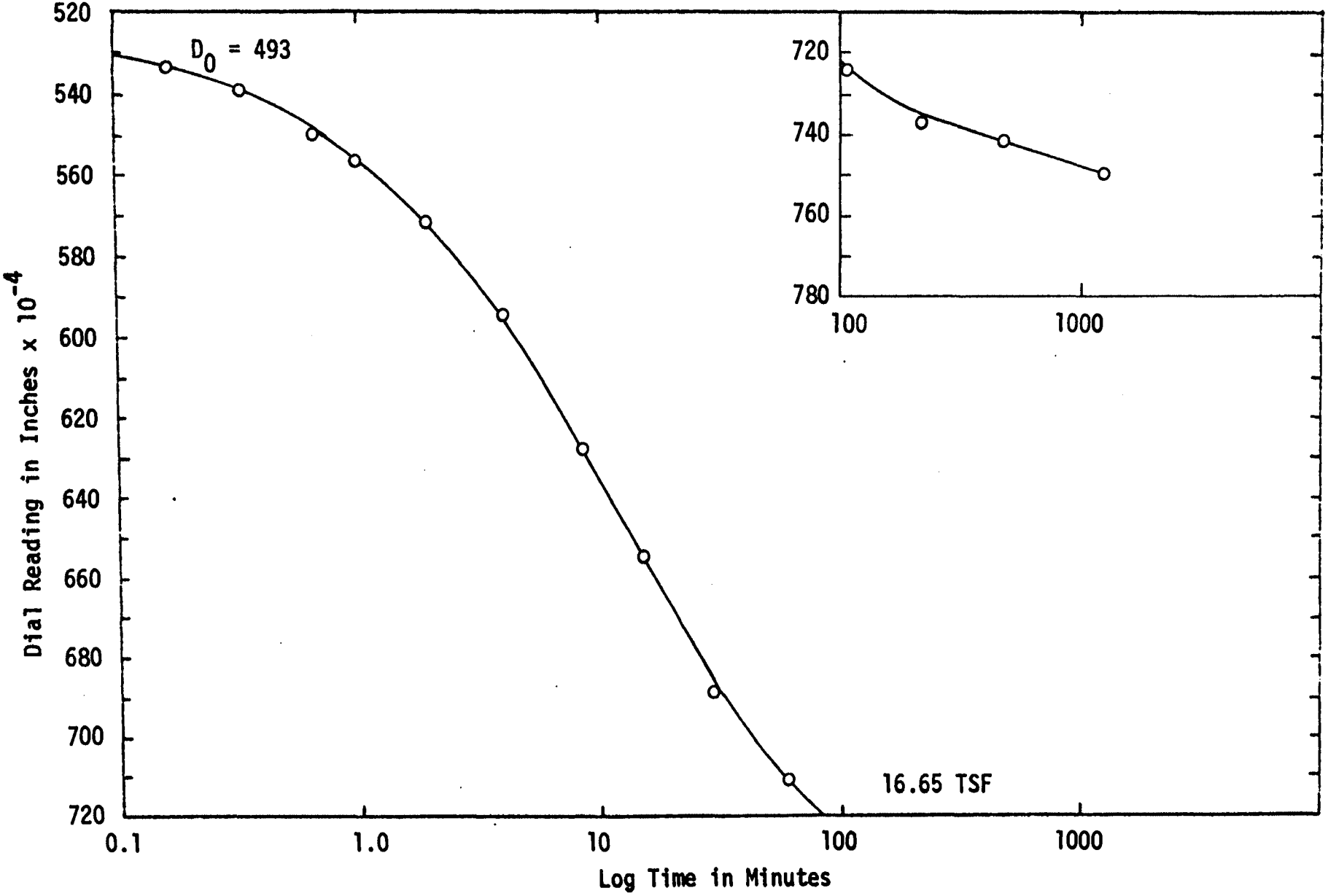

FIGURE 23-d. DIAL READING VERSUS LOG TIME FOR SAMPLE SCN

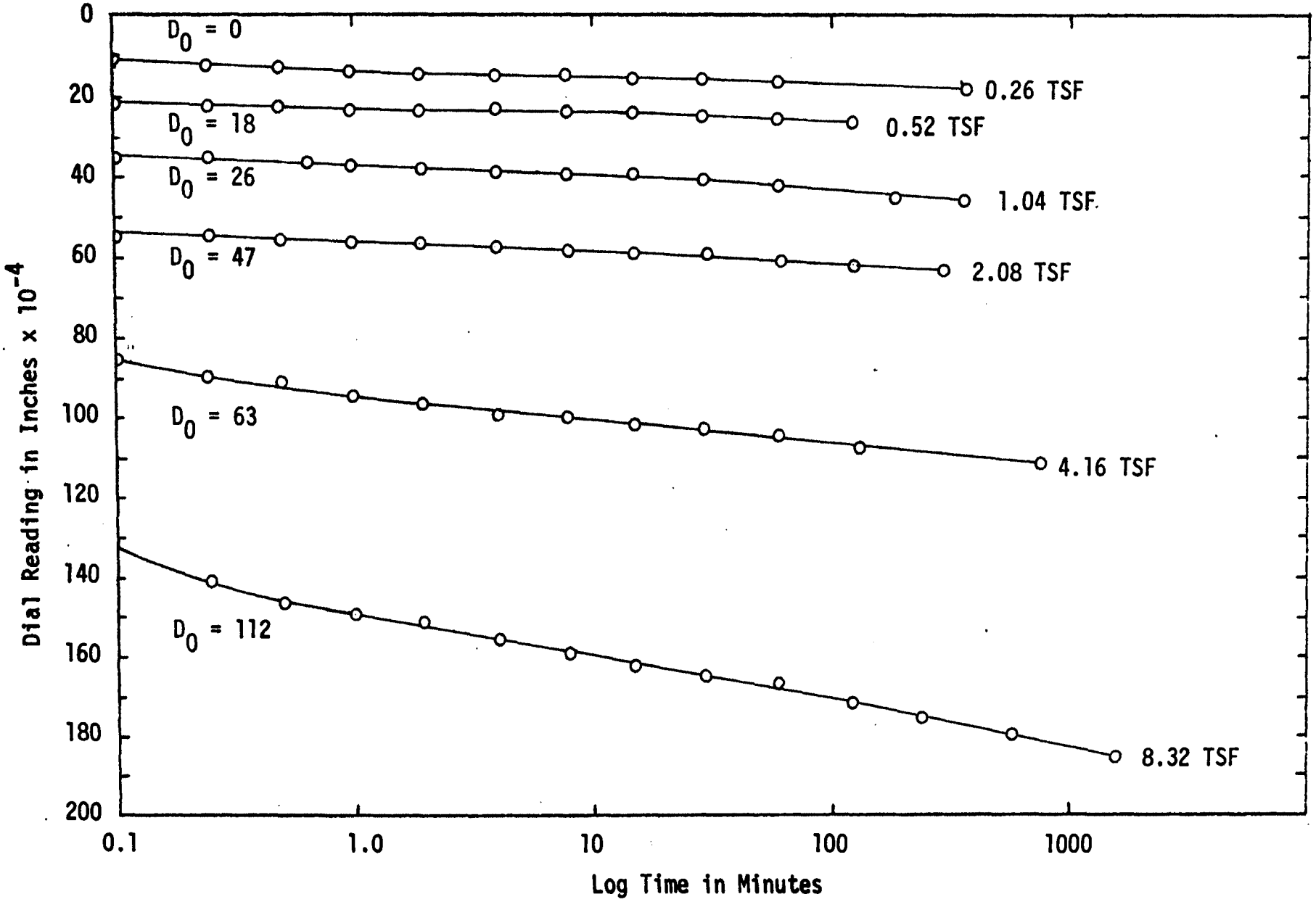

FIGURE 24-a. DIAL READING VERSUS LOG TIME FOR SAMPLE SCC

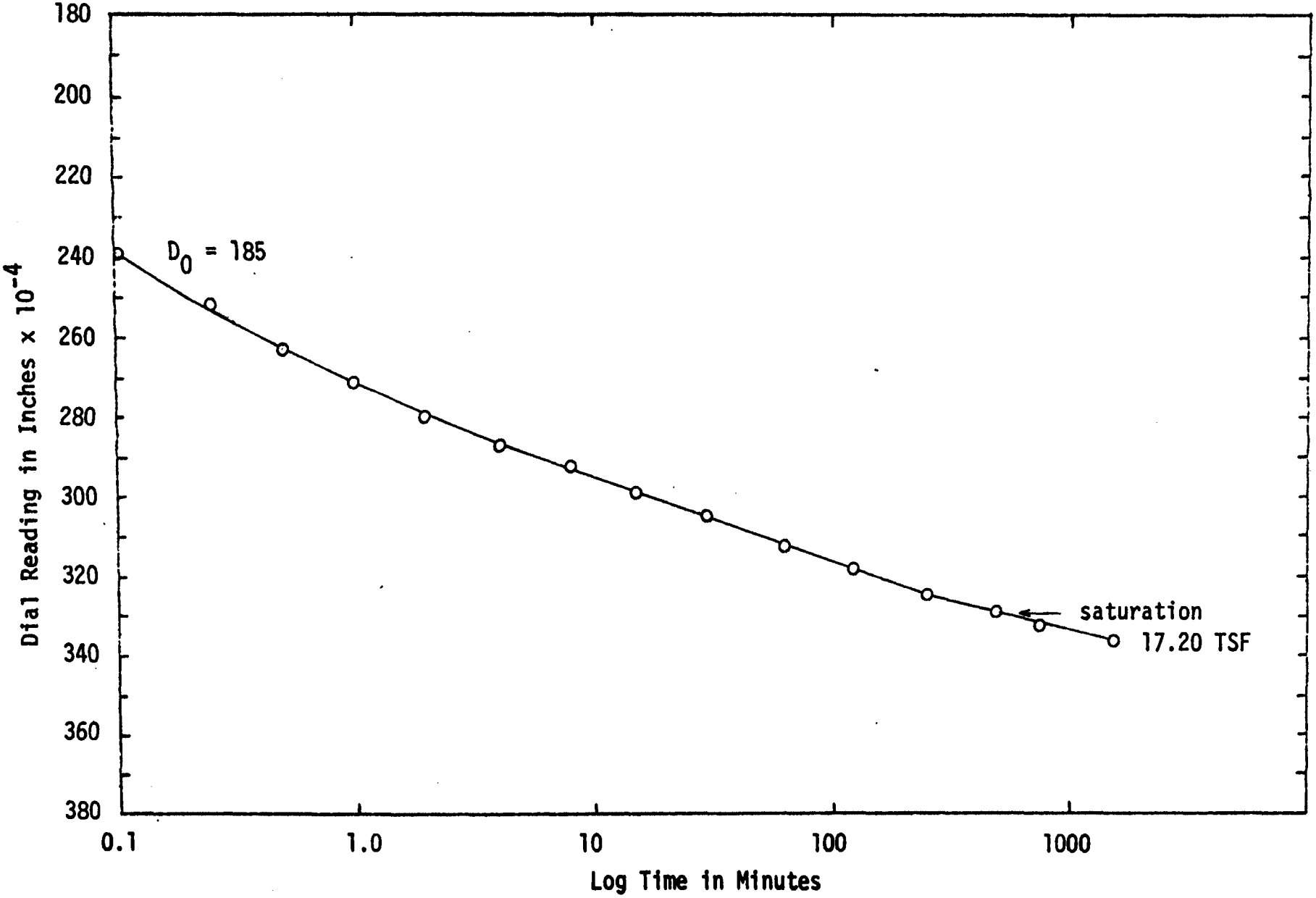

FIGURE 24-b. DIAL READING VERSUS LOG TIME FOR SAMPLE SCC

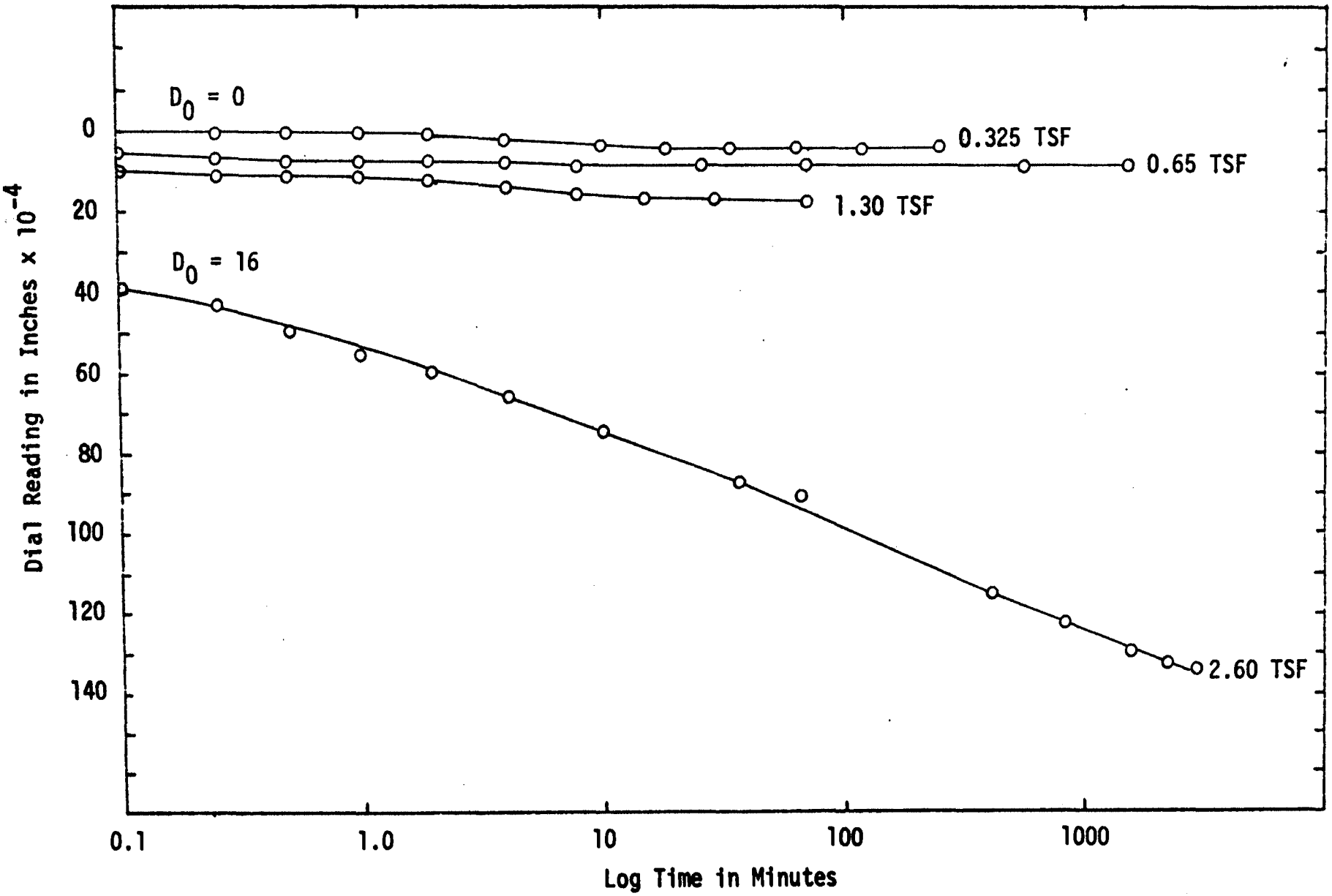

FIGURE 25-a. DIAL READING VERSUS LOG TIME FOR SAMPLE SCS

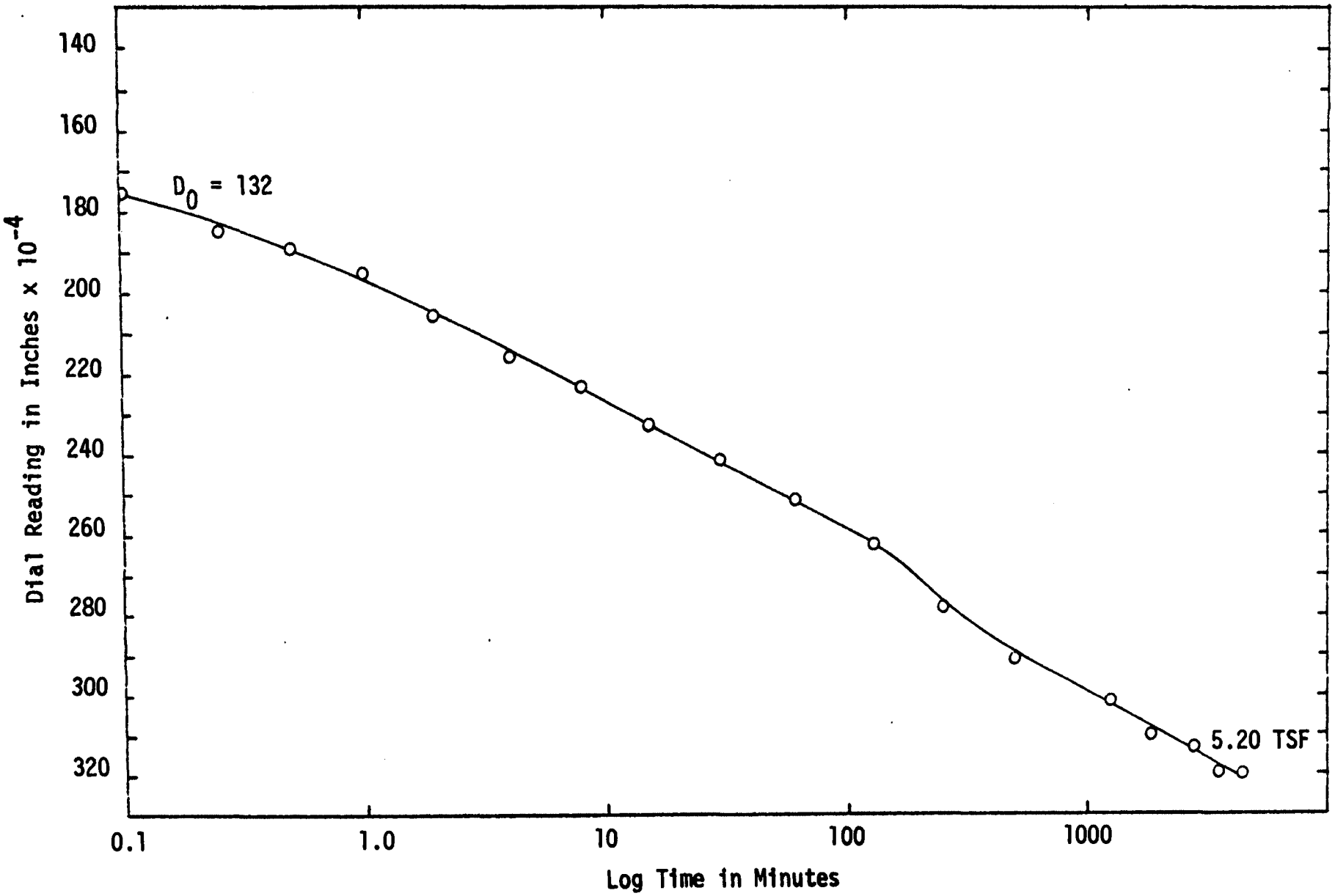

FIGURE 25-b. DIAL READING VERSUS LOG TIME FOR SAMPLE SCS

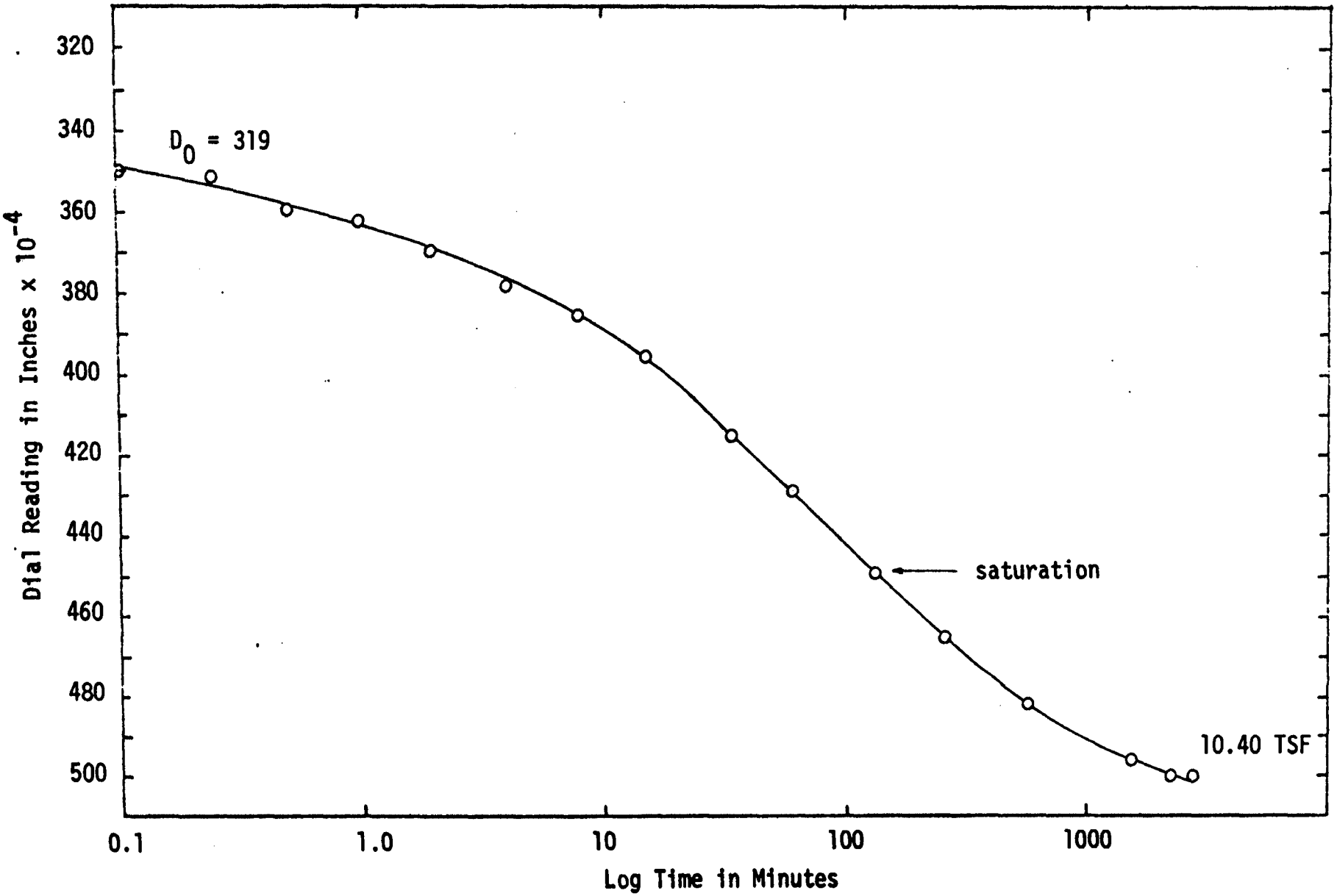

FIGURE 25-c. DIAL READING VERSUS LOG TIME FOR SAMPLE SCS

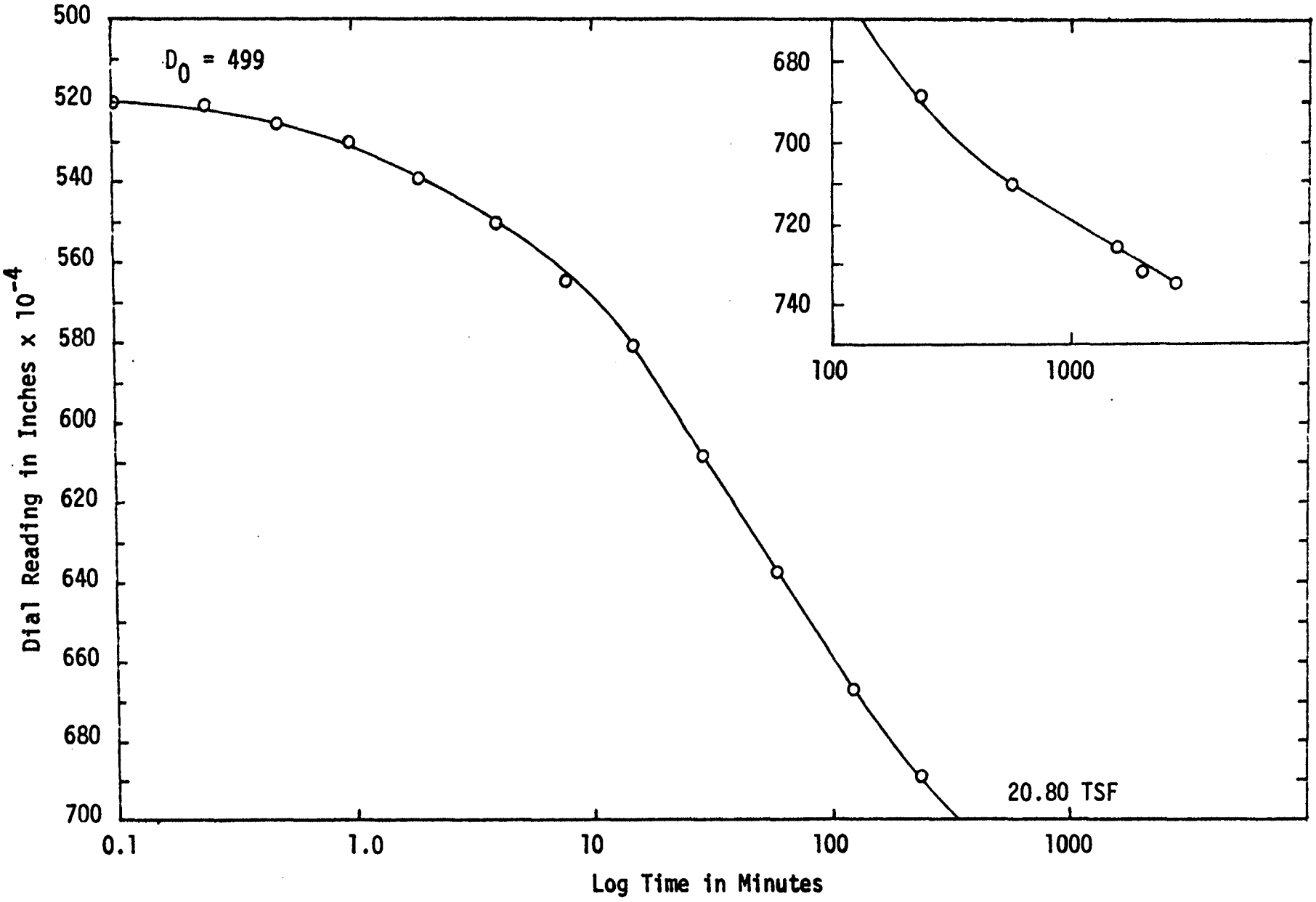

FIGURE 25-d. DIAL READING VERSUS LOG TIME FOR SAMPLE SCS

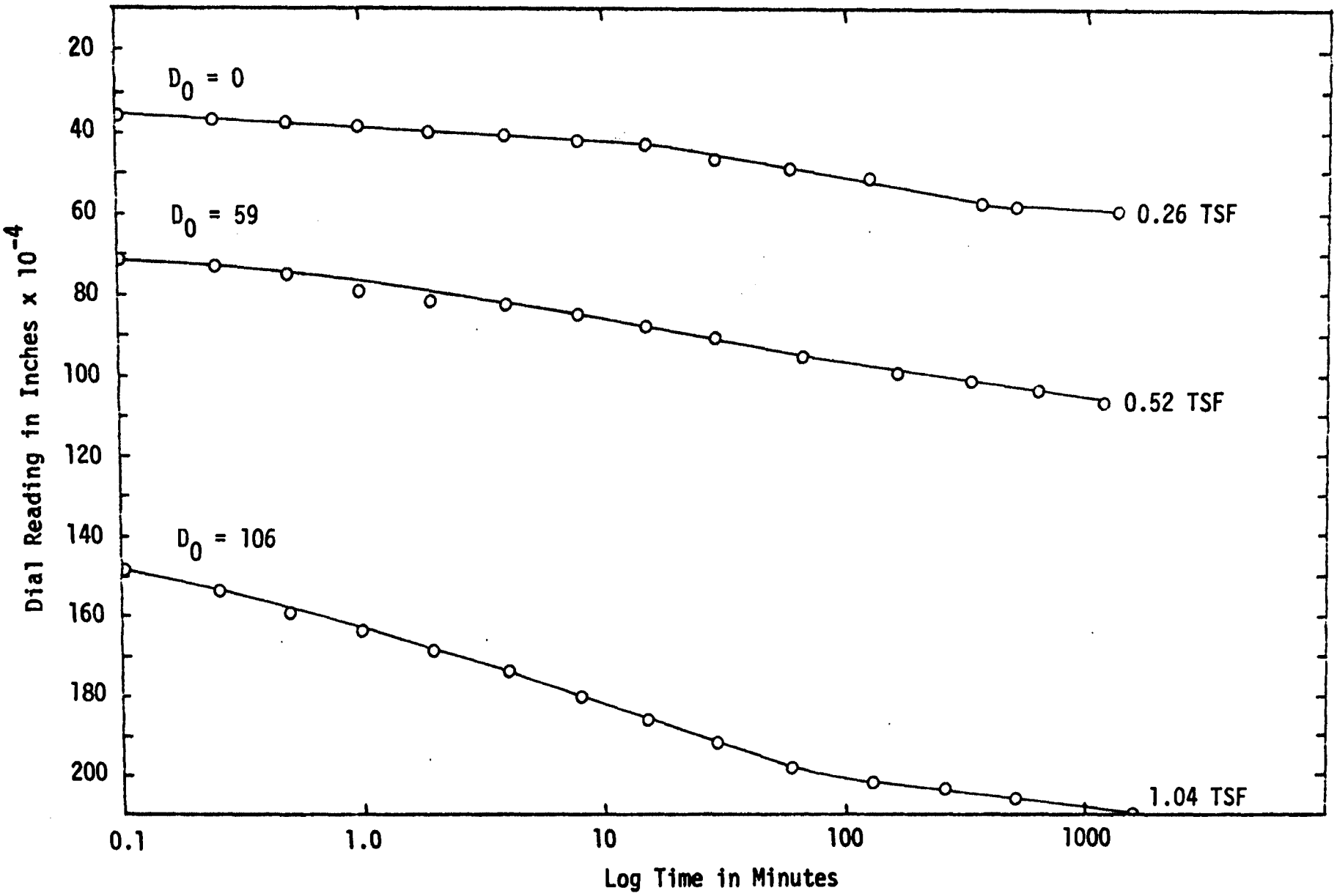

FIGURE 26-a. DIAL READING VERSUS LOG TIME FOR SAMPLE LCN

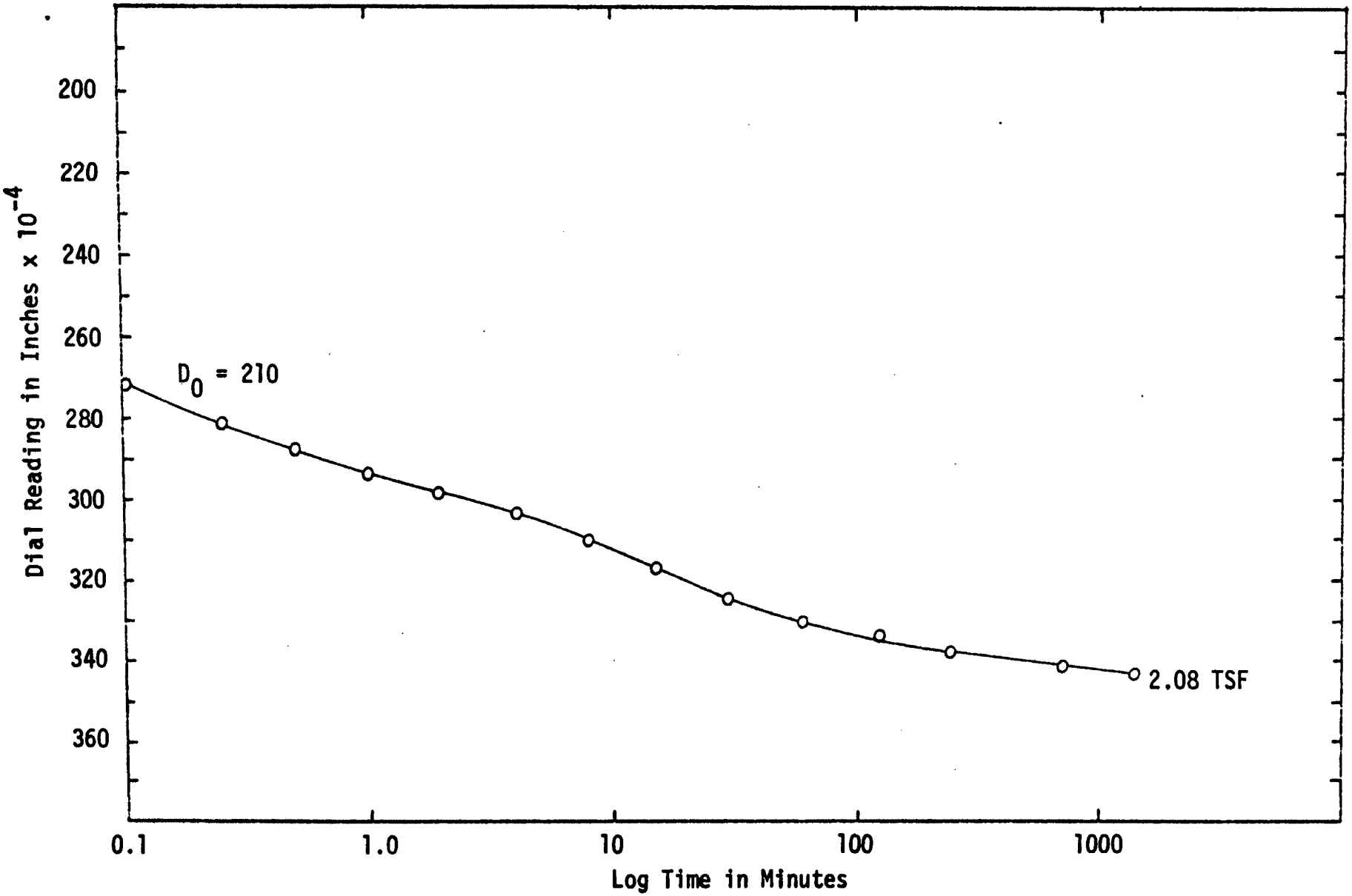

FIGURE 26-b. DIAL READING VERSUS LOG TIME FOR SAMPLE LCN

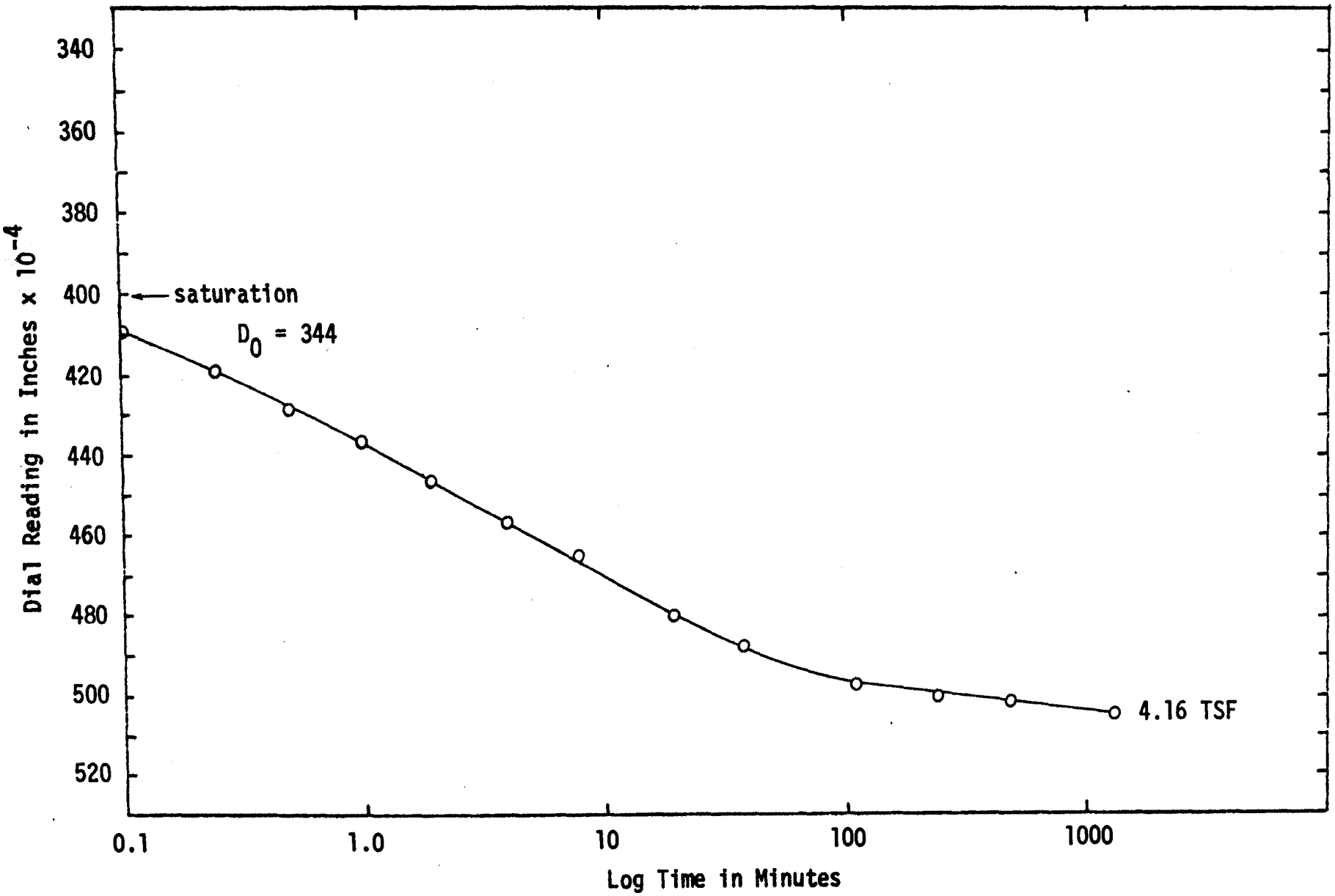

FIGURE 26-c. DIAL READING VERSUS LOG TIME FOR SAMPLE LCN

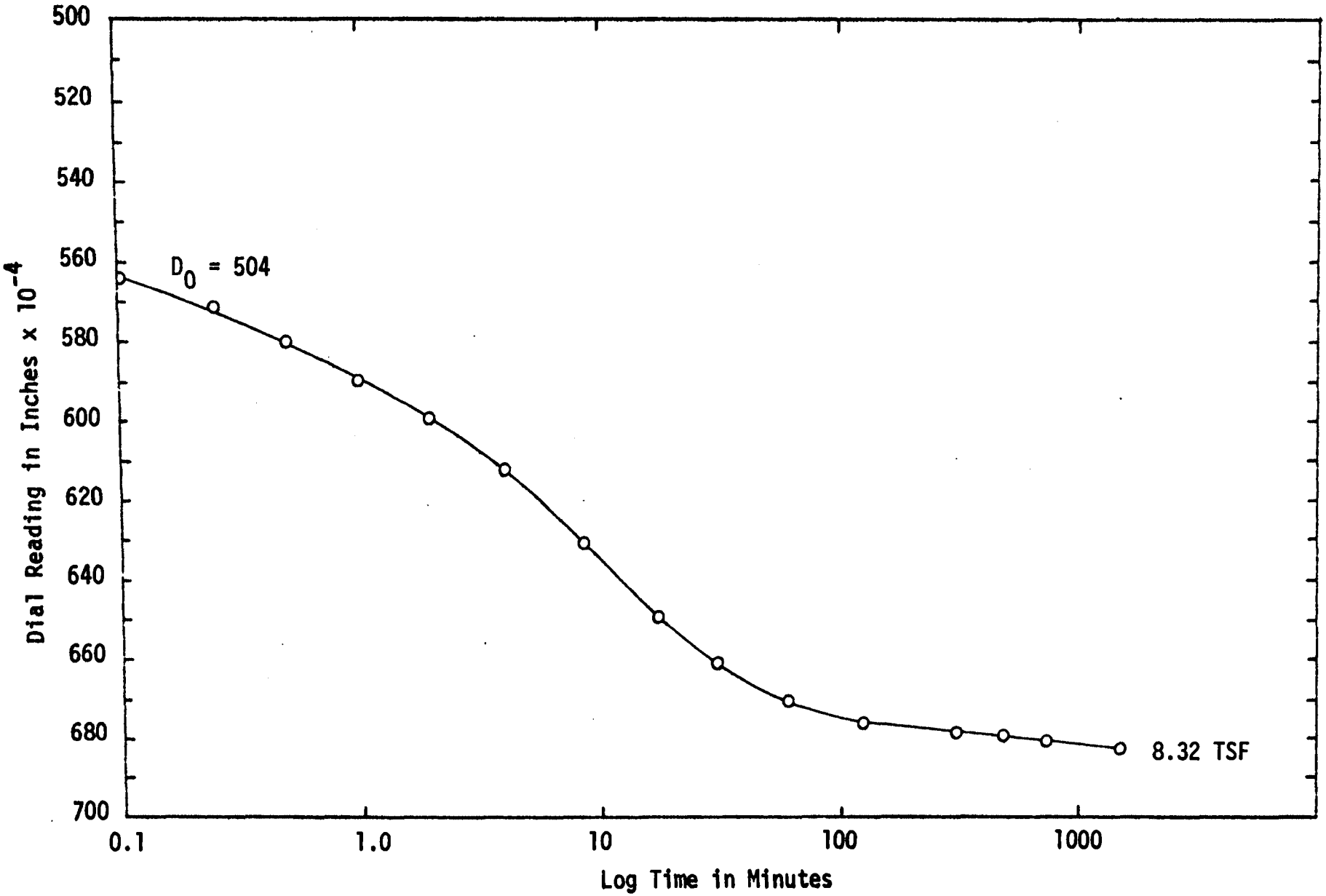

FIGURE 26-d. DIAL READING VERSUS LOG TIME FOR SAMPLE LCN

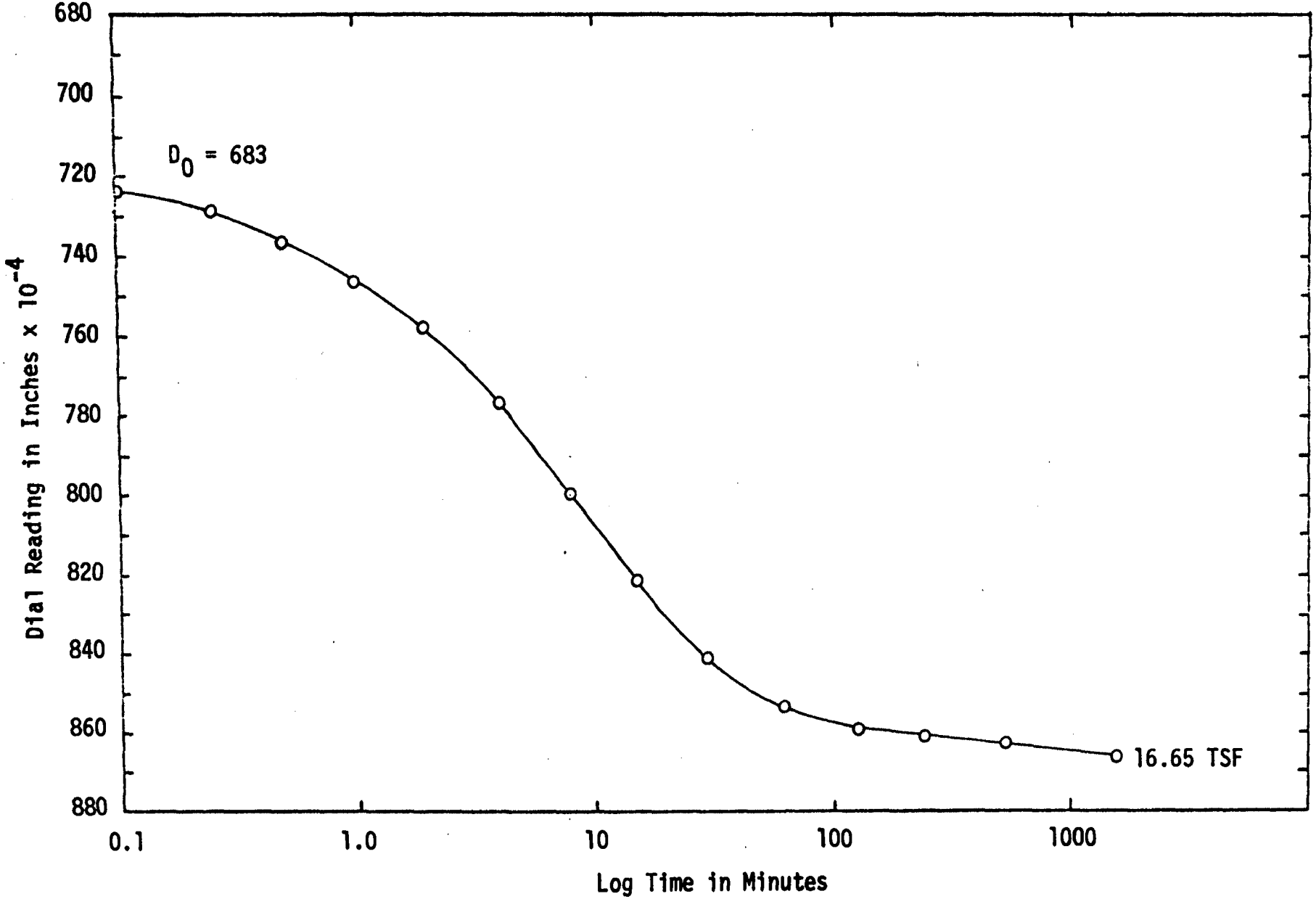

FIGURE 26-e. DIAL READING VERSUS LOG TIME FOR SAMPLE LCN

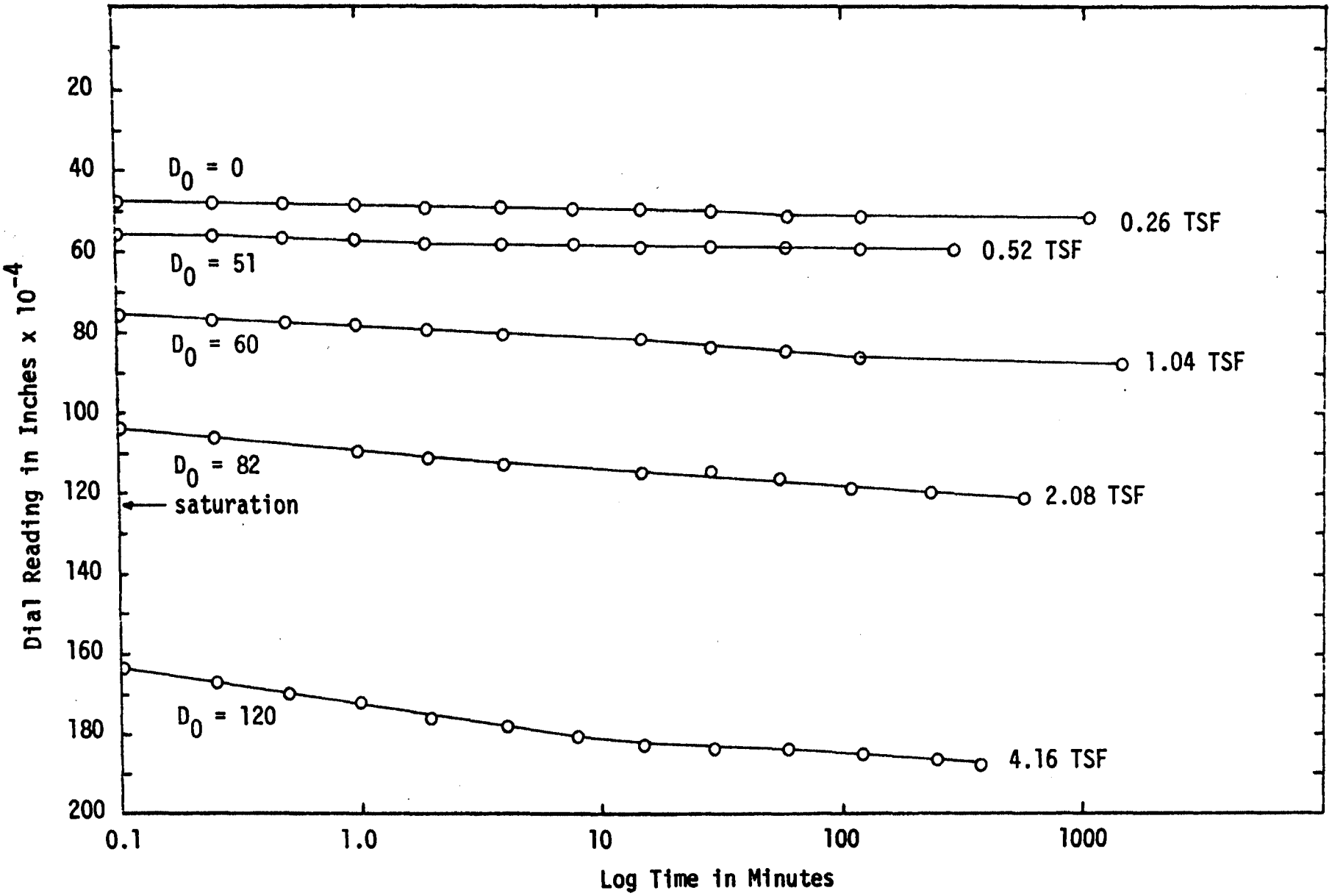

FIGURE 27-a. DIAL READING VERSUS LOG TIME FOR SAMPLE LCC

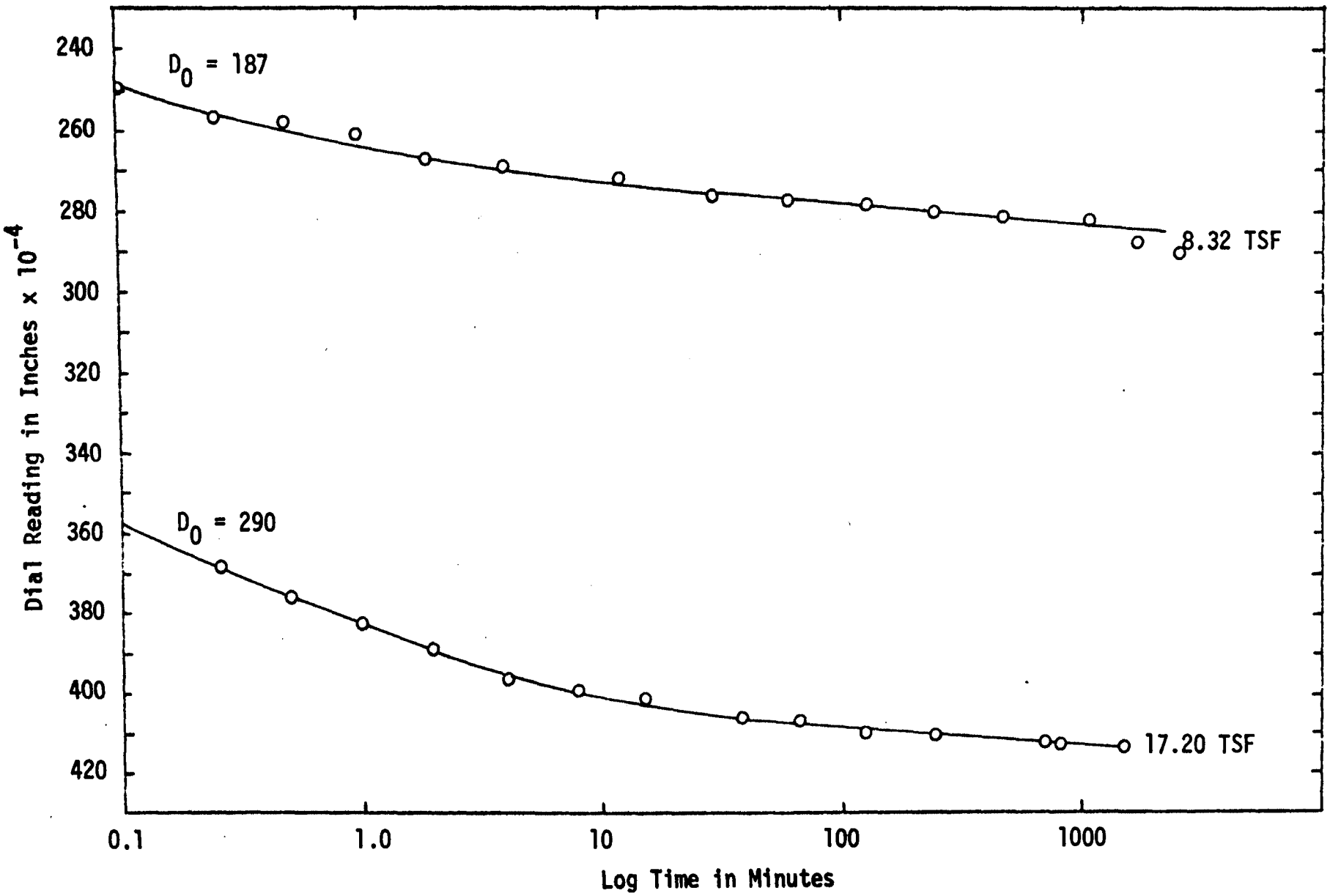

FIGURE 27-b. DIAL READING VERSUS LOG TIME FOR SAMPLE LCC

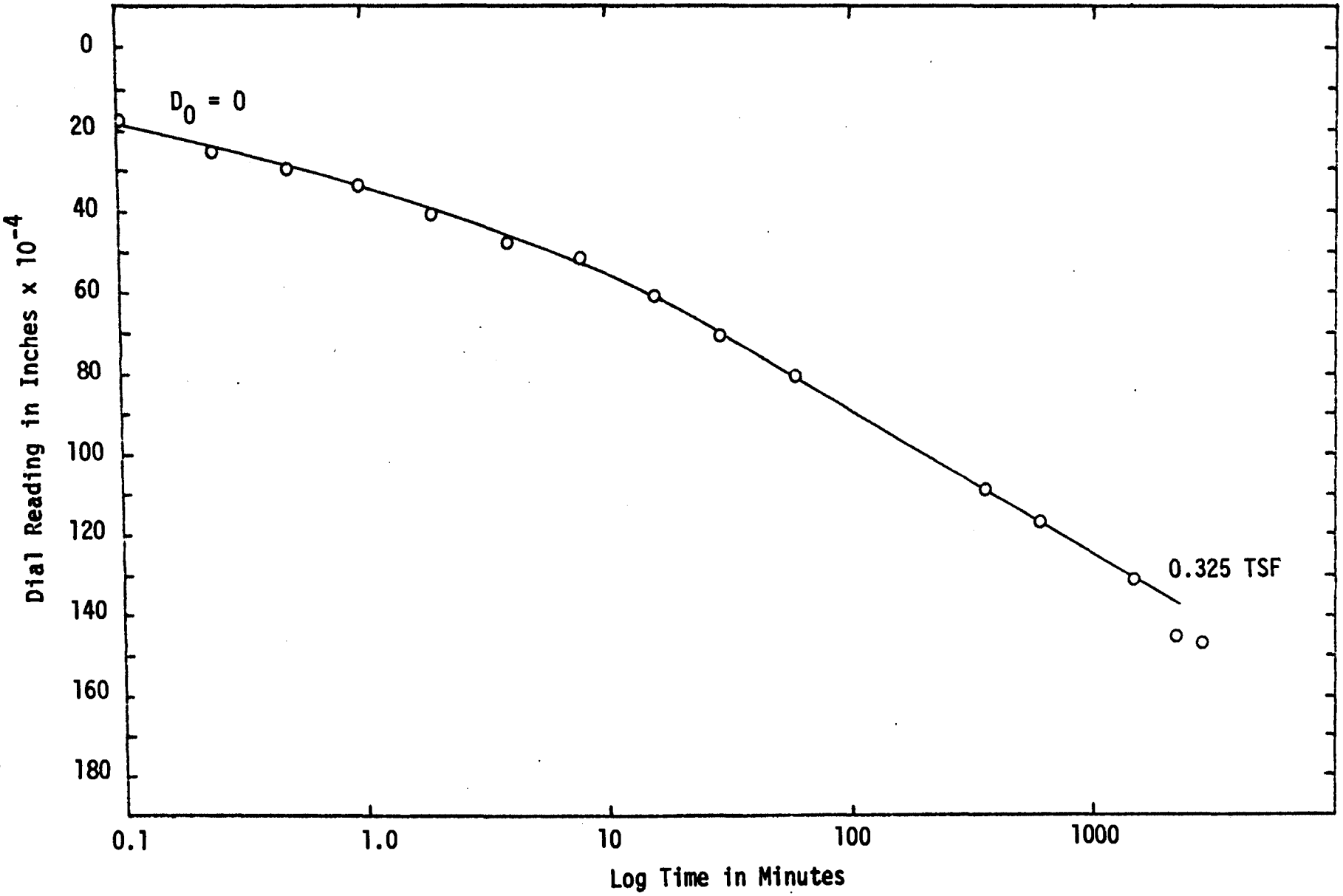

FIGURE 28-a. DIAL READING VERSUS LOG TIME FOR SAMPLE LCS

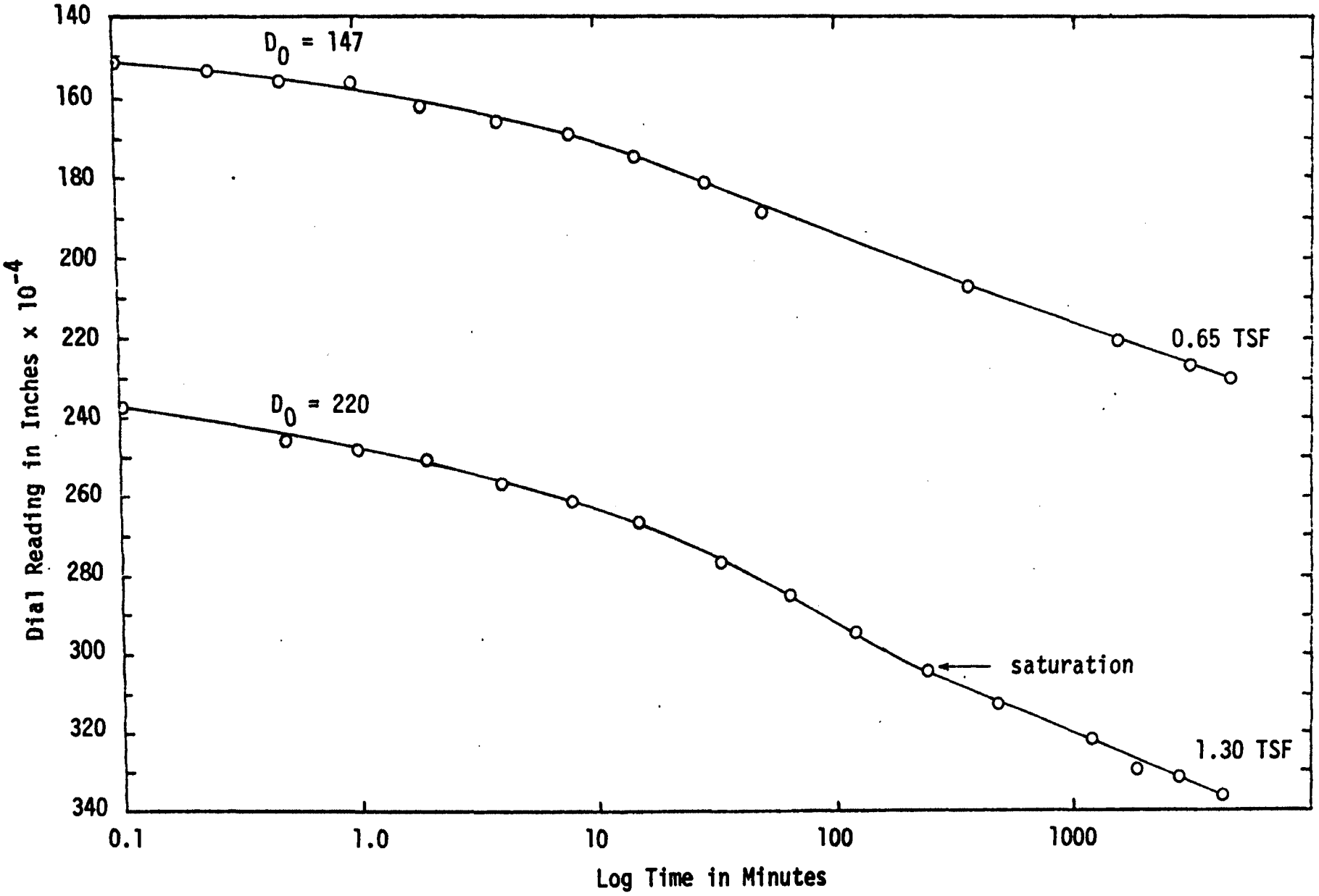

FIGURE 28-b. DIAL READING VERSUS LOG TIME FOR SAMPLE LCS

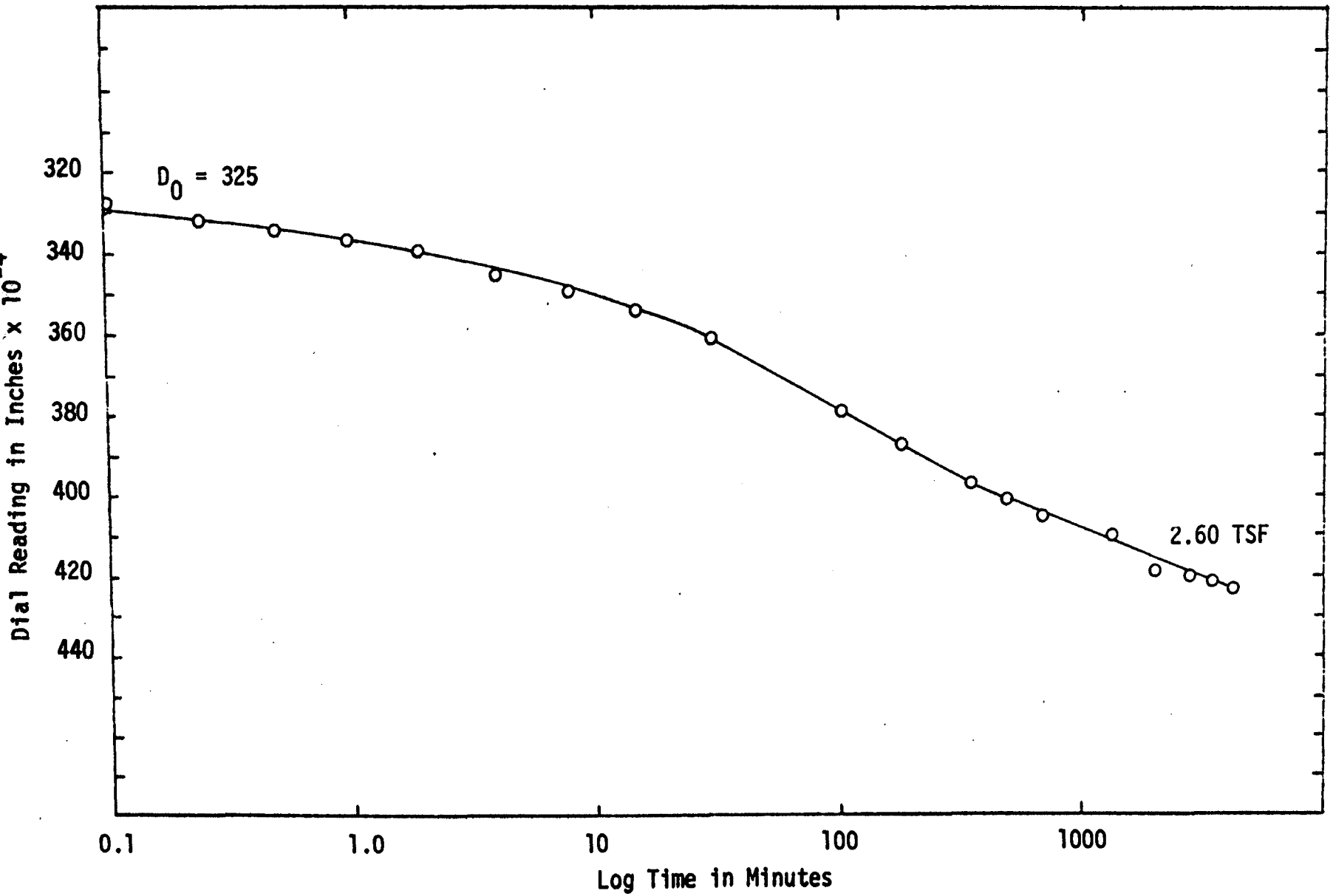

FIGURE 28-c. DIAL READING VERSUS LOG TIME FOR SAMPLE LCS

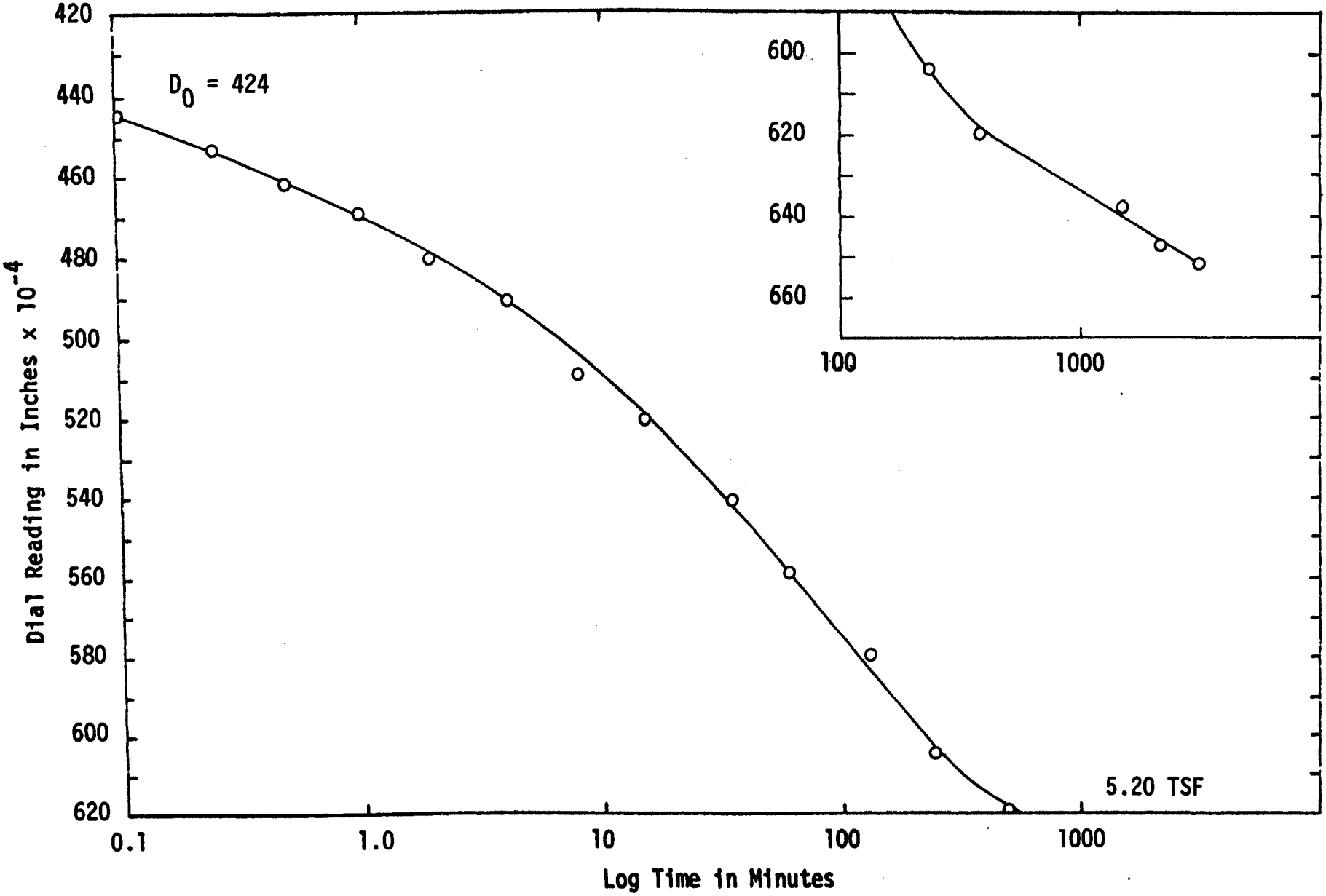

FIGURE 28-d. DIAL READING VERSUS LOG TIME FOR SAMPLE LCS

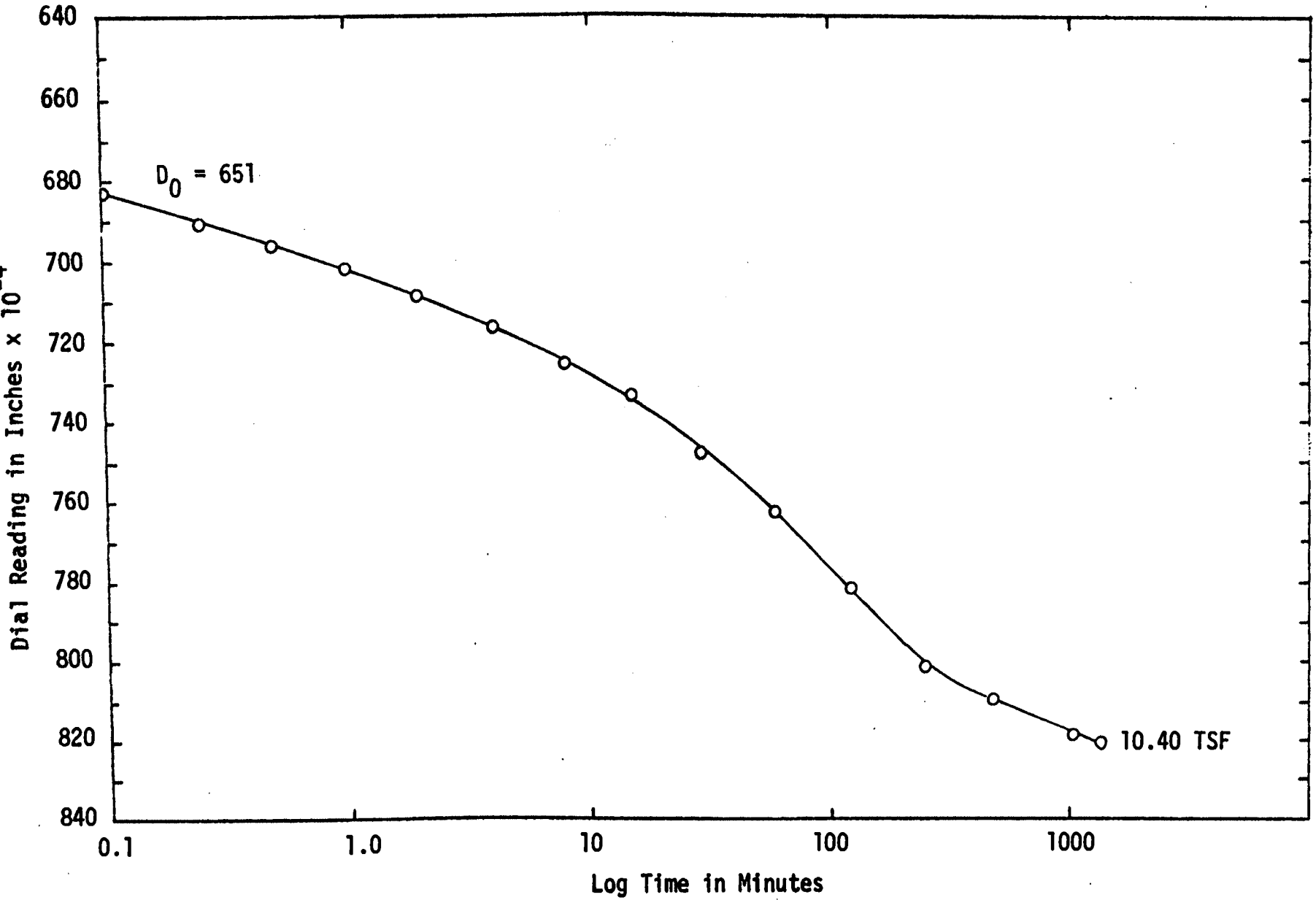

FIGURE 28-e. DIAL READING VERSUS LOG TIME FOR SAMPLE LCS

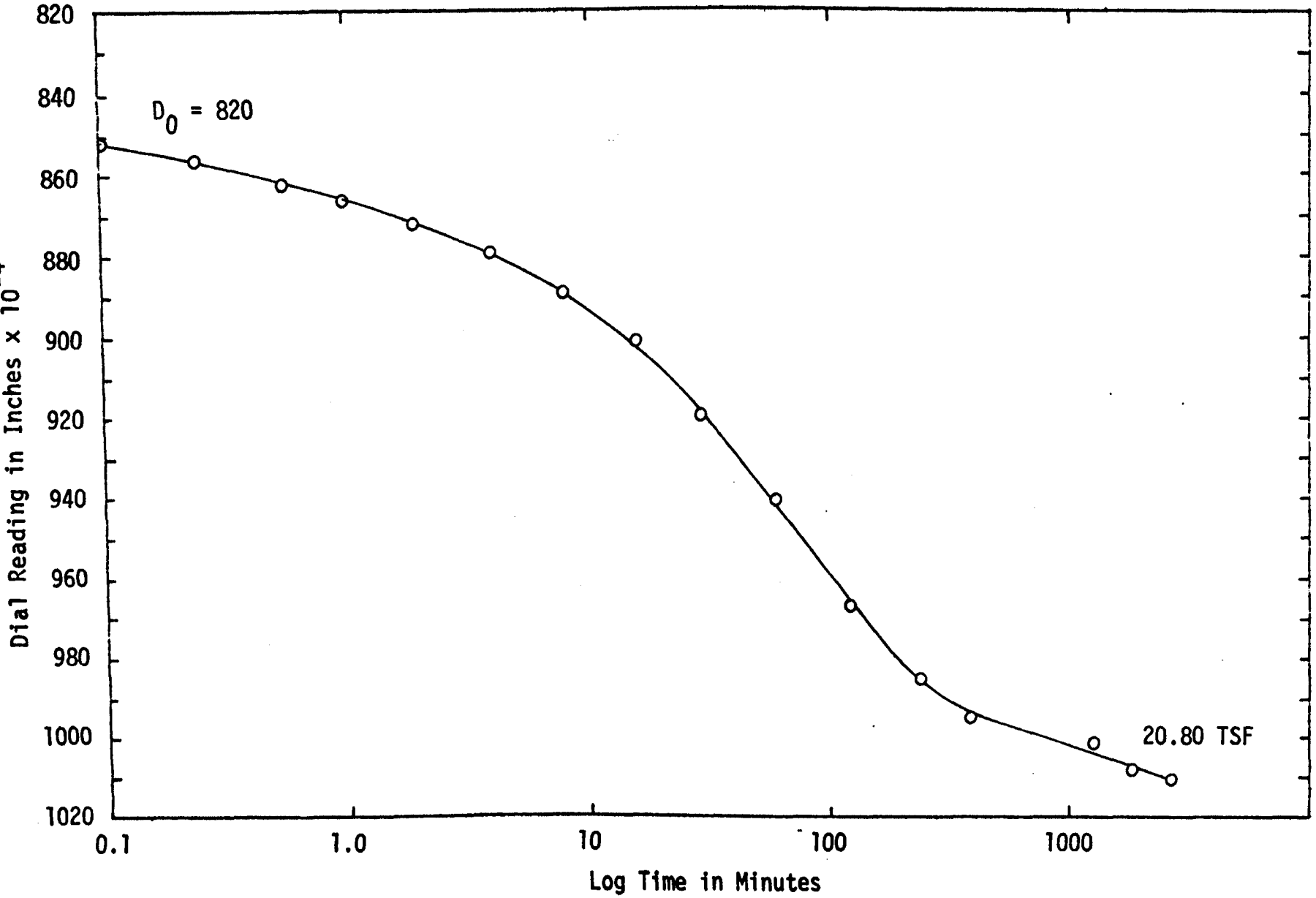

FIGURE 28-f. DIAL READING VERSUS LOG TIME FOR SAMPLE LCS

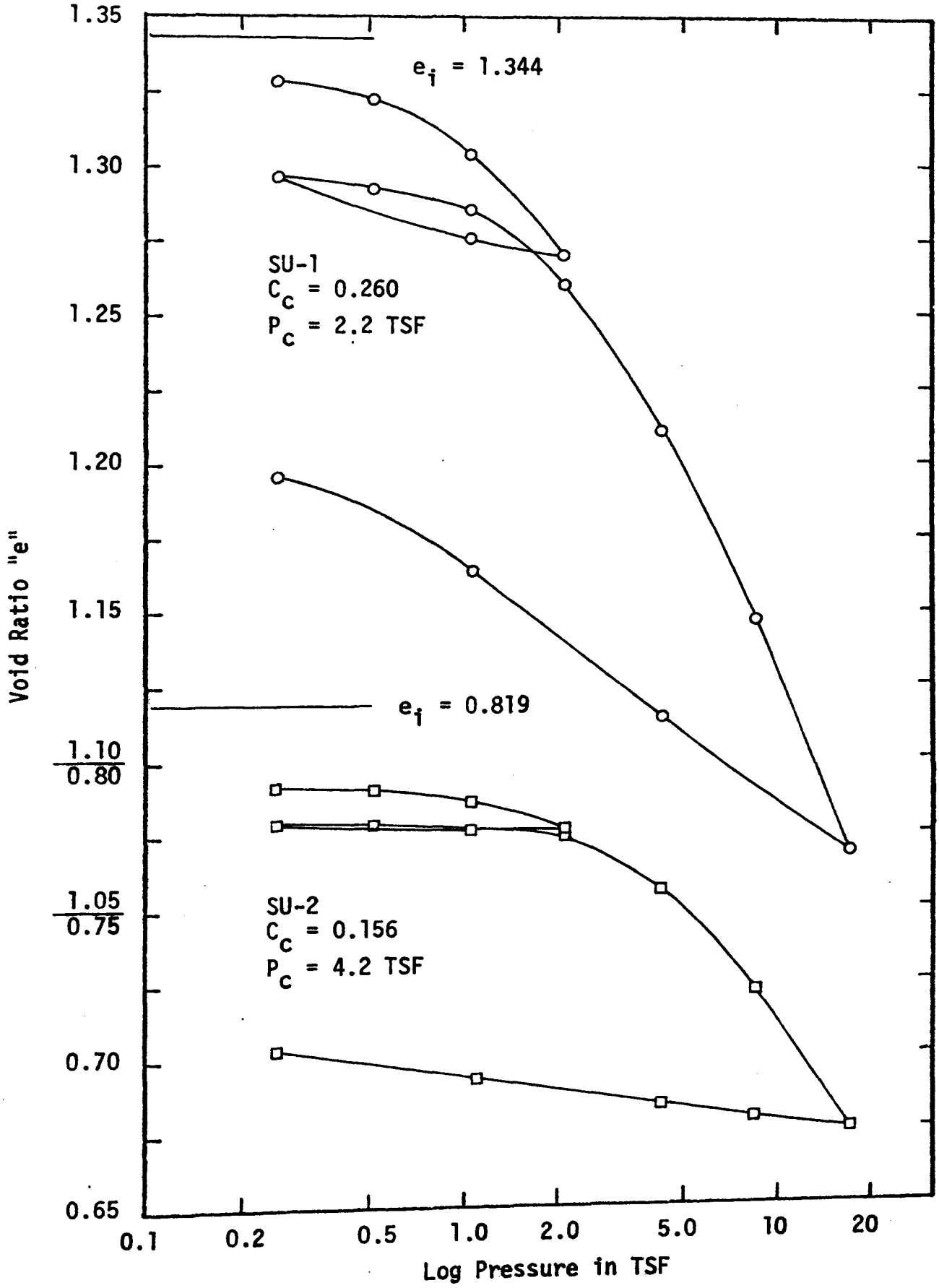

FIGURE 29. VOID RATIO-LOG PRESSURE CURVES, SU-1 AND SU-2

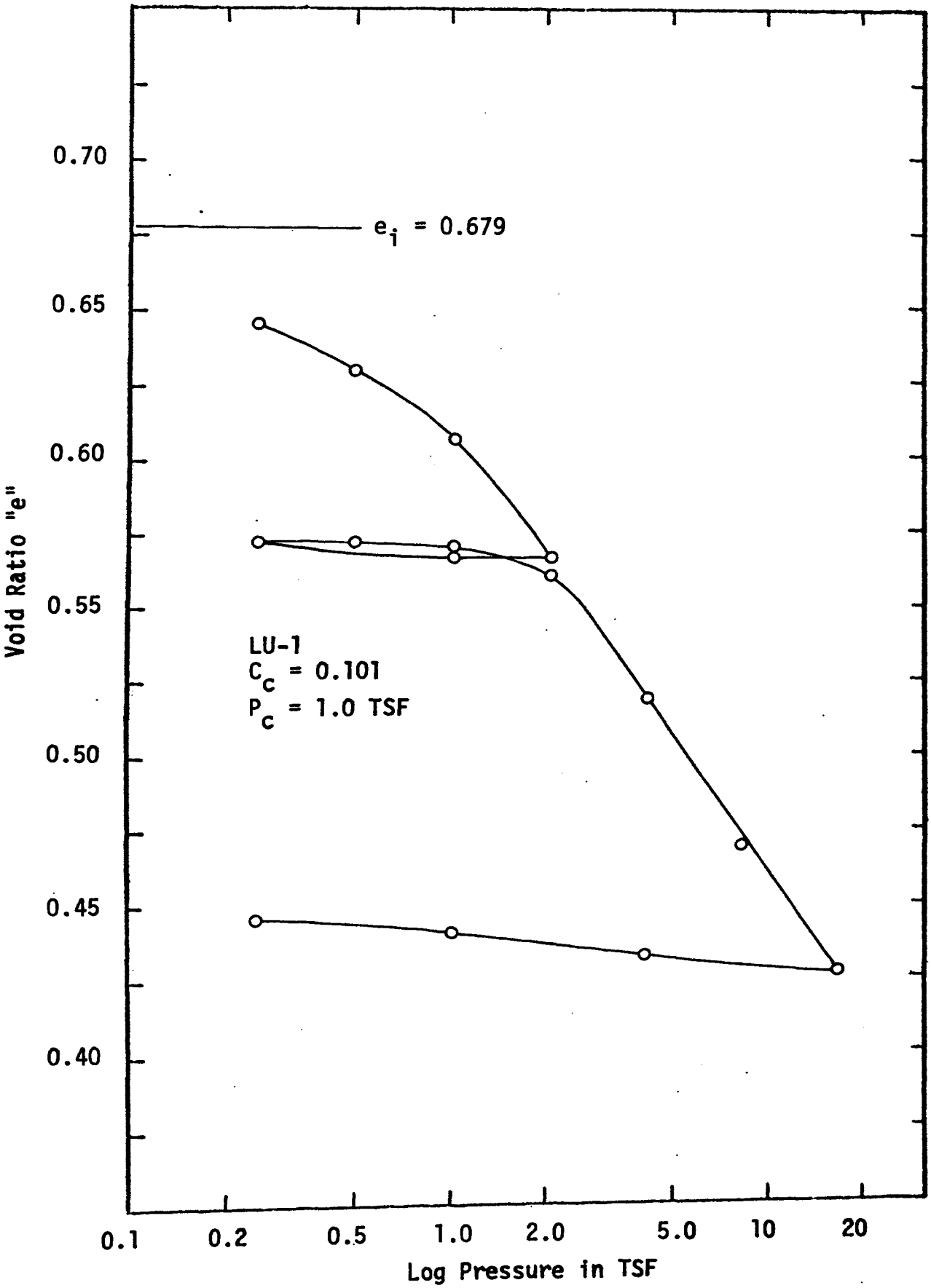

FIGURE 30. VOID RATIO-LOG PRESSURE CURVE, LU-1

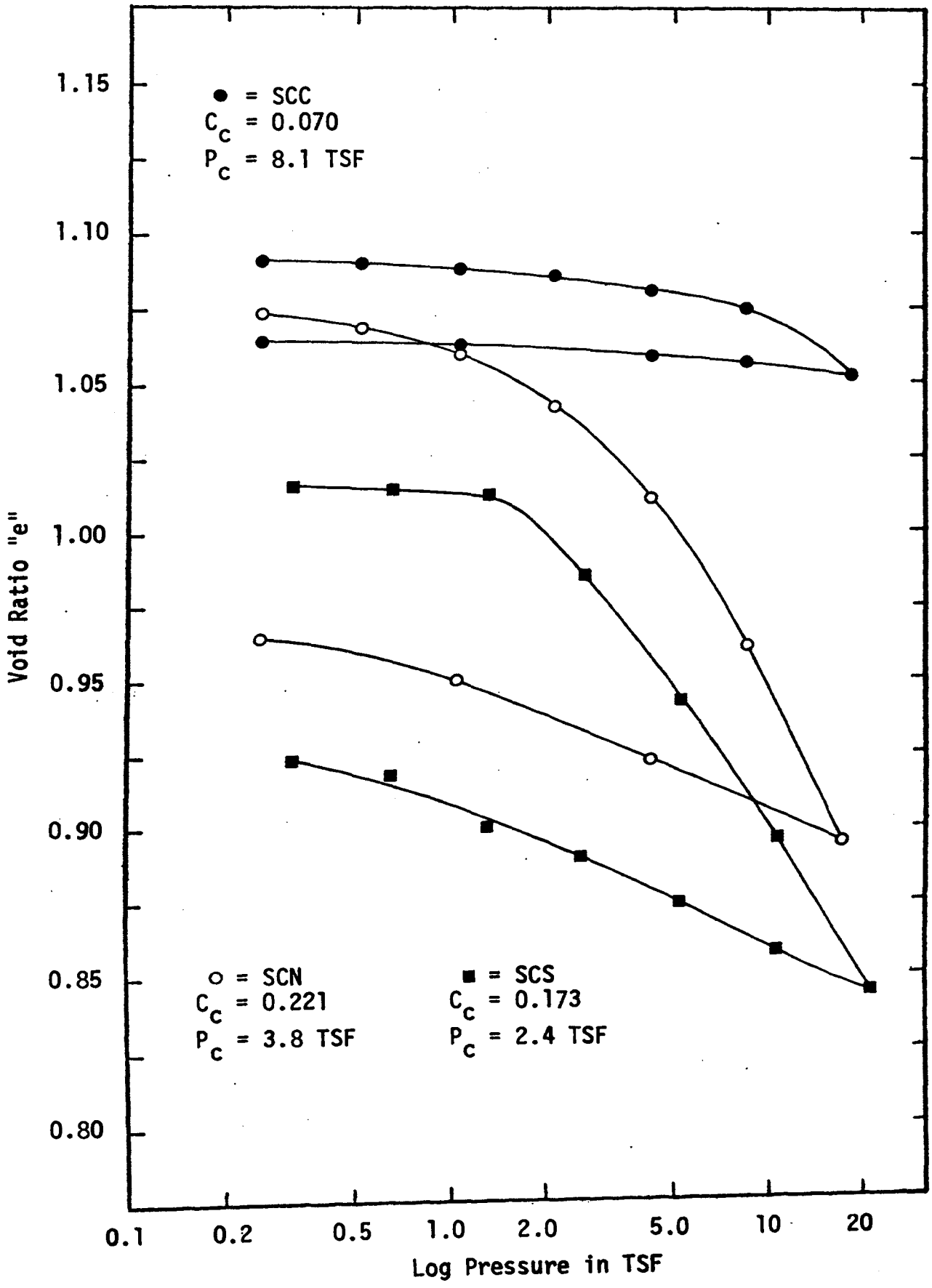

FIGURE 31. VOID RATIO-LOG PRESSURE CURVES, SCN, SCC, AND SCS

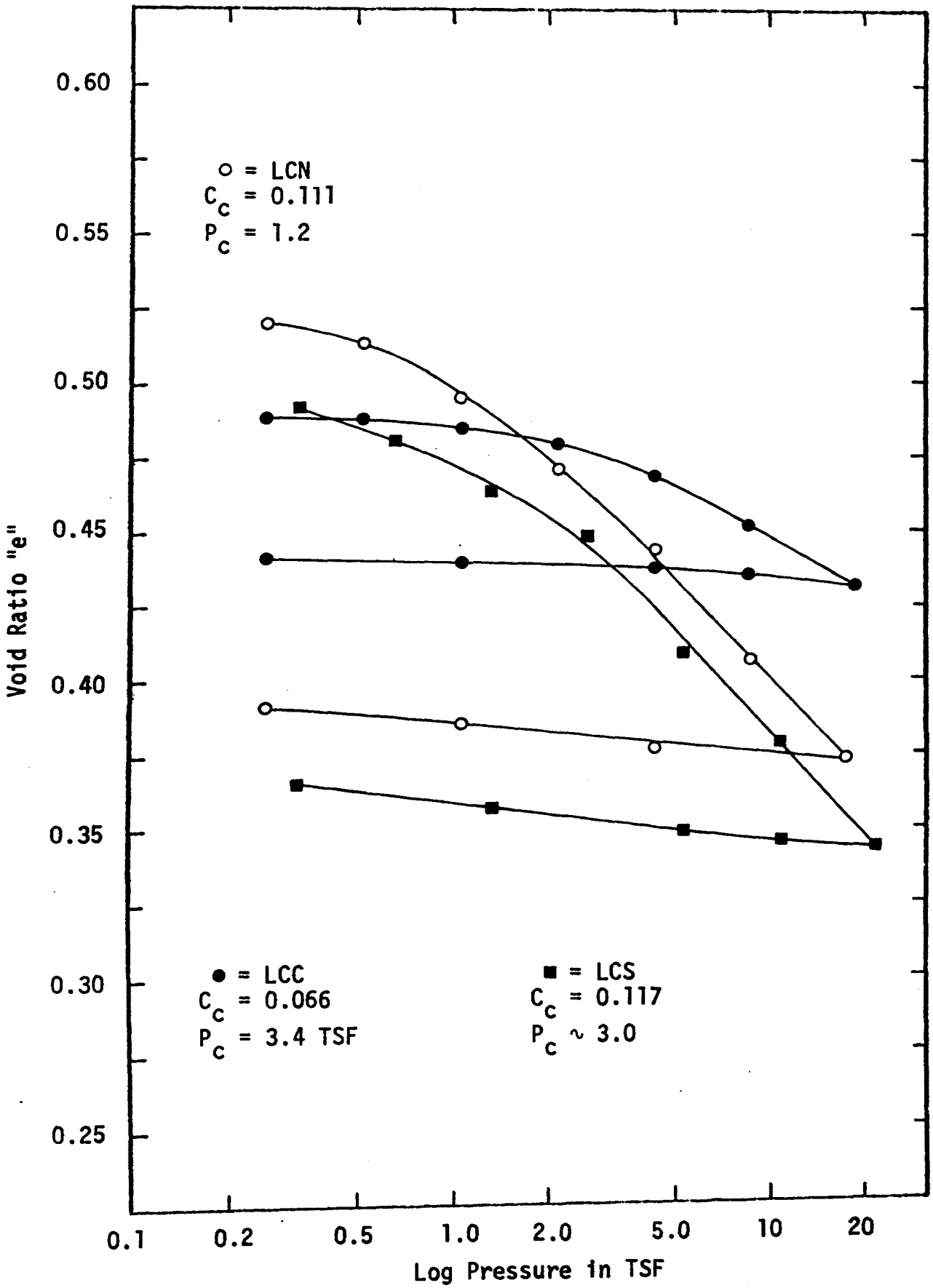

FIGURE 32. VOID RATIO-LOG PRESSURE CURVES, LCN, LCC, AND LCS

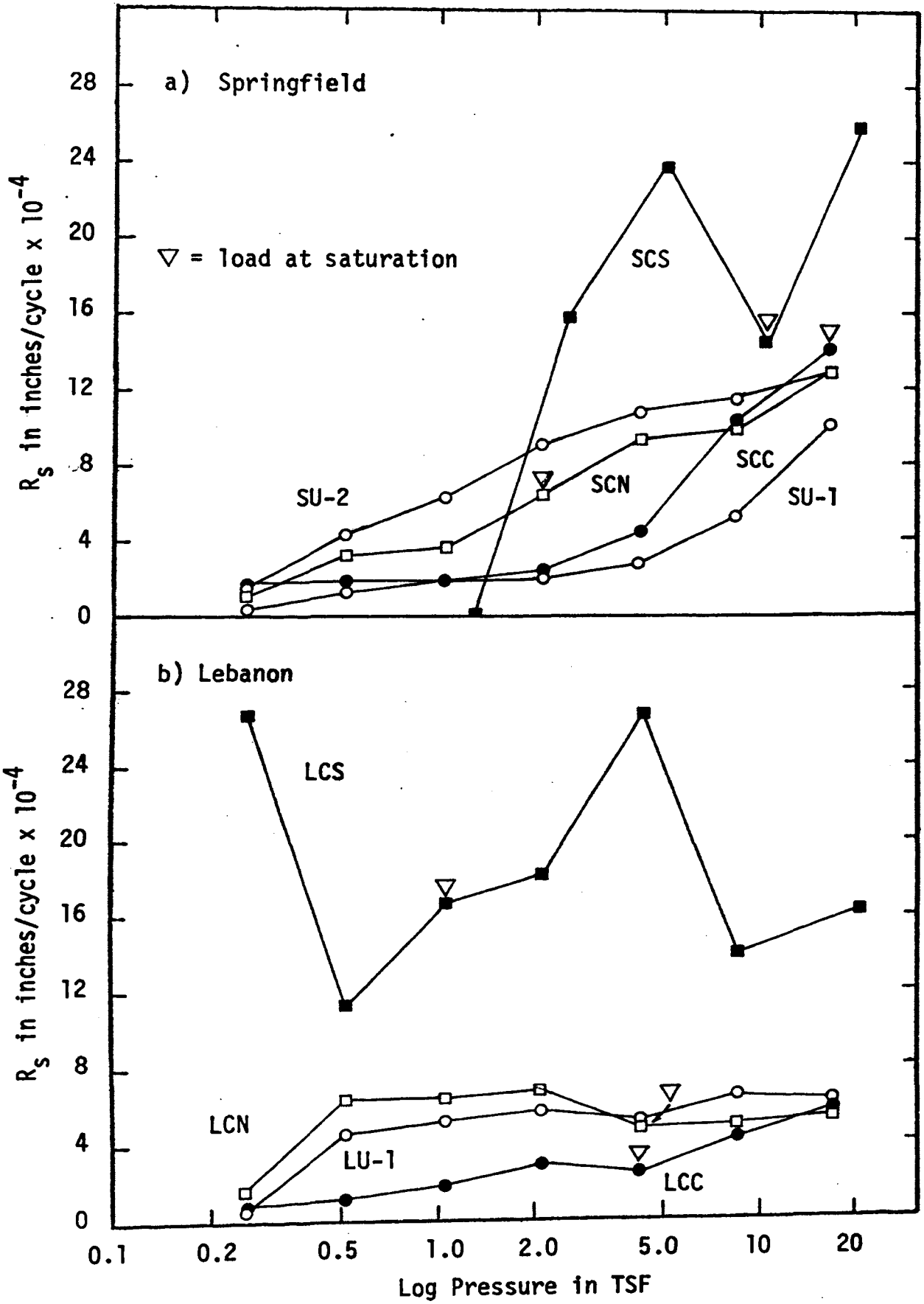

FIGURE 33. RATE OF SECONDARY COMPRESSION VERSUS LOG PRESSURE

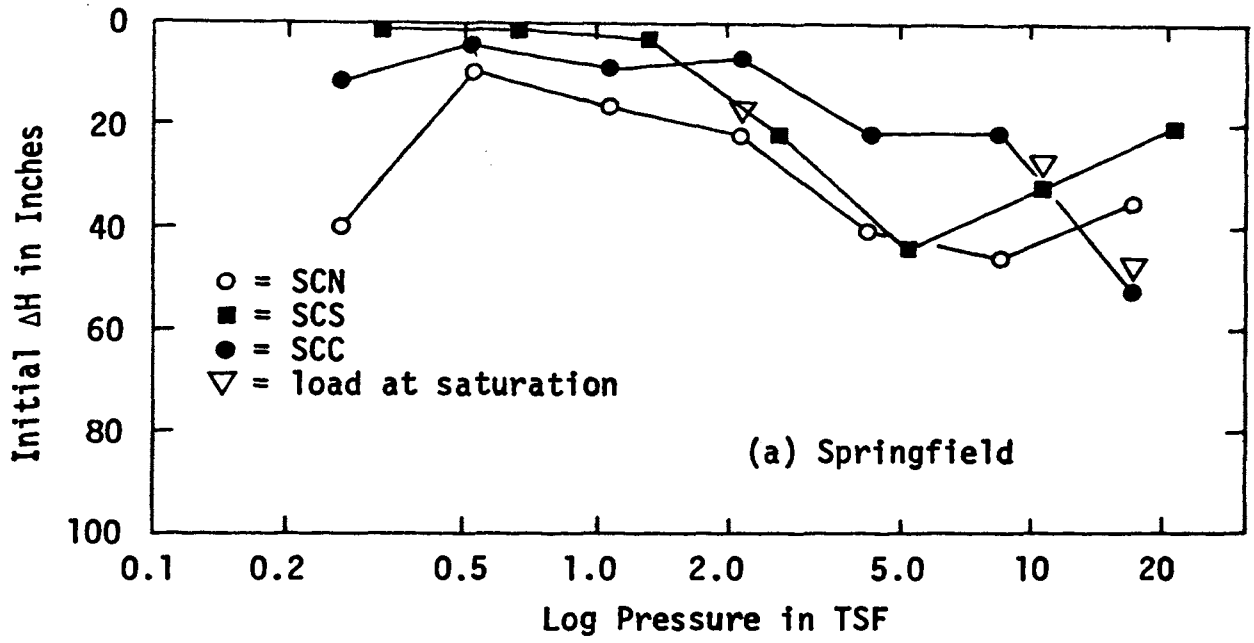

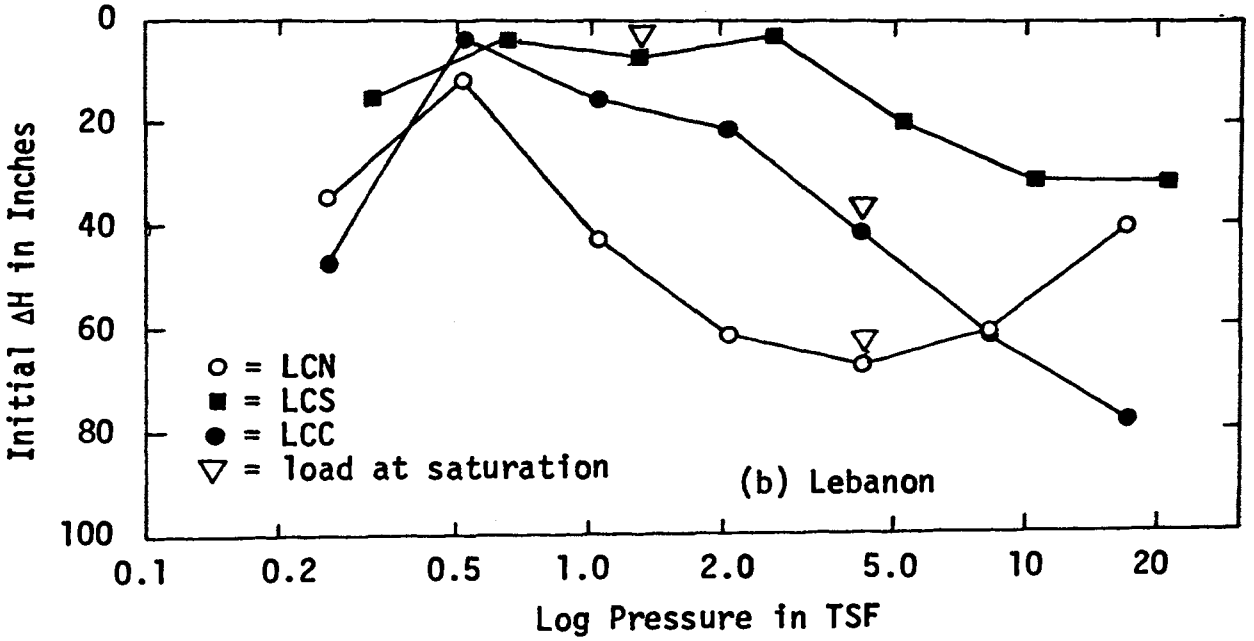

FIGURE 34. ACTUAL INITIAL COMPRESSION VERSUS LOG PRESSURE

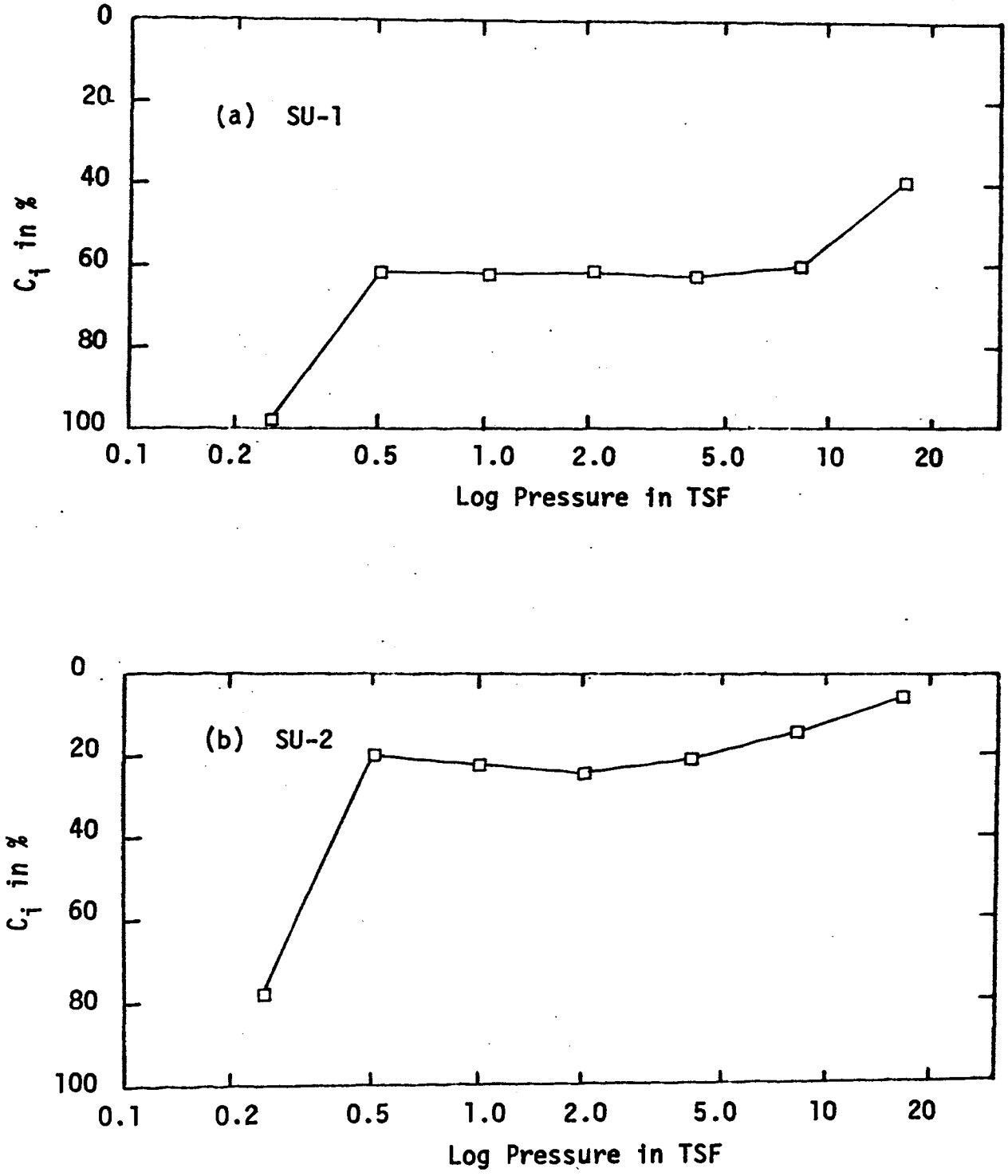

FIGURE 35. ACTUAL AND CALCULATED PERCENT INITIAL COMPRESSION VERSUS LOG PRESSURE FOR SPRINGFIELD SOILS

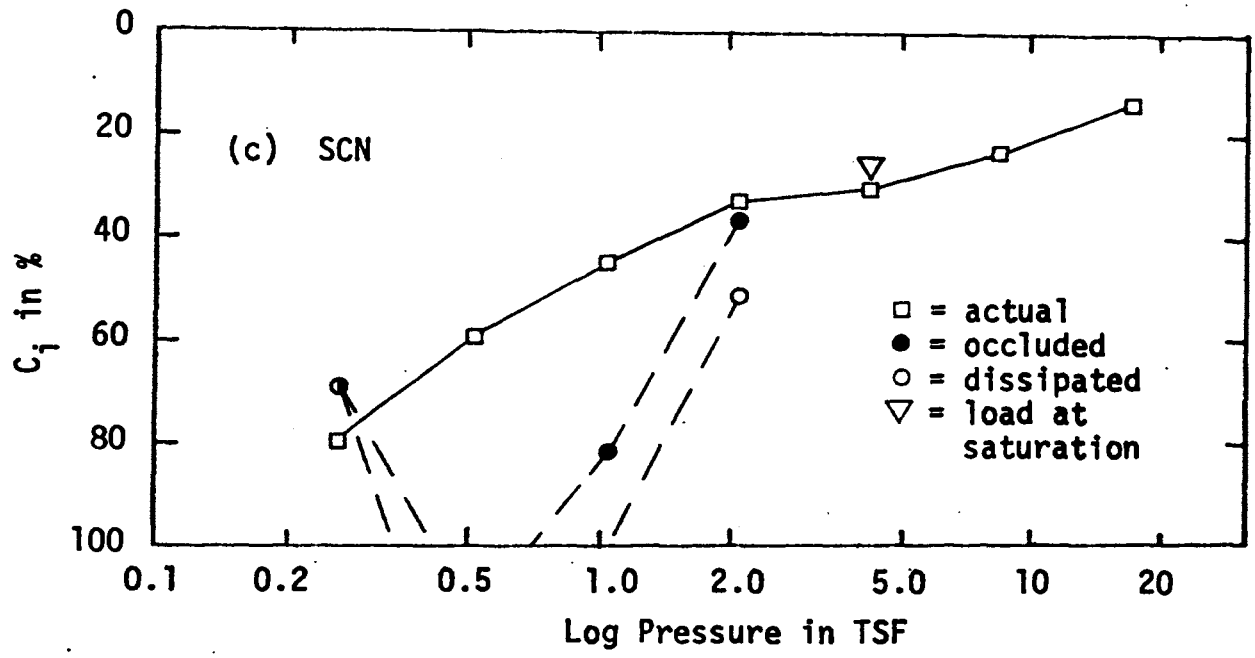

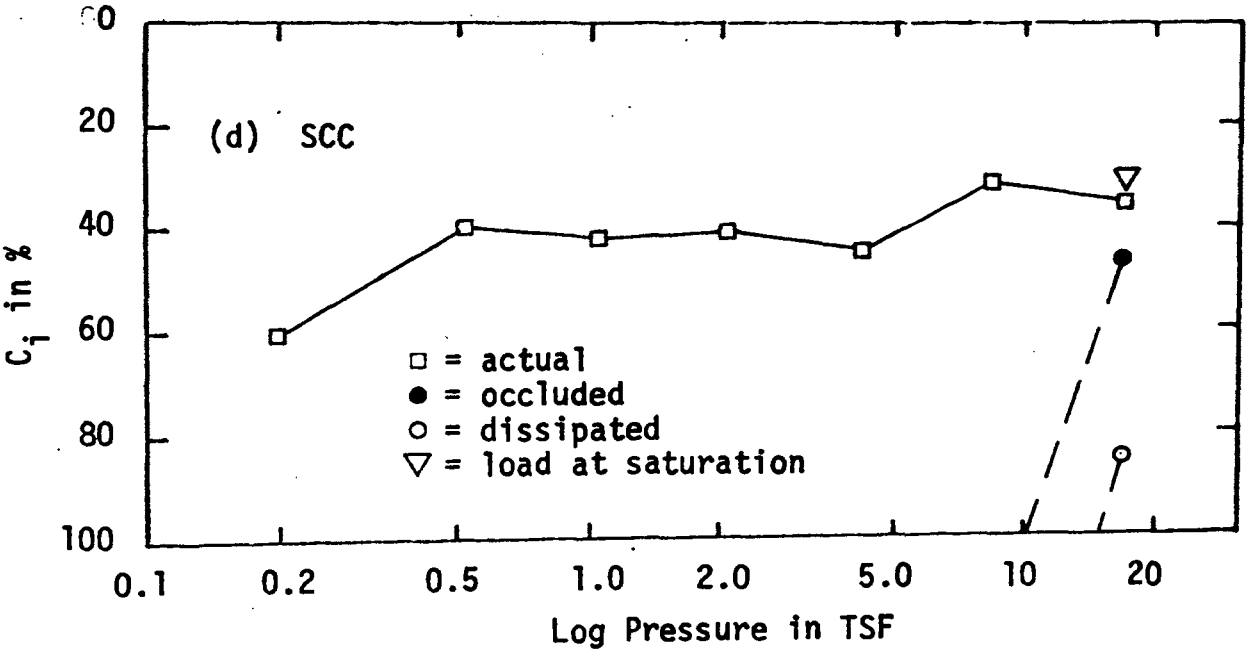

FIGURE 35, CONTINUED. ACTUAL AND CALCULATED PERCENT INITIAL COMPRESSION VERSUS LOG PRESSURE FOR SPRINGFIELD SOILS

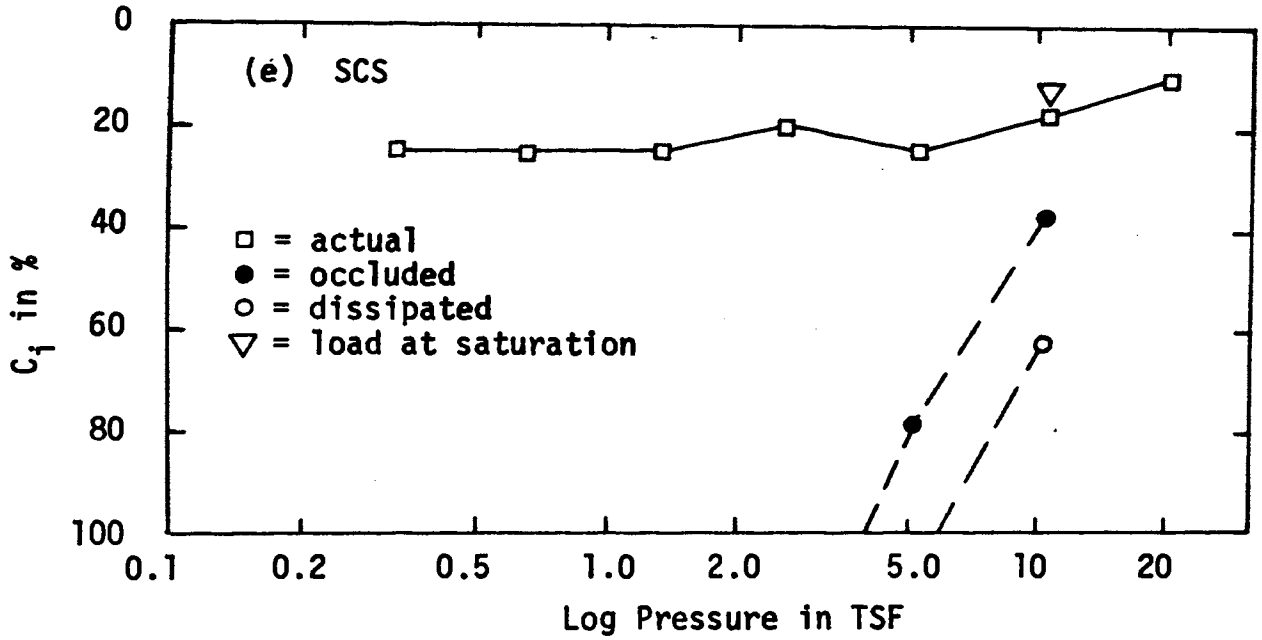

FIGURE 35, CONTINUED. ACTUAL AND CALCULATED PERCENT INITIAL COMPRESSION VERSUS LOG PRESSURE FOR SPRINGFIELD SOILS

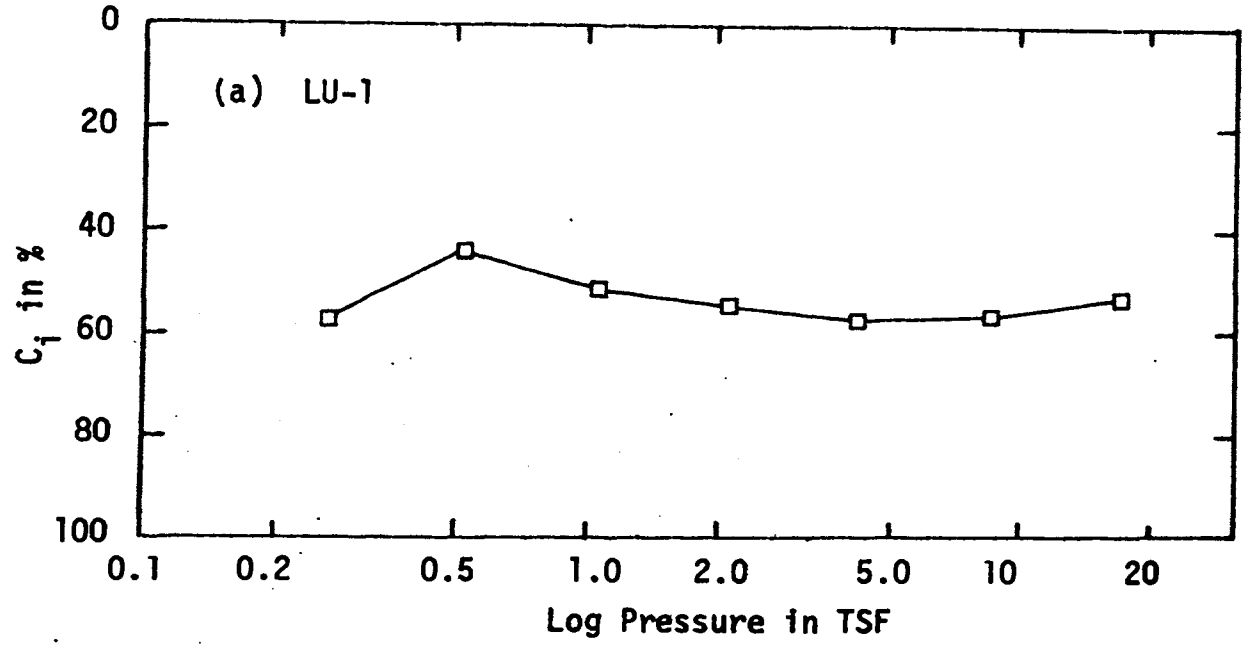

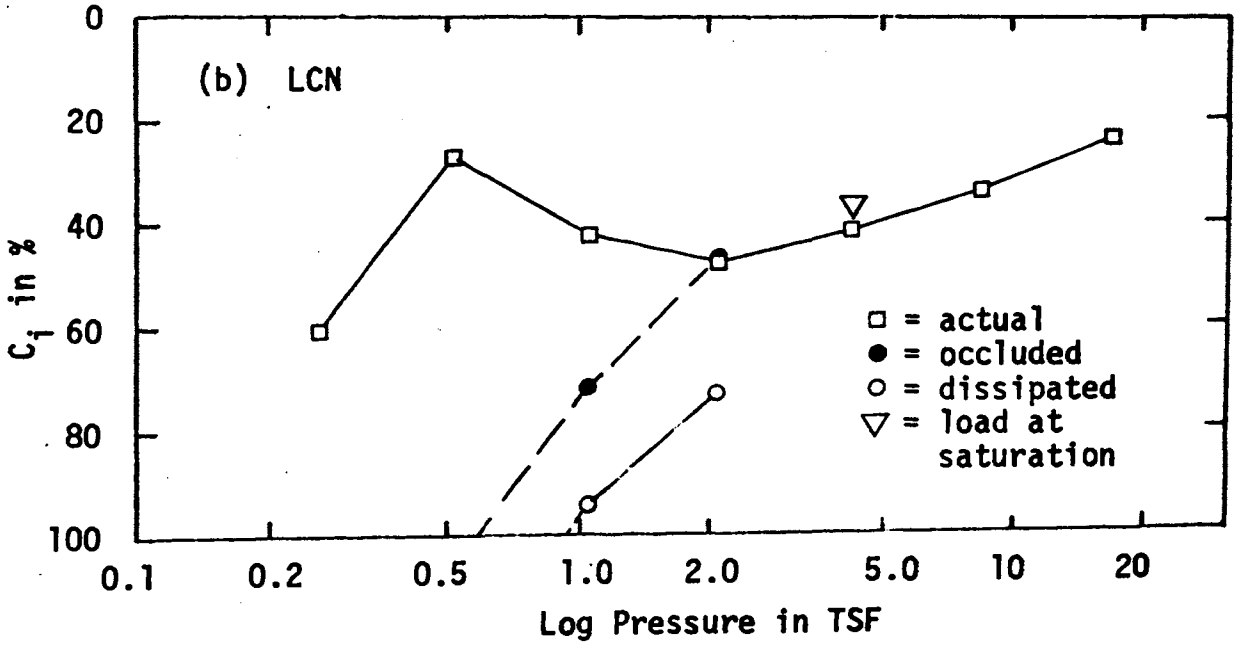

FIGURE 36. ACTUAL AND CALCULATED PERCENT INITIAL COMPRESSION VERSUS LOG PRESSURE FOR LEBANON SOILS

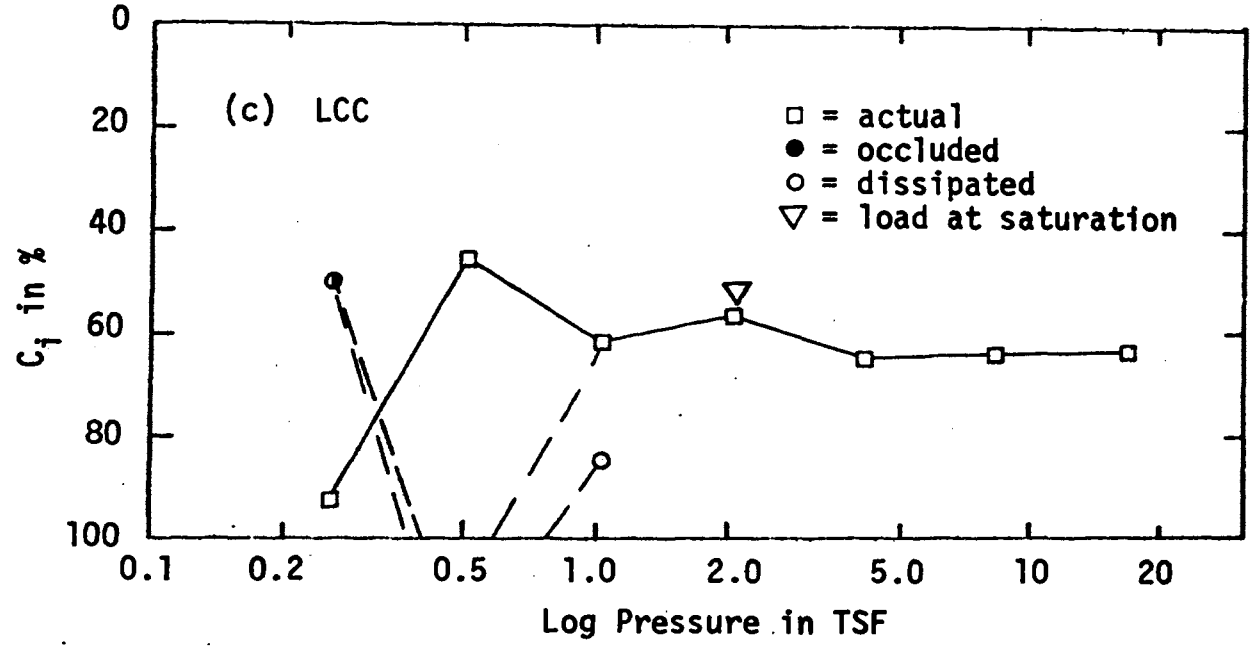

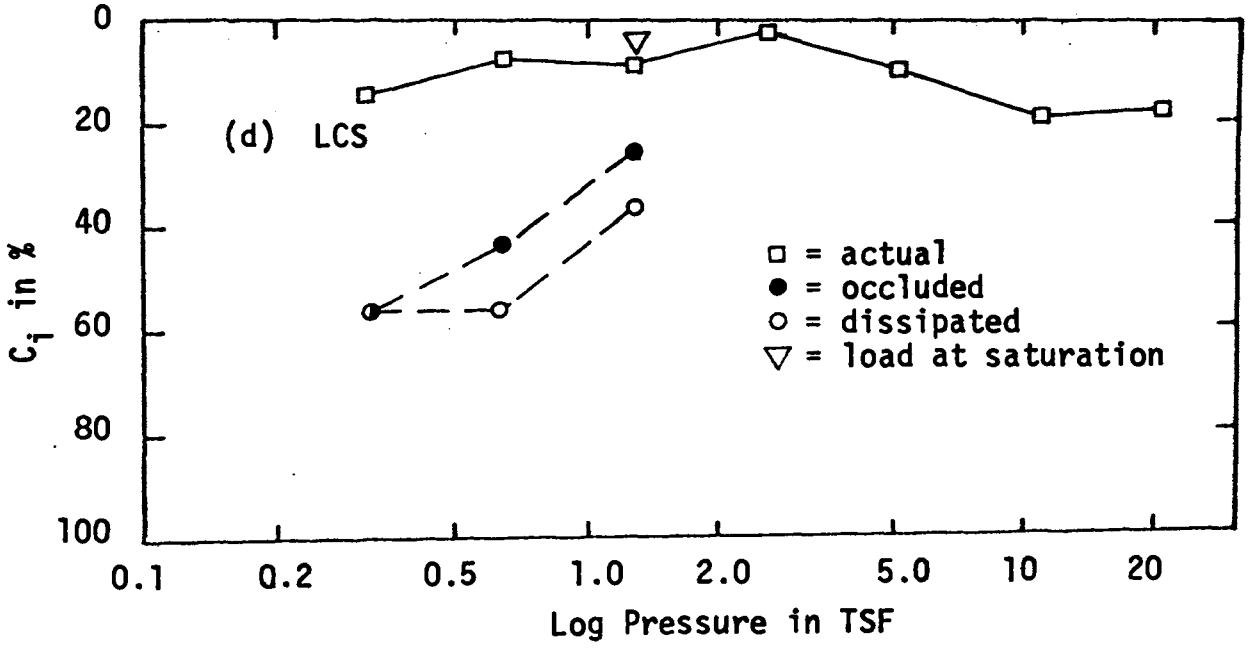

FIGURE 36, CONTINUED. ACTUAL AND CALCULATED PERCENT INITIAL COMPRESSION VERSUS LOG PRESSURE FOR LEBANON SOILS

VITA

William Joseph Graham was born October 29, 1944 in Portsmouth, New Hampshire. For most of his youth he lived in Fredericktown, Missouri, where he received his primary and secondary education. He received a Bachelor of Science Degree and Master of Science Degree in Civil Engineering from the University of Missouri at Rolla in 1967 and 1969, respectively.

Mr. Graham is married to the former Diane M. Winkler, of St. Louis, Missouri.